ANALYTICAL AND EXPERIMENTAL STUDIES OF COLD-FORMED STEEL SHEAR PANELS

by

Burak Karabulut

B.S., Civil Engineering, Kocaeli University, 2012

Submitted to the Institute for Graduate Studies in
Science and Engineering in partial fulfillment of
the requirements for the degree of
Master of Science

Graduate Program in Civil Engineering

Boğaziçi University

2016

ANALYTICAL AND EXPERIMENTAL STUDIES OF COLD-FORMED STEEL SHEAR PANELS

APPROVED BY:

Assoc. Prof. Serdar Soyöz (Thesis Supervisor)	.....
Prof. Gülay Altay	.....
Assist. Prof. Barlas Özden Çağlayan	.....

DATE OF APPROVAL: 30.12.2015

To my grandfather Vassaf Karabulut and my uncle Orhan Turhan...

ACKNOWLEDGEMENTS

Firstly, I would like to show best of my gratitude to my advisor and thesis supervisor, Assoc. Prof. Serdar Soyöz for his incredible help and support through this study and research. He has always been very encouraging and supportive for my success and he has been a great example for me with his passion and love to his job. His patience and guidance extraordinarily helped me progress in my studies and thesis.

In addition, I would like to present my gratefulness to Prof. Gülay Altay and Assist. Prof. Barlas Özden Çağlayan for their great and supportive attitude towards me, and for their valuable recommendations as well as supervision.

I owe special appreciation to the corporations Akşan and Dalsan for their great contribution to this thesis since they provided a significant number of specimens to be used as a part of this project.

I would also like to show my appreciation to Liza Doilnitsyna who has never stopped motivating and supporting me during my education just like she does for all the parts she takes place in my life.

I would like to express my sincere gratitude to my beloved friends, Serhat Aksu, Utku Demir, Sinan Karçıka, Uğur Keleş and Orbay Özkan for their great support and joy of living.

Lastly, I wish to thank the beloved members of my family, my sister Elif Karabulut, my aunt Gül Karabulut, my father Nebil Karabulut, my mother and grandmother Zuhal Karabulut, who have always unconditionally supported me and helped me be strong throughout my life. Without them, none of my dreams could have come true in my life journey.

ABSTRACT

ANALYTICAL AND EXPERIMENTAL STUDIES OF COLD-FORMED STEEL SHEAR PANELS

In the scope of this thesis, lateral load resisting capacity of cold-formed steel framed shear panels have been observed experimentally as well as analytically. Experimental observations on different configuration of shear panels and analytical study have been performed respectively in order to examine the match between experimental and analytical results. In residential applications, cold-formed steel frame is mostly sheathed with gypsum wallboard (GWB), oriented strand board (OSB) or plywood depending on the design purposes and architectural considerations. When a cold-formed steel frame is coated with one of these sheathings, it starts to behave analogous to an entire shear panel which can resist lateral loading. The behavior of these shear panels depends significantly on screw spacing, board thickness, cold-formed steel thickness, aspect ratio, strength of fasteners and sheathing type. In order to determine the effect of these factors as well as to receive various experimental results to be used in the new Turkish Earthquake Code which is planned to be published and renewed in 2016, a significant sum of experiments have been conducted for different panel configurations in Structures Laboratory of Bogaziçi University. In addition to experimental studies, analytical model representing one of the particular shear panels has been developed in SAP2000 software. After obtaining a good match between experimental and analytical results, a new model was constructed representing a typical one-story structure located in Turkey, and the performance of this structure was examined against the design earthquake specified in Turkish Earthquake Code 2007. The ultimate goal here was not only to obtain a satisfactory match between experimental and analytical results but also to prove that constructing cold-formed steel framed shear panels in seismic-prone regions such as Turkey is safe and sound.

ÖZET

HAFİF ÇELİK KAYMA PANELLERİNİN DENEYSEL VE ANALİTİK ÇALIŞMASI

Bu tezin kapsamında, hafif çelik çerçeveli kayma panellerinin yanal yük taşıma kapasitesi deneysel ve analitik olarak incelenmiştir. Farklı yapılara sahip kayma panellerinin deneysel ve analitik sonuçları arasındaki benzerliği tespit edebilmek için bu paneller üzerinde deneysel çalışmalar gerçekleştirilmiştir. Konut yapımı uygulamalarında hafif çelik çerçeve, mimari ve tasarım amacına bağlı olarak çoğunlukla alçı malzemeli kaplama, yönlendirilmiş yonga levha (OSB) veya kontroplak (plywood) ile kaplanır. Hafif çelik çerçeve yukarıda bahsedilen kaplamalardan biri ile kaplandığı zaman bir bütün olarak kayma paneline benzer bir biçimde, yanal yüklemeye karşı direnç göstermeye başlar. Bu kayma panellerinin davranışı önemli ölçüde vida aralığına, kaplama kalınlığına, hafif çelik kalınlığına, en-boy oranına, vidaların dayanımına ve kaplamanın türüne bağlıdır. Bu faktörlerin etkisini incelemek amacıyla ve 2016 yılında yenilenip basılması beklenen yeni Türk Deprem Yönetmeliğinde kullanılmak maksadıyla, Boğaziçi Üniversitesi Yapı Laboratuvarında farklı paneller üzerinde önemli sayıda deneysel çalışma gerçekleştirilmiştir. Buna ek olarak, deneylerde kullanılan panellerden biri dikkate alınarak, SAP2000 bilgisayar programı aracılığıyla bu paneli temsil eden bir analitik model geliştirilmiştir. Bu panel üzerinde geliştirilen analitik model ile deneysel sonuçlar arasında başarılı bir benzerlik elde edildikten sonra, Türkiye'de konumlanmıs olan tipik bir katlı bir yapıyı temsil eden yeni bir model de üretilmiştir. Bu yapının performansı, 2007 Türk Deprem Yönetmeliği içeriğinde sunulan tasarım depremi altında kontrol edilmiştir. Burada yapılan çalişmanın amacı yalnızca deneysel ve analitik çalışma sonuçları arasında bir benzerlik elde etmek degil, aynı zamanda Türkiye gibi depreme yatkın ülkelerde hafif çelik çerçeveli kayma panellerinin inşa edilmesinin güvenli ve sağlıklı olduğunu göstermektir.

TABLE OF CONTENTS

ACKNOWLEDGEMENTS iv
ABSTRACT v
ÖZET vi
LIST OF FIGURES x
LIST OF TABLES xviii
LIST OF SYMBOLS xx
LIST OF ACRONYMS/ABBREVIATIONS xxv
1. INTRODUCTION 1
1.1. General 1
1.2. An Introduction to Cold-Formed Steel Structures 2
1.2.1. Cold-Formed Steel Applications 2
1.2.2. Construction Procedure of Cold-Formed Steel Framed Structures 3
1.2.3. Load Carrying Methodology of CFS Framed Structures 5
1.3. Literature Review 6
1.3.1. Existing Codes, Standards and Software 7
1.3.2. Review on the Research 8
1.4. Scope and Objective of the Thesis 24
1.5. Thesis Overview 25
2. EXPERIMENTAL STUDY ON VARIOUS CFS SHEAR PANELS 27
2.1. Introduction 27
2.2. List of Shear Panels 27
2.3. Reaction Frame and Hydraulic Actuator 28
2.4. Loading Protocol 29
2.4.1. Test Method A (Sequential-Phased Displacement Procedure) . . 29
2.4.2. Test Method B (ISO 16670 Protocol) 30
2.4.3. Test Method C (CUREE Basic Loading Protocol) 32
2.5. Experiments of Shear Panels Sheathed with Board Type 1 33
2.5.1. Panel Properties 34
2.5.2. Results 34

2.5.3. Photos of Experiment 38
2.6. Experiments of Shear Panels Sheathed with Board Type 2 (0.9 mm Steel Thickness) 40
2.6.1. Panel Properties 41
2.6.2. Results 41
2.6.3. Photos of Experiment 42
2.7. Experiments of Shear Panels Sheathed with Board Type 2 (1.5 mm Steel Thickness) 43
2.7.1. Panel Properties 44
2.7.2. Results 44
2.7.3. Photos of Experiment 45
2.8. Observations on the Experiments 46
3. ANALYTICAL STUDY OF BARE FRAME AND SHEAR PANEL 52
3.1. Introduction 52
3.2. Procedure behind Analytical Approach 52
3.3. Experimental Result of the Bare Frame 53
3.4. Analytical Study of the Bare Frame 55
3.5. Analytical Study of the CFS Shear Panel Sheathed with Board Type 1 60
4. ANALYTICAL STUDY OF A TYPICAL ONE-STORY CFS STRUCTURE 63
4.1. Introduction 63
4.2. Properties of the Structure 63
4.3. Model of the Structure 64
4.4. Modification of the Nonlinear Links Due to the Effect of Gravity Load 67
4.5. Pushover Analysis of the Structure 69
4.6. Force-Based Performance Assessment of the CFS Structure 73
4.7. Displacement-Based Performance Assessment of the CFS Structure . . 76
5. CONCLUSIONS AND FUTURE WORKS 82
5.1. List of Conclusions 82
5.2. List of Future Works 84
APPENDIX A: PANEL TECHNICAL DRAWINGS (AUTOCAD) 85
A.1. L1001 Shear Panels 85
A.2. L1002 Shear Panels 86

APPENDIX B: PHOTOS OF DAMAGES OBSERVED AT CERTAIN TOP DISPLACEMENT LEVELS 87
REFERENCES 96

LIST OF FIGURES

Figure 1.1. Cold-Formed Steel Framing. 2

Figure 1.2. Completed CFS Structure. 2

Figure 1.3. Roll-Forming Machine. 3

Figure 1.4. Geometry and Component of Typical Sheathed CFS Shear Wall (Fiorino *et al.*, 2009 [19]). 4

Figure 1.5. Construction of a CFS Building Erecting on Raft-Type Foundation. 5

Figure 1.6. Typical Hold-Down Anchor. 5

Figure 1.7. Experimental Setup of Screw Connections (Fiorino *et al.*, (2007) [16]). 15

Figure 1.8. "LD Nomographs" (Fiorino *et al.*, 2009 [19]). 17

Figure 1.9. "NS Nomographs" (Fiorino *et al.*, 2009 [19]). 18

Figure 1.10. "OC Nomographs" (Fiorino *et al.*, 2009 [19]). 20

Figure 1.11. Deformation Component of a Sheathed CFS Shear Wall (Fiorino *et al.*, 2009 [19]). 21

Figure 2.1. Reaction Frame and Hydraulic Actuator. 28

Figure 2.2. Loading Protocol-Test Method A. 30

Figure 2.3. Loading Protocol-Test Method B. 31

Figure 2.4. Loading Protocol-Test Method C. 33

Figure 2.5. CFS Shear Panels Sheathed with Board Type 1. 34

Figure 2.6. Force-Displacement Hysteresis Curves of Specimens Sheathed with Board Type 1. 35

Figure 2.7. Force-Displacement Bilinear Relationship of Specimens Sheathed with Board Type 1. 36

Figure 2.8. Damages Observed on Shear Panels Sheathed with Board Type 1 at a Top Displacement of 50 mm. 39

Figure 2.9. Damages Observed on Shear Panels Sheathed with Board Type 1 at a Top Displacement of 100 mm. 39

Figure 2.10. Damages Observed on Shear Panels Sheathed with Board Type 1 at a Top Displacement of 112.5 mm. 40

Figure 2.11. CFS Shear Panels Sheathed with Board Type 2 (0.9 mm Steel Thickness). 40

Figure 2.12. Force-Displacement Hysteresis Curves of Shear Panels Sheathed with Board Type 2 (0.9 mm Steel Thickness). 42

Figure 2.13. Damages Observed on Shear Panels Sheathed with Board Type 2 (0.9 mm Steel Thickness) at a Top Displacement of 35 mm. 42

Figure 2.14. Damages Observed on Shear Panels Sheathed with Board Type 2 (0.9 mm Steel Thickness) at a Top Displacement of 50 mm. 42

Figure 2.15. Damages Observed on Shear Panels Sheathed with Board Type 2 (0.9 mm Steel Thickness) at a Top Displacement of 100 mm. . . . 43

Figure 2.16. CFS Shear Panels Sheathed with Board Type 2 (1.5 mm Steel Thickness). 43

Figure 2.17. Force-Displacement Hysteresis Curves of Shear Panels Sheathed with Board Type 2 (1.5 mm Steel Thickness). 45

Figure 2.18. Damages Observed on Shear Panels Sheathed with Board Type 2 (1.5 mm Steel Thickness) at a Top Displacement of 35 mm. 45

Figure 2.19. Damages Observed on Shear Panels Sheathed with Board Type 2 (1.5 mm Steel Thickness) at a Top Displacement of 50 mm. 45

Figure 2.20. Damages Observed on Shear Panels Sheathed with Board Type 2 (1.5 mm Steel Thickness) at a Top Displacement of 100 mm. . . . 46

Figure 2.21. Location of Strain Gauges on a Particular Shear Panel. 48

Figure 2.22. A Closer View of the Placement of Strain Gauges. 48

Figure 2.23. Force-Strain Curve of Shear Panel Sheathed with Board Type 1. . 49

Figure 2.24. Force-Strain Curve of Shear Panel Sheathed with Board Type 2 (0.9 mm Steel Thickness). 50

Figure 2.25. Force-Strain Curve of Shear Panel Sheathed with Board Type 2 (1.5 mm Steel Thickness). 50

Figure 3.1. Deformed Shape of the Bare Frame in Lateral Displacement Level of 100 mm. 53

Figure 3.2. Deformed Shape of the Bare Frame in Lateral Displacement Level of 200 mm. 54

Figure 3.3. Force-Displacement Hysteresis Curve of Bare Frame System. . . . 54

Figure 3.4. Richard and Abbott Model (Fiorino *et al.*, 2009 [19]). 56

Figure 3.5. Load-Displacement Curves of Sheathing Fasteners (Fiorino *et al.*, 2009 [19]). 56

Figure 3.6. Richard-Abbott Model vs. Analytical Screw Model. 58

Figure 3.7. Analytical Model of the Bare Frame. 59

Figure 3.8. Comparison between Analytical and Experimental Curves of Bare Frame. 59

Figure 3.9. Analytical Model of the CFS Shear Panel with Board Type 1. . . 61

Figure 3.10. Nonlinear Links Representing Sheathing-to-Frame Fasteners and Frame Fasteners. 61

Figure 3.11. Comparison between Analytical and Experimental Curves of CFS Shear Panel Sheathed with Board Type 1. 62

Figure 4.1. Top View of the Structure. 63

Figure 4.2. Model of the CFS Structure Including Distribution of Gravity Loads. 67

Figure 4.3. Shear Panel with Gravity Load and Analytical Model of the Shear Panel. 68

Figure 4.4. Modified Screw Model Including the Effect of Gravity Loading. . . 68

Figure 4.5. Comparison between Analytical and Experimental Pushover Curves under the Effect of Gravity Loading for CFS Shear Panels Sheathed with Board Type 1. 69

Figure 4.6. Deformed Shape of the Structure after Pushover Analysis. 70

Figure 4.7. Pushover Curve of the Structure. 70

Figure 4.8. Initial Stiffness of the Nonlinear Link Elements. 72

Figure 4.9. Period Calculation via Structural Modal Analysis. 73

Figure 4.10. Spectrum Coefficient (TEC 2007 [3]). 74

Figure 4.11. Amplitude of the First Mode Shape in x-direction. 77

Figure 4.12. Pushover Curve of the Structure. 78

Figure 4.13. Modal Capacity Curve of the Structure. 78

Figure 4.14. Performance Point of the Structure. 80

Figure A.1. L 1001 Panel Technical Drawing. 85

Figure A.2. L 1002 Panel Technical Drawing. 86

Figure B.1. Damages Observed on Shear Panels Sheathed with Board Type 1 at a Top Displacement of 10 mm. 87

Figure B.2. Damages Observed on Shear Panels Sheathed with Board Type 1 at a Top Displacement of 15 mm. 87

Figure B.3. Damages Observed on Shear Panels Sheathed with Board Type 1 at a Top Displacement of 20 mm. 87

Figure B.4. Damages Observed on Shear Panels Sheathed with Board Type 1 at a Top Displacement of 35 mm. 88

Figure B.5. Damages Observed on Shear Panels Sheathed with Board Type 1 at a Top Displacement of 50 mm. 88

Figure B.6. Damages Observed on Shear Panels Sheathed with Board Type 1 at a Top Displacement of 62.5 mm. 88

Figure B.7. Damages Observed on Shear Panels Sheathed with Board Type 1 at a Top Displacement of 75 mm. 89

Figure B.8. Damages Observed on Shear Panels Sheathed with Board Type 1 at a Top Displacement of 87.5 mm. 89

Figure B.9. Damages Observed on Shear Panels Sheathed with Board Type 1 at a Top Displacement of 100 mm. 89

Figure B.10. Damages Observed on Shear Panels Sheathed with Board Type 1 at a Top Displacement of 112.5 mm. 90

Figure B.11. Damages Observed on Shear Panels Sheathed with Board Type 2 (0.9 mm Steel Thickness) at a Top Displacement of 10 mm. 90

Figure B.12. Damages Observed on Shear Panels Sheathed with Board Type 2 (0.9 mm Steel Thickness) at a Top Displacement of 15 mm. 91

Figure B.13. Damages Observed on Shear Panels Sheathed with Board Type 2 (0.9 mm Steel Thickness) at a Top Displacement of 20 mm. 91

Figure B.14. Damages Observed on Shear Panels Sheathed with Board Type 2 (0.9 mm Steel Thickness) at a Top Displacement of 35 mm. 91

Figure B.15. Damages Observed on Shear Panels Sheathed with Board Type 2 (0.9 mm Steel Thickness) at a Top Displacement of 50 mm. 91

Figure B.16. Damages Observed on Shear Panels Sheathed with Board Type 2 (0.9 mm Steel Thickness) at a Top Displacement of 62.5 mm. . . . 92

Figure B.17. Damages Observed on Shear Panels Sheathed with Board Type 2 (0.9 mm Steel Thickness) at a Top Displacement of 75 mm. 92

Figure B.18. Damages Observed on Shear Panels Sheathed with Board Type 2 (0.9 mm Steel Thickness) at a Top Displacement of 87.5 mm. . . . 92

Figure B.19. Damages Observed on Shear Panels Sheathed with Board Type 2 (0.9 mm Steel Thickness) at a Top Displacement of 100 mm. . . . 93

Figure B.20. Damages Observed on Shear Panels Sheathed with Board Type 2 (1.5 mm Steel Thickness) at a Top Displacement of 10 mm. 93

Figure B.21. Damages Observed on Shear Panels Sheathed with Board Type 2 (1.5 mm Steel Thickness) at a Top Displacement of 15 mm. 93

Figure B.22. Damages Observed on Shear Panels Sheathed with Board Type 2 (1.5 mm Steel Thickness) at a Top Displacement of 20 mm. 94

Figure B.23. Damages Observed on Shear Panels Sheathed with Board Type 2 (1.5 mm Steel Thickness) at a Top Displacement of 35 mm. 94

Figure B.24. Damages Observed on Shear Panels Sheathed with Board Type 2 (1.5 mm Steel Thickness) at a Top Displacement of 50 mm. 94

Figure B.25. Damages Observed on Shear Panels Sheathed with Board Type 2 (1.5 mm Steel Thickness) at a Top Displacement of 62.5 mm. . . . 94

Figure B.26. Damages Observed on Shear Panels Sheathed with Board Type 2 (1.5 mm Steel Thickness) at a Top Displacement of 75 mm. 95

Figure B.27. Damages Observed on Shear Panels Sheathed with Board Type 2 (1.5 mm Steel Thickness) at a Top Displacement of 87.5 mm. . . . 95

Figure B.28. Damages Observed on Shear Panels Sheathed with Board Type 2 (1.5 mm Steel Thickness) at a Top Displacement of 100 mm. . . . 95

LIST OF TABLES

Table 2.1. List of Shear Panels. 28

Table 2.2. Loading Protocol-Test Method A. 29

Table 2.3. Loading Protocol-Test Method B. 31

Table 2.4. Loading Protocol-Test Method C. 32

Table 2.5. Properties of CFS Shear Panels Sheathed with Board Type 1. . . . 34

Table 2.6. Detailed Calculations of Specimens Sheathed with Board Type 1. . 38

Table 2.7. Results of CFS Shear Panels Sheathed with Board Type 1. 38

Table 2.8. Properties of Shear Panels Sheathed with Board Type 2 (0.9 mm Steel Thickness). 41

Table 2.9. Results of Shear Panels Sheathed with Board Type 2 (0.9 mm Steel Thickness). 41

Table 2.10. Properties of Shear Panels Sheathed with Board Type 2 (1.5 mm Steel Thickness). 44

Table 2.11. Results of Shear Panels Sheathed with Board Type 2 (1.5 mm Steel Thickness). 44

Table 2.12. Summary of Average Experimental Results. 46

Table 2.13. Calculation of Yield Strain of St 37 Grade Steel. 49

Table 2.14. Variation of Maximum Strain vs. Shear Strength. 50

Table 3.1. Wall Parameters (Fiorino *et al.*, 2009 [19]). 57

Table 3.2. Sheathing Fasteners Parameters (Fiorino *et al.*, 2009 [19]). 57

Table 3.3. Mechanical Properties of Board Type 1 and CFS. 60

Table 4.1. Parameters of the Structure. 64

Table 4.2. Calculation of Gravity Loads Resulting from Walls and Floor. . . . 65

Table 4.3. Calculation of Gravity Loads Distributed along the Slab. 66

Table 4.4. Weight of the Structure. 71

Table 4.5. Period Calculation via Structural Modal Analysis. 72

Table 4.6. Spectrum Characteristic Periods (TEC 2007 [3]). 74

Table 4.7. Effective Ground Acceleration Coefficient, A_0 (TEC 2007 [3]). . . . 75

Table 4.8. Building Importance Factor, I_0 (TEC 2007 [3]). 75

Table 4.9. Calculation of Essential Parameters for Modal Capacity Curve. . . 78

Table 4.10. Calculation of Essential Parameters for Performance Point. 80

LIST OF SYMBOLS

a	Shear anchor spacing
A	Gross cross-sectional area of an end stud
A_o	Efficient ground acceleration coefficient
A_{str}	Area of the plan view of the structure
A_{sp}	Area of one shear panel (for 2400/1200 mm dimensions)
$A(T1)$	Spectral acceleration coefficient for the first mode of vibration
$a_1^{(i)}$	Modal acceleration defined for the first mode of vibration in x-direction for ith step of the pushover analysis
a_{y1}	Equivalent yield acceleration related to the first mode
b	Width of the sheathing panel
C_{R1}	Ratio of spectral displacement
D	Dead Load
c	Spacing of the studs
d	Generic displacement
d_a	Overturning deformation
d_b	Bending deformation
d_c	Seismic displacement capacity
d_D	Seismic displacement demand
D_{max}	Referance deformation
d_f	Sheathing fasteners deformation
$d_1^{(i)}$	Modal displacement defined for the first mode of vibration in x-direction for ith step of the pushover analysis
d_s	Sheathing panels shear deformation
d_u	Ultimate displacement
d_Y	Yield displacement
E	Modulus of elasticity of the panel material
e	Edge distance
F_e	Conventional elastic load
f_H	Function representing wall shear strength

f_K	Function representing wall shear stiffness
F_p	Conventional peak load
F_0	Intersection between the hardening line and the δ=0 axis
f_{sad}	Function of spectral acceleration
f_u	Function representing wall ultimate displacement
ft	Nominal tensile strength
F_u	Conventional ultimate load
f_y	Function representing wall yield displacement
fy	Nominal yield strength
G	Shear modulus of elasticity of the panel material
g	Gravitational acceleration
G'	Secant shear modulus
h	Height of wall
H_c	Seismic strength capacity
H_D	Seismic action demand
$\bar{H}_c$	Wall shear strength per wall unit length
$\bar{H}_{c,f}$	Resistance of sheathing fasteners
$\bar{H}_{c,s}$	Resistance of studs
$\bar{H}_{c,ha}$	Resistance of hold-down anchors
$\bar{H}_{c,sa}$	Resistance of shear anchors
$\bar{H}_{c,s,k}$	Shear characteristic strength of studs per wall unit length
$\bar{H}_{c,ha,k}$	Shear characteristic strength of hold-down anchors per wall unit length
$\bar{H}_{c,sa,k}$	Shear characteristic strength of shear anchors per wall unit length
$\bar{H}_{c,f,d}$	Shear design strength of sheathing fasteners per wall unit length
I_0	Building importance factor
K_a	Axial stiffness of the hold-down device
K	Wall shear stiffness
K_e	Elastic stiffness

k_h	Slope of the straight line asymptote of the assumed Richard-Abbott's curve
k_o	Initial stiffness of experimental curve
l	Length of the shear panel
m	Mass of the structure
M_{x1}	Effective mass defined for the first mode of vibration in x-direction
M_1	Modal mass defined for the first mode of vibration
N_{ha}	Tension axial strength of hold-down anchor
N_s	The stud compression axial strength
n_{sp}	Number of shear panels (for 2400/1200 mm dimensions)
n_l	Number of shear panels for length of l
P_{peak}	Maximum lateral force
p	Interior spacing
P_{yield}	Yield force
Q	Live Load
R_r	Resistance
R	Strength reduction factor
$R_a(T_1)$	Seismic load reduction factor for the first mode of vibration
R_μ	Strength reduction factor based on ductility
R_Ω	Strength reduction factor based on over-strength
R_{y1}	Strength reduction factor pertinent to the first mode
s	Sheathing-to-frame fastener exterior spacing
S_a	Spectral acceleration
S_{ae1}	Elastic spectral acceleration
$S(T)$	Spectrum coefficient
S_{del}	Linear elastic spectral displacement
S_{dil}	Nonlinear inelastic spectral displacement
T_A, T_B	Spectrum characteristic periods
$T_1^{(1)}$	First period regarding the first (dominant) mode
T	Period of vibration
t	Stud thickness

t_p	Thickness of the panel sheathing
V_{paek}	Shear strength
V_{sa}	Shear strength of the shear anchor
$V_{x1}^{(i)}$	Base shear for the first mode of vibration in x-direction for ith step of the pushover analysis
U	Ultimate limit point
$u_{xN1}^{(i)}$	Top displacement for the first mode of vibration in x-direction for ith step of the pushover analysis
V_{alum}	Volume of alum
V_t	Total base shear
W	Seismic weight
W_{alum}	Weight of alum
W_{dist}	Weight as a distributed gravity load on the slab
W_{ext}	Gravity load acting on the exterior shear panels
$W_{d,t,e}$	Weight as a distributed gravity load on the top track of the exterior shear panels
$W_{d,t,i}$	Weight as a distributed gravity load on the top track of the interior shear panels
W_{floor}	Weight of the floor
W_i	Weight of any kind
W_{live}	Weight as a distributed load on the slabs resulting from live load
W_{roof}	Weight as a distributed load on the slabs resulting from roof
W_{snow}	Weight as a distributed load on the slabs resulting from snow
W_{str}	Weight of the structure
W_{walls}	Weight of the walls
Y	Yield limit point

ξ	Viscous damping ratio
$\gamma_{ov,ha}$	Overstrength factor of hold-down anchors
$\gamma_{ov,s}$	Overstrength factor of studs

$\gamma_{ov,sa}$	Overstrength factor of shear anchors
γ_{alum}	Weight per unit volume of alum
ϕ_{xN1}	Amplitude of the first mode shape at the top of the building (N^{th} story)
Δ_e	Elastic displacement
Δ_m	Ultimate displacement
Δ_{peak}	Peak displacement corresponding to the maximum lateral force
Γ_{x1}	Participation factor defined for the first mode of vibration in x-direction
Δ_u	Ultimate displacement corresponding to the failure of the shear panel
Δ_y	Yield displacement
μ	Cyclic ductility ratio
α	Shape parameter
δ_e	Conventional elastic displacement
δ_p	Conventional peak displacement
δ_u	Conventional ultimate displacement
ϕ	Hold-down anchor diameter

LIST OF ACRONYMS/ABBREVIATIONS

AISI	American Iron and Steel Institute
ASTM	American Society for Testing and Materials
CFS	Cold-Formed Steel
CUREE	Consortium of Universities for Research in Earthquake Engineering
EEEP	Equal Energy Elastic-Plastic
FME	First Major Event
GWB	Gypsum Wallboard
IDA	Incremental Dynamic Analysis
LD	Linear Dynamic
NS	Nonlinear Static
OSB	Oriented Strand Board
PGA_d	Design Value of Peak Ground Acceleration
SAP	Structural Analysis Program
SWP	Shear Wall Panels
TEC	Turkish Earthquake Code

1. INTRODUCTION

1.1. General

Cold-formed steel (CFS) framed structures have been recently used widely throughout the world for low-rise and mid-rise buildings (Figure 1.1 and Figure 1.2). Cold-formed steel started to be considered as an acceptable construction material in the late 1800s in some parts of the USA and Great Britain. However, due to lack of codes and standards relevant to cold-formed steel material, it took time to see cold-formed steel structures widely in the world especially in seismic areas. Nonetheless, research applications were kept alive on this topic and a considerable sum of experiments as well as analytical studies regarding cold-formed steel material and CFS framed systems have been conducted. Consequently, it has been assured that cold-formed steel framed systems can resist lateral loading such as an earthquake excitation and they started to be used in earthquake-prone regions. The main advantages of cold-formed steel systems can be listed as follows:

- Lightweight nature of the material
- Easy practical applications on the site (easy erection)
- Dimensional stability
- Good structural performance
- A good potential to be reused as well as being recycled (environmental issues)

Practical applicability of cold-formed steel framed structures is one of the key factors which make them preferable; thus cost-effectiveness and time-recovery come automatically as further benefits. Time is one of the most significant parameters which mold the future of a construction project; therefore time-recovery should seriously be taken into account while counting the superiority of CFS framed structures.



Figure 1.1. Cold-Formed Steel Framing.



Figure 1.2. Completed CFS Structure.

1.2. An Introduction to Cold-Formed Steel Structures

So as to be capable of understanding the nature of cold-formed steel structures, their components, process of the material production, the ways they are manufactured and assembled in the field as well as their load carrying methodology should be conceived.

1.2.1. Cold-Formed Steel Applications

Cold-formed steel (CFS) fundamentally consists of steel produced and shaped by roll-forming machine or hydraulic pressing machine (Figure 1.3). Practically, roll-

forming machines are more commonly used since they have the capability of producing and shaping the steel in a considerably short time. With today's technological developments, roll-forming machines can produce a really large number of steel sections in a day. Usually, these sections are manufactured in the factory and sent to the field to be assembled there. Since, the sections are sent fully combined and processed, the application at the site purely depends on assembling the sections to each other and constructing an entire building. This provides a really significant time gain on the site. Apart from this, with the technological developments obtained nowadays, roll-formers can be sent to the site and manufacturing can be carried out at the site depending upon the size of the project. This is a very important factor which contributes to cost-effectiveness in terms of transportation as well as labor expenses.



Figure 1.3. Roll-Forming Machine.

1.2.2. Construction Procedure of Cold-Formed Steel Framed Structures

A typical cold-formed steel framed shear wall mainly consists of a frame system connected to sheathing panels with a certain number and spacing of screws which are called sheathing to frame fasteners (Figure 1.4). Since sheathing of the cold-formed steel shear panel provides the system with stiffness and strength, the type of sheathing plays a truly significant role in load-bearing capacity. Mostly, wood-based material or gypsum-based material is picked up as a sheathing type for cold-formed steel framed

systems. Oriented strand board (OSB), plywood, steel sheet or gypsum board can be given as a good variety of examples for sheathing panels. However, in the scope of this thesis, gypsum board is used as the main sheathing in both experimental and analytical study, where N is axial force acting on the end stud / hold-down anchor and V is shear force acting on a shear anchor.

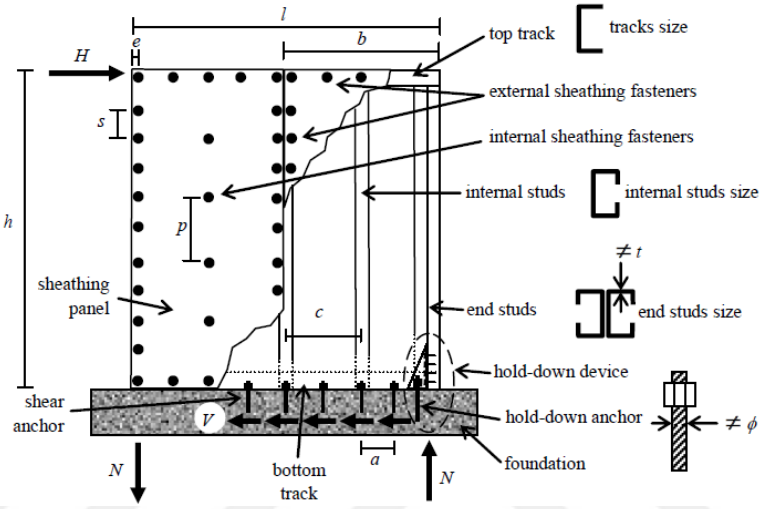

Figure 1.4. Geometry and Component of Typical Sheathed CFS Shear Wall (Fiorino *et al.*, 2009 [19]).

A cold-formed steel shear panel basically involves bottom track and top track, vertical studs, bracing, sheathing to frame fasteners, hold-down anchors, shear anchors and sheathing. Self-drilling or self-tapping screws are mostly used as fasteners connecting the sheathing to the frame. Cold-formed steel sections are generally manufactured with a thickness between 0.50 mm and 2.5 mm. Experimental study of interest in the scope of this thesis includes cold-formed steel sections with a thickness of 0.9 mm and 1.5 mm. C-shaped sections are mainly used as tracks and C-shaped sections with lips are preferred as vertical studs of a cold-formed steel shear panel. For low-rise and mid-rise cold-formed steel framed structures in residential applications, raft-type foundation is mostly preferred (Figure 1.5). Hold-down anchors are assembled in the boundary of the vertical studs with screws to the surface of the vertical studs as shown in Figure 1.6. Later on, they are anchored to the foundation of the structure with anchor bolts.



Figure 1.5. Construction of a CFS Building Erecting on Raft-Type Foundation.



Figure 1.6. Typical Hold-Down Anchor.

1.2.3. Load Carrying Methodology of CFS Framed Structures

Cold-formed steel framed structures involve shear panels as a structural wall, ceiling panels as well as roof panels, floor joists and roof trusses. The primary structural

elements for CFS structures are shear wall panels (SWP), load-bearing shear panels, floor and roof panels. However, in ordinary structural steel construction, the fundamental load-carrying system is composed of columns, beams and cross-bracing. The bare frame system of a CFS structure is attached to each other with a pin connection; therefore there is no lateral stiffness of the frame system. As a result, bracing plays the key role in lateral resistance of a CFS structure and bracing can be supplied with X-bracing, K-bracing, steel cross bracing or full panel bracing with sheathing panel. However, in the scope of this thesis, full panel bracing provided by sheathing panel based on gypsum board is taken into account. Shear wall panels can resist lateral loading whereas load-bearing shear panels can take only gravity loads due to the fact that they do not have structural sheathing. In application of cold-formed steel framed structures, it is basically desired to resist the worst case lateral loading scenario, such as an earthquake excitation, with the existence of CFS shear walls. It is expected to transfer the lateral loads to the shear panel by the roof and floor diaphragms.The ultimate goal here is to transfer the lateral load to the foundation. In the first place, lateral load is taken by the top track of the CFS shear wall and transferred to the sheathing panel via screws connecting the board to the frame system. As a result, it can easily be concluded that screw spacing takes up a very important role in assuring the satisfactory structural performance of a CFS structure. The lateral load applying as a shear is planned to be transferred to the bottom track and then to the foundation by hold-down anchors. Ultimately, it is planned to make the frame system work in axial direction in which they perform the best. To sum up the main picture relevant to the load carrying mechanism of a CFS framed structure, overturning moment and shear forces are two main forces acting on a CFS shear wall when a lateral load is applied to the top track (Figure 1.4). Overturning moment is compensated with a force couple in the hold-down anchors located in the boundaries of the bottom track whereas in-plane shear forces are resisted by the sheathing and sheathing to frame fasteners.

1.3. Literature Review

This chapter covers the review on the studies valid in the literature relevant to cold-formed steel structures. The main reason for this chapter is not only to demon-

strate the contribution of the previous research about CFS structures to the study of concern in the scope of this thesis, but also to receive some additional information to enlighten the prospective future work. Mainly, experimental and analytical research conducted on cold-formed steel structures have been covered in order to enlighten the studies in the scope of this thesis. The experimental research basically consist of tests conducted on different shear panel configurations in order to see the impact of dissimilar components of shear panels to the overall behavior. Besides, analytical research are composed of developing analytical models to represent the real experimental behavior of shear panels to be used for structural analysis.

1.3.1. Existing Codes, Standards and Software

American Iron and Steel Institute (AISI) [1] proposes various editions of "Specifications for the Design of Cold-Formed Steel Structural Members". As a result of this guidance, the interest in cold-formed steel structures increased tremendously in the last century. AISI S213-07/S1-09(2012) refers to "North American Standard for Cold-Formed Steel Framing-Lateral Design" and it has been used as a key source for parts of this thesis during conducting the experiments, receiving the results and calculations.

Standard Test Methods for Cyclic (Reversed) Load Test for Shear Resistance of Vertical Elements of the Lateral Force Resisting Systems for Buildings (ASTM E2126-11) [2] proposes a general overview for the tests to be conducted on cold-formed steel elements including information about specimens, test setup, test procedure and loading protocol as well as calculations. Experimental study in the content of this thesis have been carried out via utilizing the information specified in this code.

Turkish Earthquake Code (TEC) 2007 [3] involves specifications for structures to be built in disaster areas. In section 7 of this seismic code, rules for performance assessment of existing structures have been proposed and they have been utilized in the scope of the analytical study of this thesis. Apart from this, design spectrum proposed in this code which represents the design earthquake for design purposes and performance evaluation has also been used.

SAP2000 software [4] is a structural analysis program developed by CSi Computers and Structures incorporating. This program has been used during the analytical study in the scope of this study while obtaining the pushover curve of the shear panel and the structure.

1.3.2. Review on the Research

Miller and Pekoz (1993) [5] proposed a study which includes tests of cold-formed steel shear walls under axial loading. The entire wall and vertical studs were tested and the results were compared to the ones given by AISI's [1] "cold-formed 1986" predictions. The results obtained under axial loading were observed and the behavior of the entire wall and vertical members were checked. Accordingly, some recommendations regarding the effective length coefficients were presented. Finally, the investigations were done on the issues about eccentricity and test results relevant to this topic were also presented.

Miller and Pekoz (1994) [6] conducted experiments of gypsum wall board sheathed cold-formed steel frames under axial loading. Failure modes of the frames during these experiments were investigated and they were compared to the AISI's [1] predictions. The predictions about failure modes proposed in AISI do not match with the test results. Besides that, effect of stud spacing on the capacity under axial loading was also observed and it was concluded that the capacity decreases while the spacing of the studs is increasing. This capacity reduction is also predicted well by the specifications of AISI.

Serette and Ogunfunmi (1996) [7] proposed a research including test results of cold-formed steel specimens with gypsum wallboard, flat strap X-bracing and combination of these two systems. The ultimate intention beneath this study was to investigate the contribution of board type to the level of shear force that can be resisted by the system. During the experiments, it was basically observed that gypsum wallboard sheathing provided the specimens with significant shear strength. Yet, in spite of the significant shear strength resulting from gypsum wallboard, a certain portion of the

shear force acting on the system is recommended to be resisted by the gypsum wallboard in order to compensate for the probable opening of holes which tend to occur around the screw shank.

Serette *et al.*, (1997) [8] conducted a research in order to investigate the impact of board type and screw spacing on the behavior of shear panels. In this study, experiments under monotonic lateral loading were conducted on three different panel configurations including sheathed walls, shear walls with diagonal bracing and cross-braced walls. In order to observe the effect of screw spacing on the behavior, spacing was kept constant along the intermediate members (12 in.) and decreased along the panel edges (between 6 in. and 2 in.). In the stage where the effect of board type was investigated, the strength characteristics of plywood sheathed panels and OSB sheathed panels turned out to be analogous; however shear strength results presented relatively lower values for shear panels sheathed with gypsum wallboard (GWB). During the observations on screw connections, plywood sheathed shear panels had a relatively stronger connection than that of OSB sheathed panels. Besides, the higher contribution to the total strength of the gypsum wallboard sheathed shear panels is observed at the edge of the panels. The comparison between small-scale connection test results and full-scale wall panel test results revealed that small-scale testing can propose an efficient method for estimating the behavior which arises from full-scale wall components. Finally, the stage where the influence of spacing of the screws is examined explicitly showed that shear strength as a part of the shear panel had a significant increase as the spacing of the screws decreased.

Fülöp and Dubina (2004-Part1) [9] and Fülöp and Dubina (2004-Part2) [10] have conducted an interactive study observing performance of wall-stud cold-formed steel shear panels under monotonic and cyclic loading. First part of this interactive study includes an experimental research about cold-formed steel framed shear walls with different sheathing and configuration. The results have been obtained and compared to each other, with respect to the key performance parameters such as ductility and strength, in order to see the influence of differences in terms of configurations on the behavior. Besides that, also the characteristic features of type of failure were discussed

which were experienced during the experiments. The second part of the study mainly aims to characterize the hysteresis behavior by significant pinching which causes decay in energy dissipation. Basically, it has been observed that cold-formed steel shear panels as a whole system possess considerable resistance in terms of lateral load bearing capacity as well as rigidity against shear demand and they resist lateral loading with a systematic load transfer methodology. During the experiments, it can be explicitly observed that failure firstly formed at the bottom track close to the anchor bolt region. Accordingly, it can be deduced that strengthening the system in the boundary regions may play a truly significant role via imposing additional rigidity to the system. This detail relevant to strengthening the boundary regions on the bottom track plays a significant role since it can prevent the system from a prospective brittle type of failure which may arise from large sway of the CFS shear panel.

Rogers *et al.*, (2004) [11] conducted an experimental study on a hundred and six cold-formed steel framed specimens and their ultimate goal was to investigate the effect of the dimensions of the panels on the behavior. OSB and plywood sheathed shear panels were tested under monotonic and cyclic lateral loading. Shear panels which were tested during the experiments had a standard height of 2.44 m; however the width of the shear panels had three different variations as 0.61 m, 1.22 m and 2.44 m, respectively. Shear panels which had a width of 1.22 m and 2.44 m possessed a similar behavior, but the shear panels which had a width of 0.61 m manifested a very large lateral deformation after they reached the peak lateral load strength.

Corte *et al.*, (2006) [12] have conducted a study in order to investigate seismic behavior of sheathed cold-formed steel structures. This study is mainly composed of two successive phases which contribute to two separate articles, one representing the numerical study whereas the other illustrating an experimental study. In the first place, numerical study is demonstrated here. It has been controversial for a certain period of time to understand whether cold-formed steel structures can be widely used in earthquake-prone regions instead of other ordinary reinforced concrete or masonry structure or not. To answer this question, observations must be done to see if they have adequate ductility and sufficient strength. One of the main downsides of cold-formed

steel framed structures is their relatively small ductility. Yet, due to comparatively lightweight nature of cold-formed steel framed structures, the design procedure can be carried out with low values of the strength reduction factor which stands for cost-effectiveness. Apart from cost-effectiveness, as a consequence of lightness of this kind of structures, the design procedure can be completed within the elastic field of response. As a result of a certain sum of studies completed so far relevant to cold-formed steel framed structures, it has already been proven that this sort of structures can resist the design earthquake which is represented by ten percent probability of exceedance in fifty years within many seismic codes. However, in order to answer the question whether this kind of structures can survive severe earthquakes which are described with two percent probability of exceedance in fifty years, this research has been performed. In order to receive an explanatory resolution to examine cold-formed steel framed structures for surviving violent earthquakes, reliable mathematical models of the hysteresis behavior of shear panels manufactured of light-gage cold-formed framed construction have been developed. Since sheathed cold-formed steel framed shear panels are characterized by strong nonlinearity of the lateral load-displacement relationship as well as by strong pinching of hysteresis loops, the mathematical models representing the hysteresis behavior of the shear panels plays a really significant role in estimation of seismic behavior of this kind of structures. Demand in terms of deformation has been assessed making use of a sufficiently large database of earthquake ground motions. Based on research conducted by researchers so far, it can be inferred that over-strength is a fundamental source of cold-formed steel framed structures to survive earthquake excitation. Over-strength and ductility should instead be used in order to assure that the structure can survive very rare earthquakes which represent the violent earthquakes in seismic codes. In this way, taking full benefit from the lightness of cold-formed steel framed structures, they could adequately meet the "collapse prevention" performance level, also suffering less damage than ordinary structures. In the scope of this research, a prototype structure has been developed by means of the mathematical model representing the hysteresis behavior of the cold-formed steel framed structure and it has been schematized as a single degree of freedom system, by placing the mass at the first story. A certain number of earthquake ground motions have been selected and scaled according to the design value of the peak ground acceleration (PGA_d) and the struc-

ture has been analyzed under the effect of these ground motions. As a conclusion from this research, it has been comprehended that the examined sheathed stud wall which has been designed statically for remaining elastic under design earthquake performed adequately and inter-story drift demand turned out to be smaller than the damage-limiting value obtained from experimental tests. Taking everything into account in the scope of this study, it can explicitly be inferred that performance of the observed structure against collapse is acceptable which may motivate the change of standard construction practices in earthquake prone regions where the residential building stock for one or two-story family houses is entirely represented by masonry and reinforced concrete structures.

Landolfo *et al.*, (2006) [13] have conducted an experimental study which was also a part of the previous study on behalf of numerical research. In this paper, the results of the experimental investigation on the seismic behavior of cold-formed steel stud shear walls, sheathed with wood-based (oriented strand board (OSB)), and gypsum-based (GWB) panels is presented. Two nominally identical prototypes were constructed to carry out the tests. The tests were applied with respect to monotonic loading conditions and cyclic loading conditions for the two specimens, respectively. The results of the tests revealed that all the components of this structural system can be designed according to capacity design criteria, imposing collapse in the sheathing connections of the vertical shear wall, without significant increase of the cost. All the tests conducted on different specimens agreed with the fact that failure of these specimens is most likely to be oriented among sheathing-to-wall framing connections failure. In the monotonic test, the collapse mechanism followed an invariant trend as the lateral displacement increased, whereas some modifications were experienced in cyclic tests after the peak value of the lateral load was exceeded. The reason for this was because of the local buckling experienced according to the failure type of the cyclic tests. The lateral load vs. displacement responses were practically the same before the peak strength is obtained; however considerable variations were experienced after the post-peak branch. No considerable deformation is observed at the oriented strand board (OSB) and sheathing-to-floor framing connections in both monotonic and cyclic tests.

Xu and Martinez (2006) [14] presented a research involving an interactive study between experiments under monotonic loading and development of an analytical model representing the experimental behavior. As a common conclusion drawn from OSB sheathed panels, plywood sheathed panels and gypsum wall board sheathed panels, the failure was observed to initiate at the sheathing-to-frame connections (i.e. sheathing panel failure). The failure of the sheathing was clearly seen as a result of the rupture of the sheathing-to-frame connections. During some of the experiments, it was even seen that sheathing fully severed from the cold-formed steel frame. In case of the small thickness of the vertical studs, the failure initiated as a result of buckling occurred along these studs even though they were supported by the sheathing. Besides, the failure as a result of this buckling was also observed in cases where the cold-formed steel frame is sheathed on the both sides. The reason for this can be explained by the fact that compression on the studs increased as a consequence of application of the sheathing on both sides although that increases the lateral stiffness of the panel. In addition to this experimental study, an iterative analytical method was also developed which represents the relationship between lateral load strength and top displacement of the shear panel. This method covers the material properties, thickness, board and stud dimensions, spacing of the studs, geometric arrangement of connection elements and frame members. This study accumulates experimental results obtained from various screw configurations of full-scale shear walls so as to calibrate complex spring elements. Thus, the behavior of the shear panels can be analytically represented. In cases where sufficient sum of experimental data are not readily received, this analytical approach can provide practical estimation of the behavior in a short time.

Fiorino *et al.*, (2006) [15] observed the lateral response of sheathed cold-formed shear walls with an analytical approach and presented this study. The main objective of this study was to propose an analytical approach to estimate the relationship of shear force vs. top displacement of the cold-formed steel framed shear panels under lateral loading such as an earthquake excitation. While developing this analytical model, previous experimental studies on screw connections have been taken as a reliable resource (it should be noted that in the scope of this thesis, this analytical model has also been utilized as a reference for a starting point in the analytical study section).

The comparison of analytical results with available wall test results shows that the proposed approach can provide good prediction of both strength and wall deflection. However, the prediction of strength turned out to be more accurate than the prediction of wall deflection. All of the conclusions which were drawn as a result of this study must be considered as preliminary outcomes for actual implementation since there is a limited sum of experimental data on connections and walls.

Fiorino *et al.*, (2007) [16] have conducted experimental tests on typical screw connections for cold-formed steel housing and in accordance with these experiments, an analytical research has also been implemented. Experimental test results on the screw connections between sheathing and cold-formed steel framing have been presented. The ultimate goal of this study is to see the effect of type of panels on the behavior, to illustrate the influence of the orientation of the sheathing, to demonstrate the impact of distance of loaded edge, to see the contribution of differences in cyclic loading protocols as well as to evaluate the effect of the loading pace. Experiments have been conducted on cold-formed steel frame sheathed with oriented strand board (OSB) panels and gypsum wallboard (GWB) with a certain thickness (Figure 1.7). The properties of the specimens have been listed below:

- Hot dipped galvanized (zinc coated) steel (nominal yield strength fy=350 MPa; nominal tensile strength ft=420 MPa)
- Two different sheathing types: 9 mm thick type 3 oriented strand board (OSB) and 12.5 mm thick standard gypsum wallboard (GWB)
- Two different types of screws: 4.2*25 mm (diameter*length) flat head self-drilling screws for OSB sheathing, and 3.5*25 mm bugle head self-drilling screws for GWB

The specimens have been tested under monotonic and cyclic loading separately to investigate the influence. Consequently, no considerable deformation has been observed on the connections which stick floor sheathing to the framing during neither monotonic tests nor cyclic tests. The effect of sheathing type has turned out to expose the most significant contribution to the behavior among all of the factors. It has been seen that OSB sheathings have larger strength and absorbed energy than GWB panels,

whereas GWB sheathings showed larger stiffness and ductility than OSB sheathings. There was no sign to imply failure or considerable deformation of shear and tension anchors. Besides that, it has been observed that it is not likely to draw a certain conclusion which manifests the effect of loading rate. Furthermore, cyclic test results manifested a significant strength reduction as well as energy absorption for both OSB and GWB sheathings. Taking everything into account, making use of the experimental results conducted on screw connections while estimating the lateral response of steel frame/panel shear walls turned out to be acceptable due to the satisfactory overlap between analytical and experimental curves.

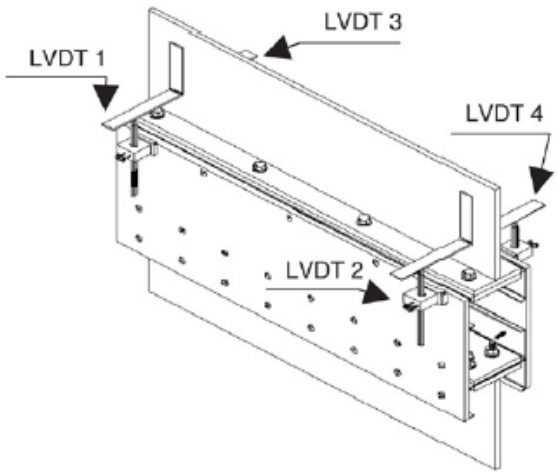

Figure 1.7. Experimental Setup of Screw Connections (Fiorino *et al.*, (2007) [16]).

Simsir and Jain (2008) [17] proposed a study about nonlinear analysis of woodframe shear walls. The ultimate objectives of this research were to develop a structural analytical model to estimate the response of woodframe wall, to include wall and ceiling returns in the structural model and to utilize the past experimental data and analytical tools which became valid in the last decade for modelling the connectors and walls. As test specimens, they used two walls which had two window openings. These specimens were sheathed with stucco on one side and gypsum wallboard on the opposite side. The researchers constructed the analytical model in finite element program SAP2000 [4] and they used shell elements to represent the stucco as well as drywall. Vertical studs were pinned at the top and bottom to represent the shear deformation which was also presented in Figure 1.11. Besides, nonlinear link elements were used to model the

load-displacement relationship of the fasteners. As a result of this modelling process, they came up with an effective analytical model which has the capability of representing the actual experimental behavior of test specimens. In addition to these applications, they also checked the stress concentration on shell elements defined in SAP2000 to identify the magnitudes of principal stresses and locations of the cracks.

Dubina (2008) [18] conducted a research on behavior and performance of cold-formed steel-framed houses under seismic action. In this research, it is basically intended to accumulate the results acquired from the previous studies and combine them on a full scale global structure. As a matter of fact, a two-story real world structure is constructed via making use of the previous experimental and numerical data which were obtained. During the construction, vibration analyses were performed at different stages of construction and a significant effect of the construction process on the dynamic characteristics of the structure was seen. After the application of oriented strand board (OSB) shear panels, the rigidity of the structure considerably increased, even the weak direction of the structure changed.

Fiorino *et al.*, (2009) [19] and Landolfo *et al.*, (2010) [20] proposed a research based on two successive phases of a study. This research eventually ends up with acquisition of design nomographs to be used for design purposes of cold-formed steel structures. Cold-formed steel housing has started to be used widely throughout the world including seismic prone regions such as Japan. The fundamental advantages of cold-formed steel systems can be listed as lightweight structure of the material, practical applicability in the field, dimensional stability, high structural performance, a good potential to be reused as well as being recycled. All of these advantageous aspects have been assured by considerable sum of experimental studies. According to the experimental studies completed so far, a satisfactory ductile seismic behavior of a CFS shear wall is accomplished when the sheathing-to-stud fasteners failure is generated. In order to ensure this structural performance, a design procedure to pick up the correct shear wall components (studs, sheathing panels, sheathing-to-frame connections and frame-to-foundation anchors) has been presented in this article. Three different phases have been adopted for this design procedure:

- Defining the wall geometry (height of wall h, spacing of the studs c) and some other parameters of the wall components: Sheathing (type, thickness, orientation), frame (steel grade, stud size, track size), sheathing to frame connections (type, interior spacing p, edge distance e), type of hold-down anchors and shear anchors
- Evaluation of the sheathing-to-frame fastener exterior spacing (s)
- Evaluation of other parameters (stud thickness t, hold-down anchor diameter ϕ, shear anchor spacing a)

All these phases have been discussed in this article excluding first phase because it is basically dependent on architectural and technological considerations as well as design for vertical loads. Determination of s is purely based on seismic analysis. This seismic analysis includes linear dynamic seismic procedure and nonlinear static seismic procedure (Figure 1.8 and Figure 1.9).

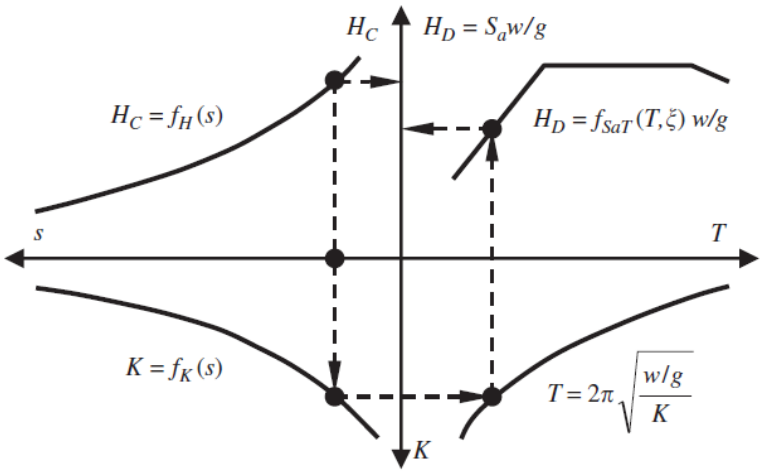

Figure 1.8. "LD Nomographs" (Fiorino *et al.*, 2009 [19]).

In LD seismic procedure, a force-based design approach is used. Besides, inelastic behavior and the structural over-strength are considered by seismic force modification factors. LD seismic procedure can simply be summarized utilizing the nomograph demonstrated above. Depending on s, stiffness (k) and Resistance (R_r) can be obtained. According to the stiffness computed, period (T) is found out knowing the seismic action

demand from Equation 1.1.

$$H_D = S_a . \frac{W}{g} \tag{1.1}$$

Spectral acceleration (S_a) can be acquired as a function of T and viscous damping ratio (ξ). That means seismic strength capacity can be compared to seismic action demand and this procedure is followed till performance and monetary considerations are satisfied (Equation 1.2).

$$H_C \geq H_D \tag{1.2}$$

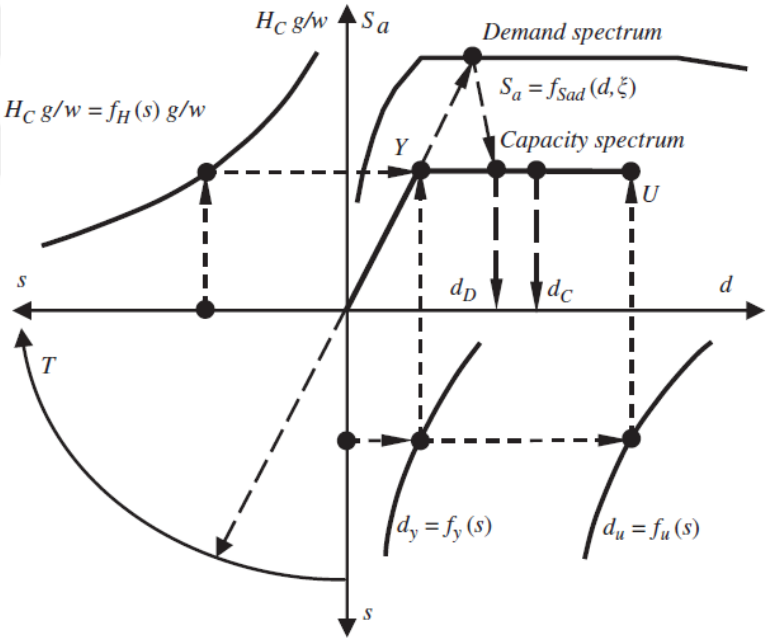

Figure 1.9. "NS Nomographs" (Fiorino *et al.*, 2009 [19]).

In NS seismic procedure, a displacement-based approach is used. The inelastic behavior and the structural over-strength are directly considered in this procedure. NS seismic procedure can simply be summarized utilizing the nomograph demonstrated above. Comparison of seismic displacement capacity to that of demand can readily be performed taking advantage of this nomograph (acceleration-displacement spectrum) which involves both demand and capacity spectra. Spectral acceleration can

be obtained as a function of spectral acceleration (f_{Sad}) with respect to the generic displacement (d) and viscous damping ratio (ξ).

$$S_a = f_{Sad}\,(d, \xi) \tag{1.3}$$

Capacity spectrum is sketched as an elastic-plastic curve which is determined by the yield (Y) and ultimate (U) limit points:

$$Y(d_y; H_C.\frac{g}{w}), U(d_u; H_C.\frac{g}{w}) \tag{1.4}$$

The yield displacement (d_y) and ultimate displacement (d_u) can be obtained as a function of the exterior spacing (s).

$$d_y = f_y\,(s)\,, d_u = f_u\,(s) \tag{1.5}$$

Utilizing the LD Nomograph, for certain values of exterior spacing (s), involvement of the computable functions f_{Sad}, f_H, f_y and fu as well as fixed quantities of seismic weight (w) and viscous damping ratio (ξ) will provide the design procedure with calculating both seismic demand (d_D) and capacity (d_C). That means seismic displacement capacity can be compared to seismic displacement demand and this procedure is followed till performance and monetary considerations are satisfied.

$$d_C \geq d_D \tag{1.6}$$

After determining sheathing-to-frame fastener exterior spacing (s), the evaluation of stud thickness (t), hold-down anchor diameter (ϕ) and shear anchor spacing (a) should be determined to complete the design.

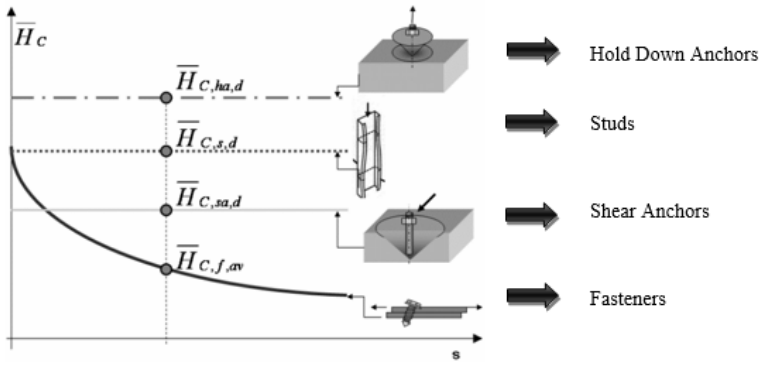

Figure 1.10. "OC Nomographs" (Fiorino *et al.*, 2009 [19]).

The nomograph presented above represents the wall shear strength per wall unit length ($\bar{H}_C$) corresponding to the resistance of sheathing fasteners ($\bar{H}_{C,f}$), studs ($\bar{H}_{C,s}$), hold-down anchors ($\bar{H}_{C,ha}$) and shear anchors ($\bar{H}_{C,sa}$). They are represented together as function of the exterior spacing (s).

$$\bar{\mathrm{H}}_{\mathrm{C,f}} = \mathrm{f_H}\,(\mathrm{s})\,, \bar{\mathrm{H}}_{\mathrm{C,s}} = \frac{\mathrm{H_{C,s}}}{\mathrm{l}} = \frac{\mathrm{N_s}}{\mathrm{h}}, \bar{\mathrm{H}}_{\mathrm{C,ha}} = \frac{\mathrm{H_{C,ha}}}{\mathrm{l}} = \frac{\mathrm{N_{ha}}}{\mathrm{h}}, \bar{\mathrm{H}}_{\mathrm{C,sa}} = \mathrm{V_{sa}}\left(\frac{1}{\mathrm{a}} + \frac{1}{\mathrm{l}}\right) \quad (1.7)$$

where N_s is the stud compression axial strength, N_{ha} is tension axial strength of hold-down anchor and V_{sa} is shear strength of the shear anchor.

$$\frac{\bar{\mathrm{H}}_{\mathrm{C,s,k}}}{\gamma_{\mathrm{ov,s}}} \geq \bar{\mathrm{H}}_{\mathrm{C,f,d}}, \frac{\bar{\mathrm{H}}_{\mathrm{C,ha,k}}}{\gamma_{\mathrm{ov,ha}}} \geq \bar{\mathrm{H}}_{\mathrm{C,f,d}}, \frac{\bar{\mathrm{H}}_{\mathrm{C,sa,k}}}{\gamma_{\mathrm{ov,sa}}} \geq \bar{\mathrm{H}}_{\mathrm{C,f,d}} \quad (1.8)$$

where $\bar{H}_{C,s,k}$ is shear characteristic strength of studs per wall unit length, $\bar{H}_{C,ha,k}$ is shear characteristic strength of hold-down anchors per wall unit length, $\bar{H}_{C,sa,k}$ is shear characteristic strength of shear anchors per wall unit length, $\bar{H}_{C,f,d}$ is shear design strength of sheathing fasteners per wall unit length, $\gamma_{ov,s}$ is overstrength factor of studs, $\gamma_{ov,ha}$ is overstrength factor of hold-down anchors and $\gamma_{ov,sa}$ is overstrength factor of shear anchors.

Making use of the OC Nomograph presented in Figure 1.10, for certain values of exterior spacing (s), the design parameters of interest (t, a and ϕ) can be obtained till the "Capacity Design" criteria are satisfied.

The applications done so far in this article demonstrated the design of CFS housing requires definition of the wall shear response (f_k, f_H, f_y and f_u) as a function of exterior spacing (s). In LD seismic analysis, only wall stiffness f_k and strength f_H must be defined, whereas in application of NS procedure, the definition of the elastic-plastic curve through the functions f_H, f_y and f_u needs the acquisition of whole force (H) - displacement (d) response curve of the wall. For this purpose, a specific analytical-numerical method has been developed by the authors allowing the prediction of the whole curve in terms of f_k, f_H, f_y and f_u. According to this methodology, the lateral displacement of a sheathed CFS shear wall can be obtained by adding four different deformation contributions as shown in Equation 1.9.

$$d = d_f + d_s + d_b + d_a \tag{1.9}$$

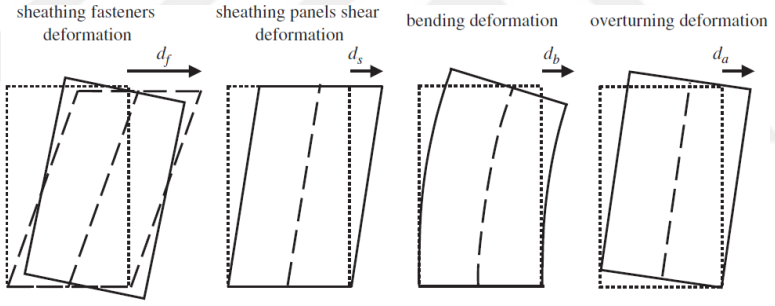

Figure 1.11. Deformation Component of a Sheathed CFS Shear Wall (Fiorino *et al.*, 2009 [19]).

The conclusions show that the best performance of CFS housing systems is obtained when sheathing-to-stud screw failure is generated. To assure this, a design procedure has been proposed in this article. After determining the shear wall geometry and technological components, the exterior spacing of the fasteners (s) is determined utilizing LD seismic analysis or NS seismic analysis. Finally all other parameters such as studs, shear and hold-down anchors are obtained. As a final step, an analytical model used to define the wall strength curves is presented.

Rogers *et al.*, (2010) [21] conducted a research on experiments of typical weld

and screw-connected single-story diagonal strap braced cold-formed steel frame configurations. The connection of diagonal strap is divided into two options by changing the width of the straps (between 4:1 and 1:1). Furthermore, different aspect ratios for the straps were also tested. Strength reduction factors represent the inelastic behavior of cold-formed steel structures and they are also used during the design process. These strength reduction factors which were acquired from the experiments were compared to the ones that are proposed by AISI S213 [1]. There was an overlap between results of experiments and values proposed by AISI S213 for the specimens possessing a width of 2:1 or smaller. However, for the specimens which have 4:1 aspect ratio, the experimental strength reduction factors did not match with the ones proposed by AISI S213. Therefore, it can be concluded that AISI S213 cannot make a good prediction for 4:1 aspect ratio.

Schafer *et al.*, (2010) [22] proposed a study about computational modeling of cold-formed steel. The ultimate objective in this research was to see the effect of choice of element and mesh type during modeling process. Finite element analyses have been carried out using the developed computational model. Besides, a wide emphasis was also put on elastic buckling and nonlinear collapse analysis. It has been eventually concluded that the greatest impact on the behavior of cold-formed steel members has turned out to be resulting from mesh type. Computational modeling which was composed of coarse meshes turned out to estimate global and distortional buckling modes well however it could not catch the local buckling modes accurately enough. Yet, mesh densities defined by medium and fine types could adequately represent global, local and distortional buckling modes.

Fiorino *et al.*, (2012) [23] presented an article about seismic analysis of sheathing-braced cold-formed steel structures. In this study, the results of a wide range of nonlinear dynamic analyses performed on one-story cold-formed framed buildings are presented. Coming from the fundamental background related to cold-formed steel structures, if cold-formed steel (CFS) structures are designed with respect to the "sheathing-design" methodology which imposes prevention of brittle type of failure, the overall behavior of the structure is mainly affected by the response of sheathing-to-frame fas-

teners which is characterized by strong nonlinearity of the lateral load-displacement relationship as well as by strong pinching of hysteresis loops. Parameters such as type of sheathing panel, wall dimensions, screw spacing, seismic weight and soil type have been taken into account with a certain number of specific shear panel configurations. Dynamic analyses have been carried out by means of incremental dynamic analysis (IDA) on various one-story cold-formed steel framed buildings via applying an ad hoc model of the hysteresis response of the sheathed cold-formed shear panels. Ultimately, it was planned to come up with a design nomograph to be used in order to design single degree of freedom sheathed cold-formed steel framed structures.

Peterman *et al.*, (2014) [24] proposed a paper about hysteretic characterization of cold-formed steel stud-to-sheathing connections. On behalf of this study, various experimental studies have been conducted in order to obtain the characteristic behavior of the connection between cold-formed steel frame and sheathing when in-plane lateral forces are of concern. The contribution of the connection to the energy absorption capacity of shear panels have been stated in this research. Besides, the significance of connections in terms of providing bracing to the studs under gravity loads and out-of-plane loads has also been emphasized in the scope of this paper. The impact of configuration of sheathing, spacing of fasteners, thickness of steel and type of fasteners on the performance of connections has been observed experimentally and it has been deduced that the main controlling factor turned out to be resulting from type of sheathing and thickness of studs. Finally, characterization of the hysteretic behavior of shear walls based on experimental outcomes has been summarized to be used in further analytical studies including the effect of gravity and lateral loading together.

Peterman and Schafer (2014) [25] conducted a study relevant to sheathed cold-formed steel studs under axial and lateral load. The objective of this research was to identify as well as to characterize the behavior of cold-formed steel studs under axial and lateral load. The specimens in the content of this research were sheathed with dissimilar sheathing types including oriented strand board (OSB), gypsum wallboard (GWB) and combination of both. Initially, a certain determined level of axial load is applied to the stud and then lateral load was applied until the failure state occurs.

This kind of configuration yielded axial load, bending, and torsion on the stud. For the studs sheathed on one face included failure modes of torsion and/or fastener pull-through whereas studs sheathed on both faces posed failure modes of torsion, local buckling, fastener pull-through, and bearing especially for gypsum-sheathed studs. It has been concluded that sheathing type takes up an important role in limiting torsion and in determining the response of the members and fasteners. Furthermore, new computational models for estimating the strength in the connection limit states were presented. Eventually, it was observed that a model which was based on the torsional capacity of the fastener-sheathing system, limited by either pull-through or bearing failure modes, supplied the best convergence with limit states acquired from the tests.

1.4. Scope and Objective of the Thesis

The need for new construction methodologies is increasing day by day especially for regions in which construction sector is growing up rapidly. CFS framed systems have been considered as a great solution to satisfy the demand coming from growing construction sector expectations especially because of its time and cost effectiveness. As a result, cold-formed steel construction has started to spread all over the world including North and South America, Great Britain, Germany and so forth. Due to the advantageous sides of cold-formed steel construction such as high strength and ductility, dimensional stability, lightness, environmental benefits, durability, easy erection, time and cost effectiveness, the increasing interest in CFS structures has never decelerated. Especially with the publication of various editions of "Specifications for the Design of Cold-Formed Steel Structural Members" by American Steel and Iron Institute (AISI [1]), the popularity of CFS structures increased significantly.

However, some downsides of cold-formed steel structures such as instability problems arising from large width-to-thickness ratio due to small thickness, vulnerability to global buckling, local buckling and distortional buckling and isolation capability have always kept the researchers erring on the side of caution and conducting further studies to come up with solutions to these facts. In addition to these, the question which also requires an answer is whether cold-formed steel framed structures have enough

structural performance in seismic-prone regions or not. All of these questions and high potential of cold-formed steel structures throughout the world kept the research alive on this topic for many years. Recently, cold-formed steel structures have reached a tremendous accomplishment in terms of the increasing number all over the world.

Turkey is one of the countries which suffers from severe earthquakes. The rapidly growing population and accordingly increasing demand for earthquake resistant structures made cold-formed steel structures popular in Turkey. Various studies were completed upon this topic and still there are ongoing research relevant to CFS structures. In the new Turkish Earthquake Code which is planned to be published and renewed in 2016, a section will be allocated for cold-formed steel structures. In order to be used in this section, various experimental studies have been performed with different panel sheathings all based on gypsum in the Structures Laboratory of Bogaziçi University. A detailed information regarding this experimental study and conclusions which were drawn with respect to the results are provided hereafter within the scope of this thesis. Apart from this, an analytical model representing one of the shear panels involved in the experiments has been developed via making use of SAP2000 software [4]. This model has been improved till acquiring the best fit between experimental results and analytical results. As long as this model works properly, representing the real-time experimental behavior, the investigations and research can be extended successfully. A typical one-story residential structure has been built by utilizing this analytical model of the CFS shear panel, and the performance of this structure was checked according to the Turkish Earthquake Code 2007 [3] in order to assure the reliability of a cold-formed steel structure in seismic-prone regions. Yet, it should be noted that this last study can be extended and developed into different stages. This was just an initial analytical study involving an entire structure in the content of this thesis.

1.5. Thesis Overview

The organization of the thesis is following the subsequent manner. Chapter 1 is involving the introduction part to the thesis. It is composed of some general information regarding the cold-formed steel structures. This chapter also includes literature survey,

thesis statement, content of the thesis and thesis objective. Chapter 2 is composed of the experimental study completed in the Structures Laboratory of Bogaziçi University. A detailed information relevant to the pre and post process of experiments is provided in this chapter. Chapter 3 contains development of an analytical model representing one of the CFS shear panels. Chapter 3 is followed by Chapter 4 which includes analytical performance assessment of a typical one-story structure constructed with the model of one of the cold-formed steel shear panels. Conclusions are drawn in Chapter 5 according to the investigations completed upon the experimental study and analytical study. Chapter 5 is also composed of future works which are likely to be conducted in the future as an extended study following the works completed in the scope of this thesis.

2. EXPERIMENTAL STUDY ON VARIOUS CFS SHEAR PANELS

2.1. Introduction

In Turkish Earthquake Code which is planned to be renewed as well as to be published in 2016, Section 10 will be allocated for "Special Rules for the Design of Load Carrying Systems of Cold-Formed Steel Structures under Earthquake Effect". Shear strength per unit length and strength reduction factors (R) of cold-formed steel shear panels sheathed with variety of boards to be used in Section 10 have been presented hereafter in the scope of this research. Strength reduction factor is obtained as a multiplication of strength reduction factors calculated based on ductility and over-strength. Displacement-controlled cyclic tests have been accomplished three times for each system and average of the results for these three experiments have been used to represent the system (as long as the difference between two successive experimental results does not exceed 10%).

2.2. List of Shear Panels

A considerable sum of experiments have been conducted in the Structures Laboratory of Bogaziçi University including different configurations of shear panels. However, only the tests conducted on shear panels showing the effect of type of sheathing and thickness of steel on the behavior are presented in the scope of this thesis in accordance with the forthcoming analytical study. List of shear panels used during tests is presented as follows (Table 2.1). There are two sheathing types used on the specimens for the tests:

- Board Type 1: White gypsum based sheathing that is used for the construction of partition walls, drywall linings and suspended ceilings
- Board Type 2: Gypsum based exterior sheathing that is used for exterior walls

with its reinforced core against humidity and with special orange fiberglass mats. Felt type fibers as an ingredient are used to improve the performance of this type of sheathing

Table 2.1. List of Shear Panels.

Specimens	Number of Experiments
1. CFS Shear Panel Sheathed with Board Type 1	3
2. CFS Shear Panels Sheathed with Board Type 2 (0.9 mm Steel Thickness)	3
3. CFS Shear Panels Sheathed with Board Type 2 (1.5 mm Steel Thickness)	3

2.3. Reaction Frame and Hydraulic Actuator

The experiments have been completed at Bogaziçi University in Structures Laboratory. Dartec brand hydraulic actuators which have 25 tons of capacity have been used during the experiments. With the contribution of the hydraulic actuator connected transversely to the reaction frame, displacement-controlled loading was applied to the test specimen with the test setup illustrated below (Figure 2.1).



Figure 2.1. Reaction Frame and Hydraulic Actuator.

2.4. Loading Protocol

There are three loading protocols proposed by ASTM E2126-11 [2] (Standard Test Methods for Cyclic (Reversed) Load Test for Shear Resistance of Vertical Elements of the Lateral Force Resisting Systems for Buildings), which are also used by AISI S213-07/S1-09(2012) [1] (North American Standard for Cold-Formed Steel Framing-Lateral Design).

2.4.1. Test Method A (Sequential-Phased Displacement Procedure)

According to this protocol, experiment steps and number of cycles have been demonstrated in the table as well as the figure below (Table 2.2 and Figure 2.2).

Table 2.2. Loading Protocol-Test Method A.

Pattern	Step	Number of Cycles	Amplitude of Primary Cycle, (% FME)
1	1	3	25
-	2	3	50
-	3	3	75
2	4	7	100
-	5	7	125
-	6	7	150
-	7	7	175
-	8	7	200
-	9	7	250
-	10	7	300
-	11	7	350
-	12		Additional increments of 50 (until specimen failure)

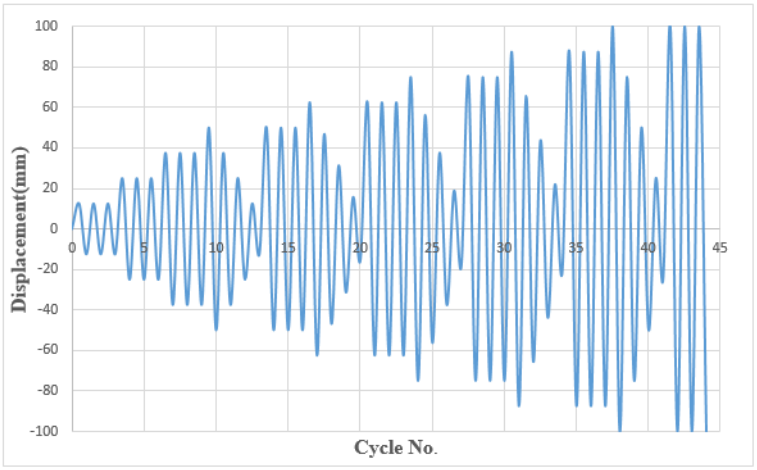

Figure 2.2. Loading Protocol-Test Method A.

The rules below relevant to the protocol have been listed.

- The first displacement pattern consists of three phases, each containing three fully reversing cycles of equal amplitude, at displacements representing 25%, 50%, and 75% of anticipated first major event (FME).
- Each phase is associated with a respective displacement level and contains one initial cycle, three decay cycles, and a number of stabilization cycles.
- For nailed wood-frame walls, three stabilization cycles are sufficient to obtain a stabilized response. The amplitude of each consecutive decay cycle decreases by 25% of the initial displacement.

2.4.2. Test Method B (ISO 16670 Protocol)

According to this protocol, experiment steps and number of cycles have been demonstrated in the table as well as the figure below (Table 2.3 and Figure 2.3).

Table 2.3. Loading Protocol-Test Method B.

Pattern	Step	Number of Cycles	Amplitude, (% Δ_m)
1	1	1	1.25
-	2	1	2.5
-	3	1	5
2	4	1	7.5
-	5	1	10
-	6	3	20
-	7	3	40
-	8	3	60
-	9	3	80
-	10	3	100
-	11	3	Additional increments of 20 (until specimen failure)

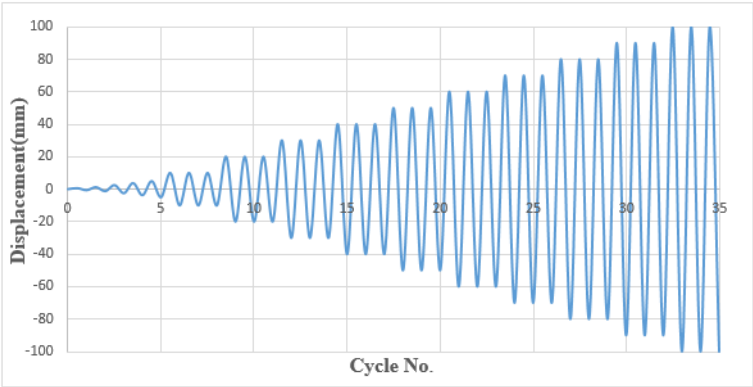

Figure 2.3. Loading Protocol-Test Method B.

The rules below relevant to the protocol have been listed.

- ISO Displacement Schedule-Displacement controlled loading procedure that involves displacement cycles grouped in phases at incrementally increasing displacement levels.

- The ISO loading schedule consists of two displacement patterns and is illustrated in Figure 2.3.
- The first displacement pattern consists of five single fully reversed cycles at displacements of 1.25%, 2.5%, 5%, 7.5%, and 10% of the ultimate displacement Δ_m.
- The second displacement pattern consists of phases, each containing three fully reversed cycles of equal amplitude, at displacements of 20%, 40%, 60%, 80%, 100%, and 120% of the ultimate displacement Δ_m.

2.4.3. Test Method C (CUREE Basic Loading Protocol)

CUREE Basic Loading Protocol has been used during the experiments which were conducted in the scope of this thesis. Experiment steps and number of cycles have been demonstrated in the table as well as the figure below (Table 2.4 and Figure 2.4).

Table 2.4. Loading Protocol-Test Method C.

Pattern	Step	Number of Cycles	Amplitude of Primary Cycle, (% D_{max})
1	1	6	5
2	2	7	7.5
-	3	7	10
3	4	4	20
-	5	4	30
4	6	3	40
-	7	3	70
-	8	3	100
-	9	3	100+50
-	10	3	Additional increments of 50 (until specimen failure)

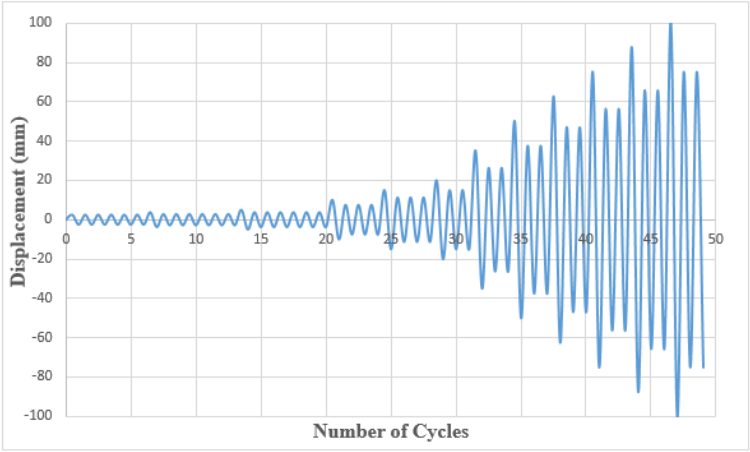

Figure 2.4. Loading Protocol-Test Method C.

The rules below relevant to the protocol have also been applied.

- Each phase of the loading history consists of a primary cycle with amplitude expressed as a fraction (percent) of the reference deformation, D_{max}, and subsequent trailing cycles with amplitude of 75% of the primary one. The reference deformation D_{max} shall be an estimate of the maximum displacement at which the load in a primary cycle has not yet dropped below 0.8 P_{peak}.
- Besides, the value of D_{max} cannot exceed 0.025 times the wall height.
- The rate of displacement shall be between 1.0 and 63.5 mm/s and the cyclic frequency shall range from 0.2 to 0.5 Hz.
- The loading shall follow the corresponding procedure until the applied load diminishes more than 0.2 P_{peak}, that is, until the limit state occurs.

2.5. Experiments of Shear Panels Sheathed with Board Type 1

A typical view of the shear panels which were sheathed with board type 1 can be seen in Figure 2.5.



Figure 2.5. CFS Shear Panels Sheathed with Board Type 1.

2.5.1. Panel Properties

Properties of the panels sheathed with board type 1 are given in the table below (Table 2.5).

Table 2.5. Properties of CFS Shear Panels Sheathed with Board Type 1.

Steel Thickness	0.9 mm
Panel Height	2400 mm
Panel Width	1200 mm
Sheathing Type	Board Type 1
Sheathing Thickness	12.5 mm
Screw Spacing	Edges 20 cm between 30 cm
Screw Type/Strength	4.2*16 flat head screws

2.5.2. Results

Three of the experiments which were conducted for the same panel configuration revealed the Force-Displacement hysteresis curves as shown in Figure 2.6. Consistent

with ASTM 2126 [2], bilinear relationship has been obtained by using the envelope curve acquired from the raw Load-Displacement curves. For this purpose, Equal Energy Elastic-Plastic (EEEP) rule was taken into account. According to this rule, the area underneath the envelope curve and idealized bilinear curve is equal. Taking benefit from this bilinear relationship, design shear strength and ductility quantities have been obtained. Strength reduction factor based on ductility can be calculated for mid-range period structures making use of Equation 2.7.

The raw results from three experiments and acquisition of the bilinear relationship for one experiment have been demonstrated successively as shown in Figure 2.6 and Figure 2.7.

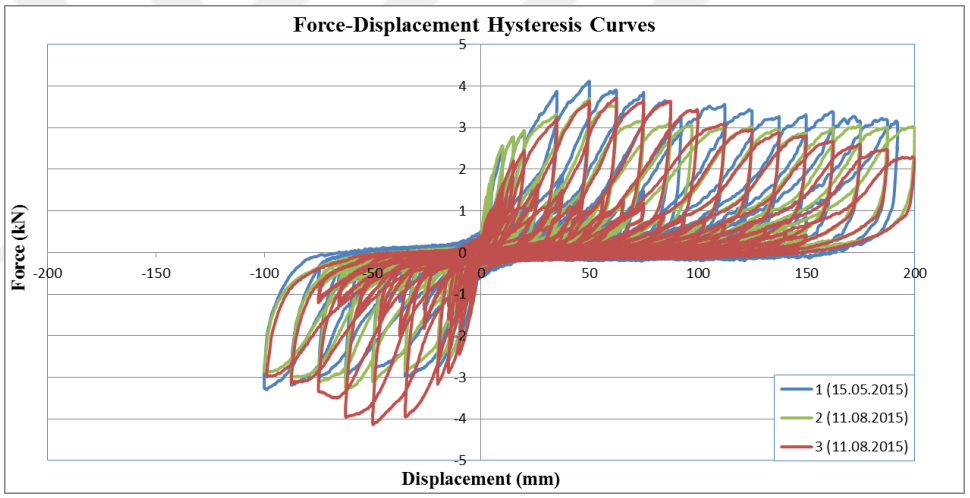

Figure 2.6. Force-Displacement Hysteresis Curves of Specimens Sheathed with Board Type 1.

While completing the calculations for each experiment, average values of the force corresponding to the same level of deformation in each direction have been used to obtain the average envelope curve in Figure 2.7. For each experiment, the values of the shear strength and strength reduction factors have been computed using the average Force-Displacement envelope curve.

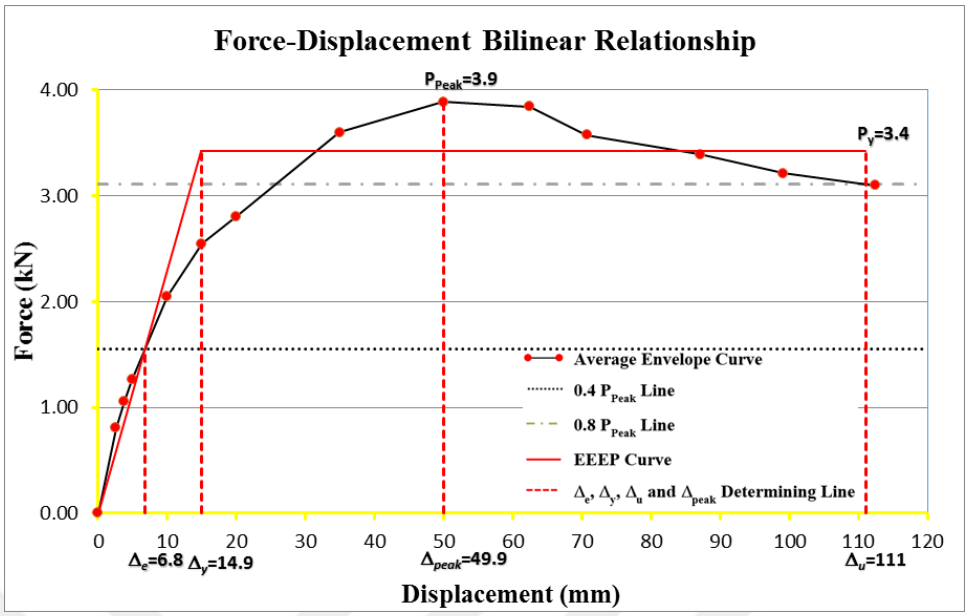

Figure 2.7. Force-Displacement Bilinear Relationship of Specimens Sheathed with Board Type 1.

A detailed calculation which shows acquisition of shear strength of the shear panel, secant shear modulus of the shear panel, cyclic ductility ratio, elastic stiffness of the shear panel, yield force of the shear panel, strength reduction factors based on ductility and over-strength is presented using the following equations. However, this detailed calculation will be presented only for this specific set of experiments. Calculation of other experiments will not be demonstrated in detail, only the summary of results of calculations and hysteresis curves of the experiments will be valid.

$$V_{Peak} = \frac{\mathrm{P_{Peak}}}{l} \tag{2.1}$$

$$\mathrm{G'at0.4P_{peak}} : \frac{0.4\mathrm{P_{Peak}}}{\Delta} * \frac{\mathrm{h}}{l} \tag{2.2}$$

$$\mathrm{G'atP_{peak}} : \frac{\mathrm{P_{Peak}}}{\Delta} * \frac{\mathrm{h}}{l} \tag{2.3}$$

$$\mu = \frac{\Delta \mathrm{u}}{\Delta \mathrm{y}} \tag{2.4}$$

$$K_e = \frac{0.4\mathrm{P_{Peak}}}{\Delta} \tag{2.5}$$

$$\mathrm{P_{Yield}} = (\Delta_u - \sqrt{\Delta \mathrm{u}^2 - \frac{2\mathrm{A}}{\mathrm{Ke}}})Ke \tag{2.6}$$

$$\mathrm{R}_\mu = \sqrt{2\mu - 1} \tag{2.7}$$

$$\mathrm{R}_\Omega = \frac{\mathrm{P_{Peak}}}{\mathrm{P_{Yield}}} \tag{2.8}$$

where V_{Peak} is shear strength of the shear panel, G' is secant shear modulus, h is height of the wall, l is length of the wall, μ is cyclic ductility ratio, P_{Peak} is maximum lateral force, μ is cyclic ductility ratio, Δ_u is ultimate displacement corresponding to the failure of the shear panel, Δ_y is yield displacement, Δ_{peak} is peak displacement corresponding to the maximum lateral force, K_e is elastic stiffness of the shear panel, P_{Yield} is yield force of the shear panel, A is the area underneath the envelope curve, R_μ is strength reduction factor based on ductility and R_Ω is strength reduction factor based on over-strength. It should be noted that only if G' at 0.4 P_{peak} is larger than G' at P_{peak}, EEEP curve as described in ASTM E2126-11 [2] can be generated. Besides, if Δ_u^2 is larger than $\frac{2A}{Ke'}P_y$ cannot be taken equal to 0.85 P_{peak}.

Table 2.6. Detailed Calculations of Specimens Sheathed with Board Type 1.

V_{Peak} (kN/m)	3.2
h (m)	2.4
l (m)	1.2
G' at $0.4P_{peak}$ (kN/m)	459
G' at P_{peak} (kN/m)	156
μ	7.4
K_e (kN/m)	229
A (kNm)	284
P_{yield} (kN)	3.4
Rμ	3.7
R_Ω	1.1

The results of three experiments on shear panels sheathed with board type 1 have been summarized in the tabular form as follows (Table 2.7).

Table 2.7. Results of CFS Shear Panels Sheathed with Board Type 1.

Experiment # (Date)	Shear Strength (kN)	Shear Strength (kN) Difference %	Ductility (μ)	Rμ	Rμ Difference %
1 (15/05/2015)	3.2	<1 %	12.1	4.8	4%
2 (11/08/2015)	3	6%	14.4	5.3	13%
3 (11/08/2015)	3.4	6%	7.4	3.7	24%
Average	3.2	-	11.3	4.6	-

2.5.3. Photos of Experiment

In this section, some representative photos which were taken during the experiment to demonstrate the damage concentration on the panel will be presented. These photos include three different stages representing the level of top displacement for which the panel reaches ultimate load bearing capacity, the panel experiences failure and ultimate lateral displacement capacity of the hydraulic actuator is exceeded (for two-sided cyclic loading). However a broader presentation of damage photos which

includes all the levels of top displacement is provided in Appendix B.



Figure 2.8. Damages Observed on Shear Panels Sheathed with Board Type 1 at a Top Displacement of 50 mm.

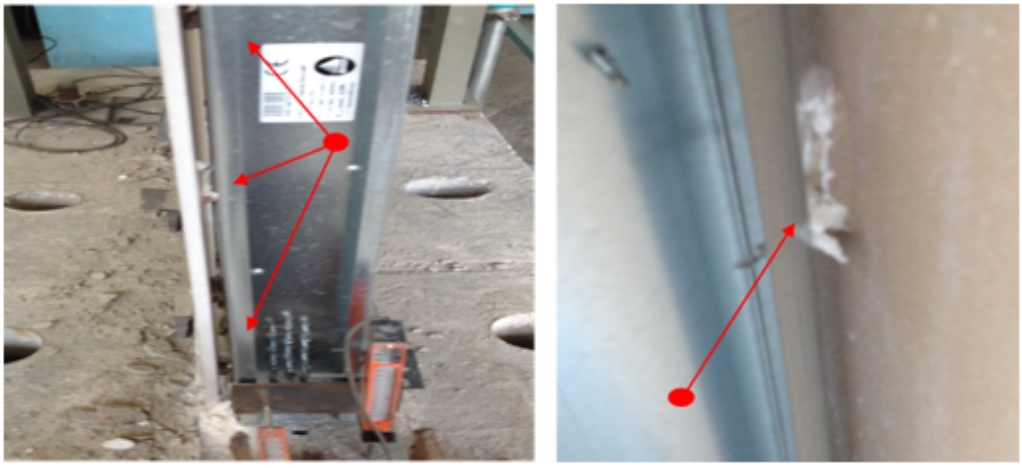

Figure 2.9. Damages Observed on Shear Panels Sheathed with Board Type 1 at a Top Displacement of 100 mm.

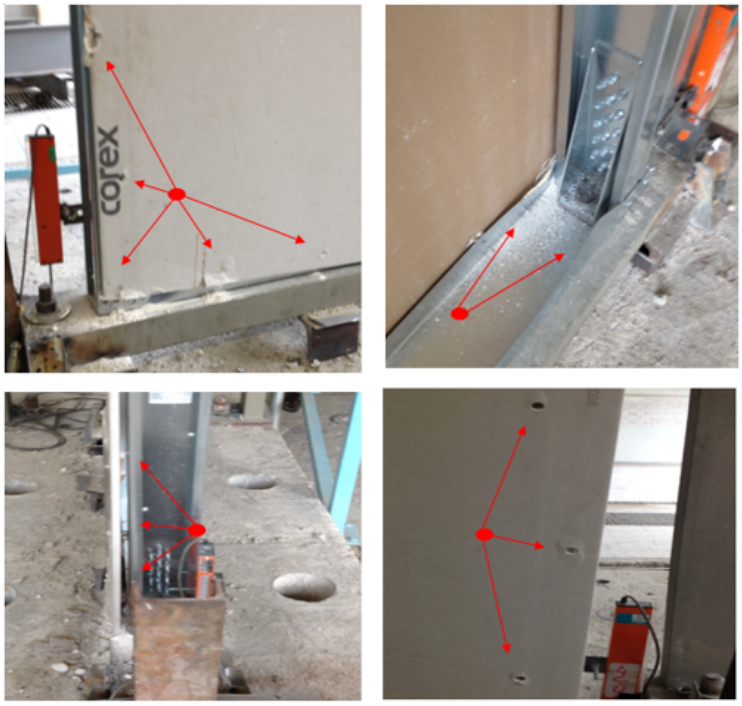

Figure 2.10. Damages Observed on Shear Panels Sheathed with Board Type 1 at a Top Displacement of 112.5 mm.

2.6. Experiments of Shear Panels Sheathed with Board Type 2 (0.9 mm Steel Thickness)

A typical view of the shear panels which were sheathed with board type 2 for 0.9 mm of steel thickness can be seen in Figure 2.11.



Figure 2.11. CFS Shear Panels Sheathed with Board Type 2 (0.9 mm Steel Thickness).

2.6.1. Panel Properties

Properties of the panels sheathed with board type 2 (0.9 mm Steel Thickness) are given in the table below (Table 2.8).

Table 2.8. Properties of Shear Panels Sheathed with Board Type 2 (0.9 mm Steel Thickness).

Steel Thickness	0.9 mm
Panel Height	2400 mm
Panel Width	1200 mm
Sheathing Type	Board Type 2
Sheathing Thickness	12.5 mm
Screw Spacing	Edges 20 cm, between 30 cm
Screw Type/Strength	4.2*16 flat head screws

2.6.2. Results

The results of three experiments of specimens sheathed with Board Type 2 (0.9 mm steel thickness) and hysteresis curves of these experiments have been summarized in the table and figure below (Table 2.9 and Figure 2.12).

Table 2.9. Results of Shear Panels Sheathed with Board Type 2 (0.9 mm Steel Thickness).

Experiment # (Date)	Shear Strength (kN)	Shear Strength (kN) Difference %	Ductility	Rμ	Rμ Difference %
1 (27/04/2015)	5.8	3%	7.4	3.7	<1 %
2 (28/04/2015)	5.9	2%	7.3	3.7	<1 %
3 (29/04/2015)	6.4	7%	7	3.6	2%
Average	6	-	7.2	3.67	-

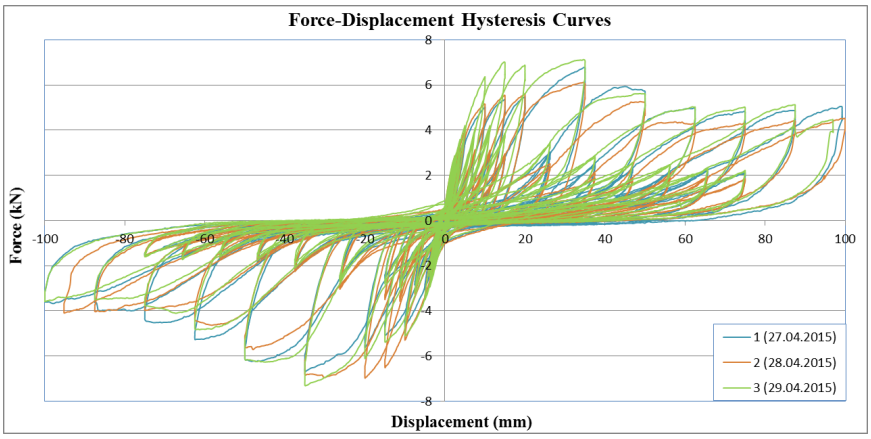

Figure 2.12. Force-Displacement Hysteresis Curves of Shear Panels Sheathed with Board Type 2 (0.9 mm Steel Thickness).

2.6.3. Photos of Experiment

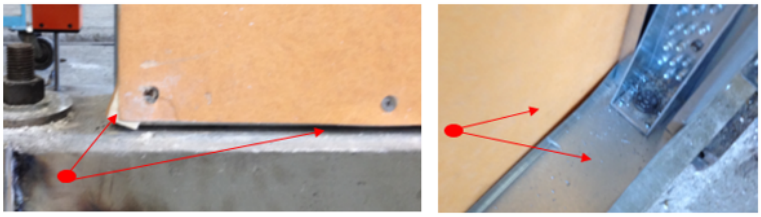

Figure 2.13. Damages Observed on Shear Panels Sheathed with Board Type 2 (0.9 mm Steel Thickness) at a Top Displacement of 35 mm.

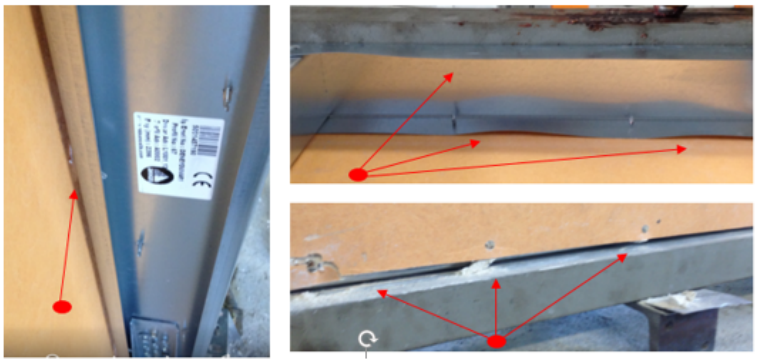

Figure 2.14. Damages Observed on Shear Panels Sheathed with Board Type 2 (0.9 mm Steel Thickness) at a Top Displacement of 50 mm.

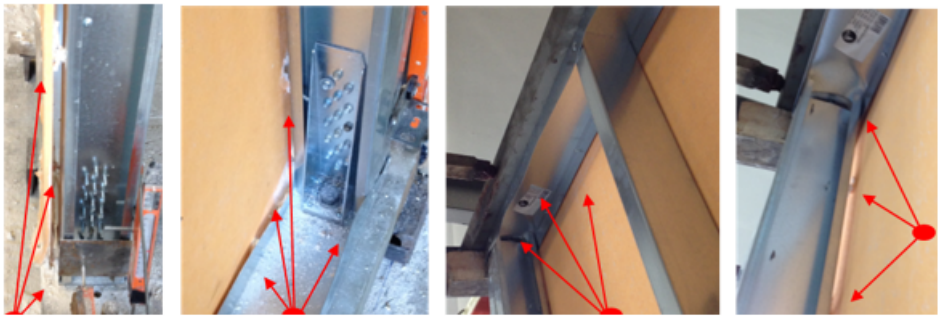

Figure 2.15. Damages Observed on Shear Panels Sheathed with Board Type 2 (0.9 mm Steel Thickness) at a Top Displacement of 100 mm.

2.7. Experiments of Shear Panels Sheathed with Board Type 2 (1.5 mm Steel Thickness)

A typical view of the shear panels which were sheathed with board type 2 for 1.5 mm of steel thickness can be seen in Figure 2.16.



Figure 2.16. CFS Shear Panels Sheathed with Board Type 2 (1.5 mm Steel Thickness).

2.7.1. Panel Properties

Properties of the panels sheathed with board type 2 (1.5 mm steel thickness) are given in the table below (Table 2.10).

Table 2.10. Properties of Shear Panels Sheathed with Board Type 2 (1.5 mm Steel Thickness).

Steel Thickness	1.5 mm
Panel Height	2400 mm
Panel Width	1200 mm
Sheathing Type	Board Type 2
Sheathing Thickness	12.5 mm
Screw Spacing	Edges 20 cm, between 30 cm
Screw Type/Strength	4.2*16 flat head screws

2.7.2. Results

The results of three experiments of specimens sheathed with board type 2 (1.5 mm steel thickness) and hysteresis curves of these experiments have been summarized in the table and figure below (Table 2.11 and Figure 2.17).

Table 2.11. Results of Shear Panels Sheathed with Board Type 2 (1.5 mm Steel Thickness).

Experiment # (Date)	Shear Strength (kN)	Shear Strength (kN) Difference %	Ductility (μ)	Rμ	Rμ Difference %
1 (05/05/2015)	7.2	3%	7.8	3.8	<1 %
2 (06/05/2015)	7.2	3%	9.2	4.2	10%
3 (07/05/2015)	7.8	5%	6.5	3.5	9%
Average	7.4	-	7.83	3.83	-

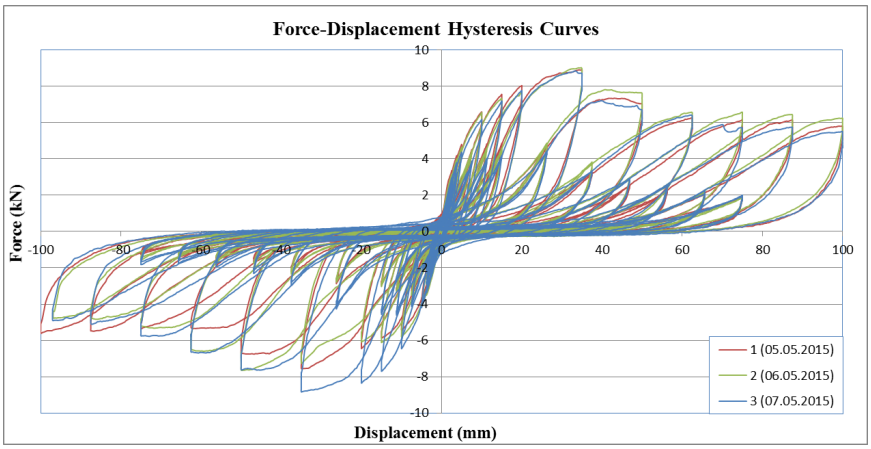

Figure 2.17. Force-Displacement Hysteresis Curves of Shear Panels Sheathed with Board Type 2 (1.5 mm Steel Thickness).

2.7.3. Photos of Experiment

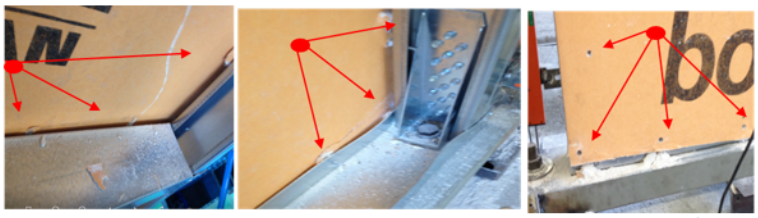

Figure 2.18. Damages Observed on Shear Panels Sheathed with Board Type 2 (1.5 mm Steel Thickness) at a Top Displacement of 35 mm.



Figure 2.19. Damages Observed on Shear Panels Sheathed with Board Type 2 (1.5 mm Steel Thickness) at a Top Displacement of 50 mm.

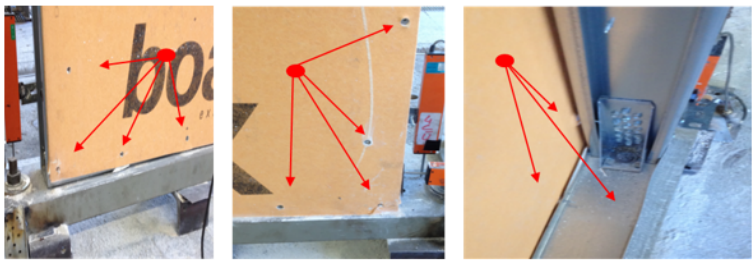

Figure 2.20. Damages Observed on Shear Panels Sheathed with Board Type 2 (1.5 mm Steel Thickness) at a Top Displacement of 100 mm.

2.8. Observations on the Experiments

Average shear strength per unit length and strength reduction factors which were calculated as a result of experiments conducted in the content of this chapter, are demonstrated in the table below (Table 2.12).

Table 2.12. Summary of Average Experimental Results.

Experiment	Shear Strength (kN)	R_μ	R_Ω	Strength Reduction Factor (R)
1. CFS Shear Panels Sheathed with Board Type 1	3.2	4.6	1.1	5.1
2. CFS Shear Panels with Board Type 2 (0.9 mm Steel Thickness)	6	3.7	1.1	4.1
3. CFS Shear Panels Sheathed with Board Type 2 (1.5 mm Steel Thickness)	7.4	3.8	1.1	4.2

Based on the results presented in the previous section and investigations during the experiments, following observations can be listed:

- When the results of all experiments were observed, the fundamental contribution to the performance of specimens is coming from high level of ductility as well as energy absorption capacity.
- The main factor which provides all of the specimens with high ductility is the screws which supply connectivity between the board and cold-formed frame system. These screws managed to open a path alongside the board and compensated

the demand coming from lateral loading via energy absorption capacity.

- These screws kept moving along the paths they created and accordingly, the connection between the board and cold-formed steel frame remained sound under relatively large values of the lateral force. This behavior can be considered as another contribution to the energy absorption capacity of the specimens sheathed with different configurations and types of gypsum wallboard (GWB).
- The comparison between shear panels sheathed with board type 1 and board type 2 revealed that specimens sheathed with Board Type 2 illustrated a considerably stiffer behavior possessing higher load bearing capacity; however, they showed slightly smaller ductility and energy absorption capacity which is quite predictable.
- This stiffer behavior was also proven visually by the particles ruptured from the board. Mainly, stiffer behavior of board type 2 can be explained by the fact that board type 2 sheathings were strengthened by felt type fibers as an ingredient. These fibers located inside the gypsum provided higher strength to board type 2 sheathings and accordingly they possessed higher load bearing capacity and rigidity.
- When the results of the experiments conducted on shear panels sheathed with board type 2 possessing 1.5 mm steel thickness are compared to the results of experiments of shear panels sheathed with board type 2 having 0.9 mm steel thickness, it can be concluded that the former has a larger load carrying capacity as well as ductility. This comparison explicitly demonstrates the positive impact of the steel thickness on performance of the shear panels.
- It can be clearly deduced that the connection between the board and cold-formed steel frame remained strong under large values of lateral force due to the aptitude of the screws to keep moving inside the path they created for a long time. This can be presented as a key factor which explains high ductility of the shear panels.
- In order to detect the stresses which appear on the cold-formed steel frame, strain measurements were carried out by using strain gauges. Since the maximum stress concentration is most likely to occur in the boundary regions close to the foundation, three strain gauges were located close to intersection point of bottom track and vertical stud in the boundary. Besides, measurement of strain has also

been actualized in the mid-height of the shear panel using three strain gauges close to the intersection point of vertical stud in the boundary and lateral track in the middle height of the shear panel. The reason for this is to see the variation of the stress along the height of the shear panel. However, as it is expected, the maximum critical stress values have always appeared to be close to the bottom track in the boundary regions. The placement of the strain gauges on a shear panel and a closer view of the placement of strain gauges are given in Figure 2.21 and Figure 2.22, respectively.

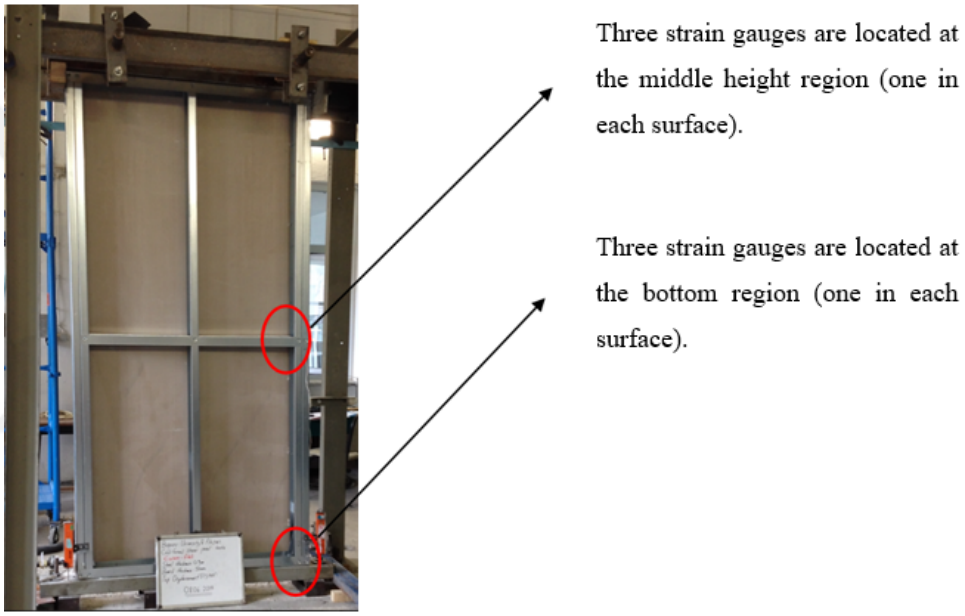

Figure 2.21. Location of Strain Gauges on a Particular Shear Panel.

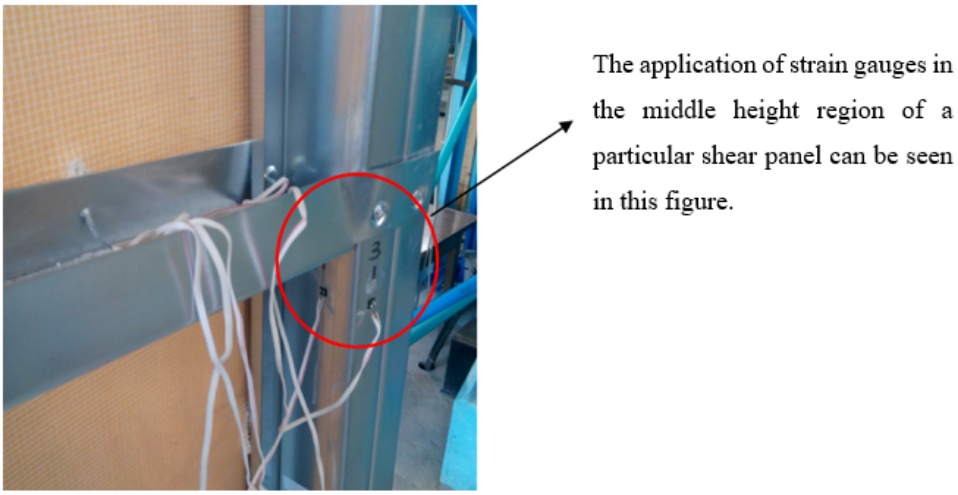

Figure 2.22. A Closer View of the Placement of Strain Gauges.

- Strain measurements have been carried out once in each three set of experiments and maximum strain values obtained from the most critical location have been compared to the yield strain of St 37 steel grade. As a result, strain values obtained during the experiments have never exceeded the yield strain of St 37 steel grade which is an indication of the fact that cold-formed steel frame has never encountered a critical level of stress during the experiments. Comparison of the maximum strain value obtained during the experiments of shear panels and yield strain of St 37 steel grade is presented here. Yield strain of St 37 grade steel can be calculated via Hooke's law in Equation 2.9, where ε_y is yield strain, σ_y is yield stress and E refers to the Young's modulus. For St 37 steel, calculations can be completed as shown in Table 2.13.

$$\varepsilon_{\mathbf{y}} = \frac{\sigma_{\mathbf{y}}}{\mathbf{E}} \tag{2.9}$$

Table 2.13. Calculation of Yield Strain of St 37 Grade Steel.

Yield Stress, σ_y (MPa)	Young's Modulus, E (MPa)	Yield Strain, ε_y (microstrain)
227.5	203395	1100

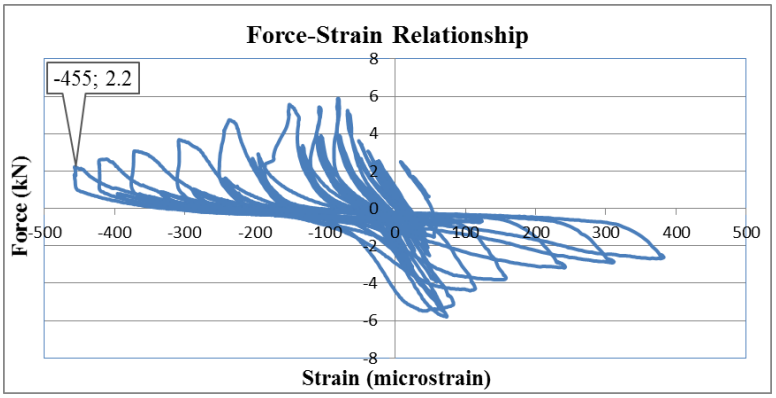

Figure 2.23. Force-Strain Curve of Shear Panel Sheathed with Board Type 1.

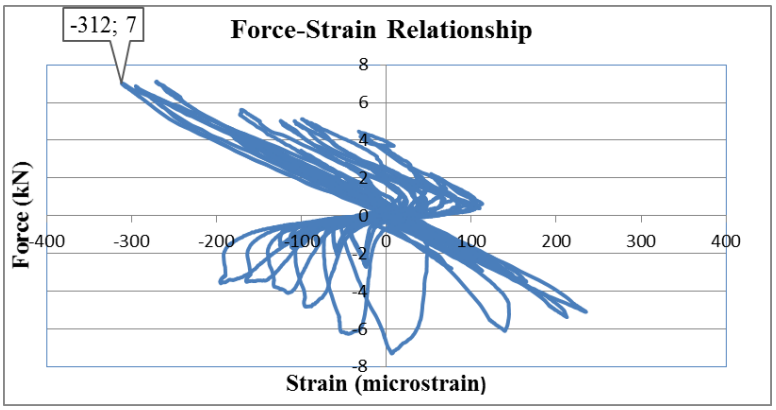

Figure 2.24. Force-Strain Curve of Shear Panel Sheathed with Board Type 2 (0.9 mm Steel Thickness).

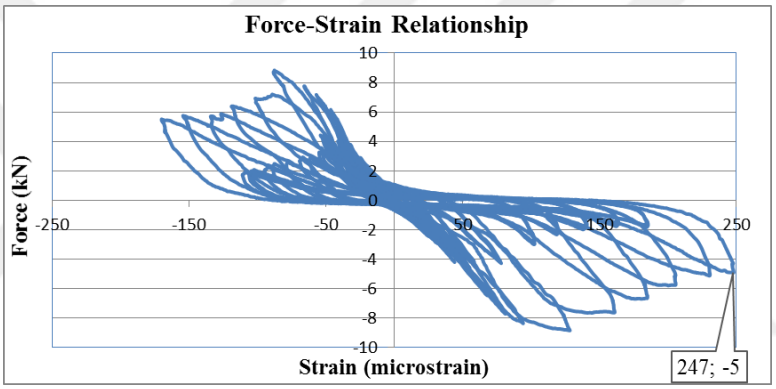

Figure 2.25. Force-Strain Curve of Shear Panel Sheathed with Board Type 2 (1.5 mm Steel Thickness).

- Maximum strain value which occurred on shear panels sheathed with board type 1, board type 2 (0.9 mm steel thickness) and board type 2 (1.5 mm steel thickness) turned out to be 455, 312 and 247 microstrain which are all smaller than the yield strain value, 1100 microstrain.

Table 2.14. Variation of Maximum Strain vs. Shear Strength.

Experiment	Shear Strength (kN)	Maximum Strain (microstrain)
1. CFS Shear Panels Sheathed with Board Type 1	3.2	455
2. CFS Shear Panels Sheathed with Board Type 2 (0.9 mm Steel Thickness)	6	312
3. CFS Shear Panels Sheathed with Board Type 2 (1.5 mm Steel Thickness)	7.4	247

- As ultimate load bearing capacity of the shear panel increased, lover strain values, thus lower stresses occurred on the cold-formed steel frame. This is quite expected because bare frame of the cold-formed steel shear panel starts to be subjected to more hardening as the ultimate load bearing capacity of the shear panel as a whole system is reached.

3. ANALYTICAL STUDY OF BARE FRAME AND SHEAR PANEL

3.1. Introduction

Subsequent to the experimental study carried out in chapter 2, sufficient emphasis was put on analytical approach in chapter 3. It was fundamentally desired to construct an analytical model of a cold-formed steel shear panel which has the capability of representing the actual behavior of the shear panel obtained from the experiments.

3.2. Procedure behind Analytical Approach

The analytical study which is elaborated on hereafter has been completed with two successive stages:

- First model was set up and advanced based on experimental results of the test of the bare frame.
- Second model was set up and developed depending on the experimental results of the tests on specimens sheathed with Board Type 1 with 200/300 mm screw spacing which represents 200 mm screw spacing in the edges and 300 mm screw spacing in between (Appendix A).

Basically there are three types of screws used on the shear panel:

- Screws connecting the frame sections to each other
- Screws connecting the sheathing to the frame sections
- Screws connecting the hold-down anchors to the surface of vertical studs

Since hold-down anchors are readily modeled by simple supports in SAP2000, the main emphasis should be put on the type of screws regarding the first two types. As it is known, frame sections are attached to each other as pin connections; therefore

the frame system itself has no lateral stiffness. In order to represent this fact, frames are modeled as moment-releases which means they do not contribute to the lateral stiffness.

Together with moment-releases, the screws are modeled as nonlinear link elements (Simsir and Jain, 2008 [17]) based on trial and error solution depending on the experimental results of the bare frame system. Similarly, for representing the screws connecting the sheathing to frame, nonlinear link elements were modeled based on trial and error till a reasonable match between analytical results and experimental results is obtained.

3.3. Experimental Result of the Bare Frame

Prior to the analytical study performed on bare frame, experimental investigation was completed on the bare frame system of the CFS shear panels. Deformed shape of the bare frame in the stages of lateral displacement of 100 mm and 200 mm can be seen as follows (Figure 3.1 and Figure 3.2). Besides that, force-displacement curve obtained at the top level of the bare frame is also presented herein (Figure 3.3).



Figure 3.1. Deformed Shape of the Bare Frame in Lateral Displacement Level of 100 mm.



Figure 3.2. Deformed Shape of the Bare Frame in Lateral Displacement Level of 200 mm.

As can be observed from the damage concentration on the bare frame for lateral displacement levels of 100 mm and 200 mm respectively, the main damage is formed as a local buckling located in the boundary regions of bottom track.

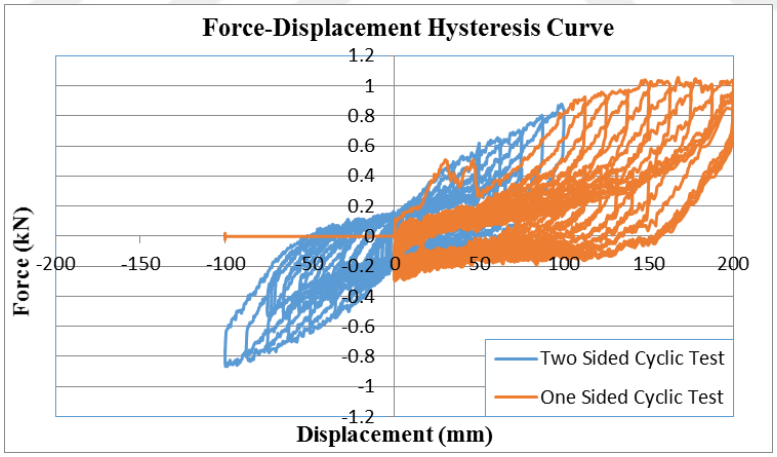

Figure 3.3. Force-Displacement Hysteresis Curve of Bare Frame System.

When the damage concentration and experimental results of the bare frame are checked simultaneously, it can easily be concluded that there is no global failure experienced by the system since the force has never dropped below 0.8 of the peak force even though the experiment was extended till the ultimate lateral loading capacity of the hydraulic actuator is reached (200 mm of lateral displacement).

3.4. Analytical Study of the Bare Frame

In order to represent the screws connecting the frame sections to each other as a pin connection, nonlinear links have been defined in SAP2000. Load-Displacement relationship characterizing the behavior of a screw can be estimated with a reasonable match by Richard and Abbott model (Fiorino *et al.*, 2009 [19]). Richard and Abbott model which can be seen in Figure 3.4 and Figure 3.5 has been developed based on experiments conducted on CFS shear panels with the properties as follows:

- Hot dipped galvanized (zinc coated) steel (nominal yield strength fy=350 MPa; nominal tensile strength ft=420 MPa)
- Two different sheathing types: 9 mm thick type 3 oriented strand board (OSB) and 12.5 mm thick standard gypsum wallboard (GWB)
- Two different types of screws: 4.2*25 mm (diameter*length) flat head self-drilling screws for OSB sheathing, and 3.5*25 mm bugle head self-drilling screws for GWB

However, the properties of the CFS shear panels in the scope of this thesis are listed subsequently:

- St37 grade steel (nominal yield strength fy=227.5 MPa; nominal tensile strength ft=310.3 MPa)
- One type of sheathing: 12.5 mm thick standard gypsum wallboard (GWB)
- One type of screw: 4.2*16 mm (diameter * length) flat head self-drilling screws for GWB sheathing

It can be explicitly interpreted that all of the main characteristic properties of the CFS shear panels used while developing Richard-Abbott model and experimental study conducted in the content of this thesis differ from each other. As a consequence, it can be deduced that it is not reasonable to adopt Richard and Abbott model directly to this study. Yet, this model has been taken as a reference for a starting point to be

used in trial and error solution.

$$\text{for}\delta \leq \delta_{\text{p}} : \text{F}\left(\delta\right) = \frac{\left(\text{k}_0 - \text{k}_{\text{h}}\right)\delta}{\left(1 + \left|\left(\text{k}_0 - \text{k}_{\text{h}}\right)\delta/\text{F}_0\right|^{1/\alpha}\right)} + \text{k}_{\text{h}}\delta \tag{3.1}$$

$$\text{for}\delta > \delta_{\text{p}} : \text{F}\left(\delta\right) = \frac{\text{F}_{\text{p}} - \text{F}_{\text{u}}}{\delta_{\text{u}} - \delta_{\text{p}}}(\delta_{\text{u}} - \delta) + \text{F}_{\text{p}} \tag{3.2}$$

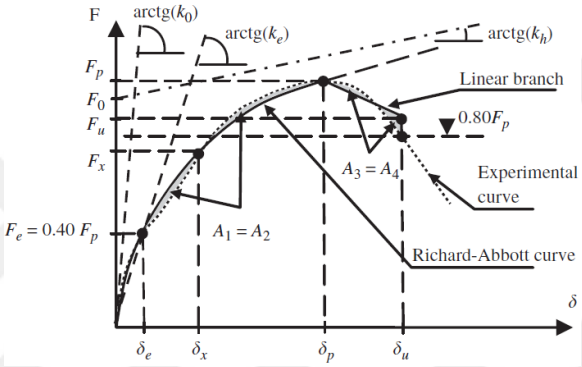

Figure 3.4. Richard and Abbott Model (Fiorino *et al.*, 2009 [19]).

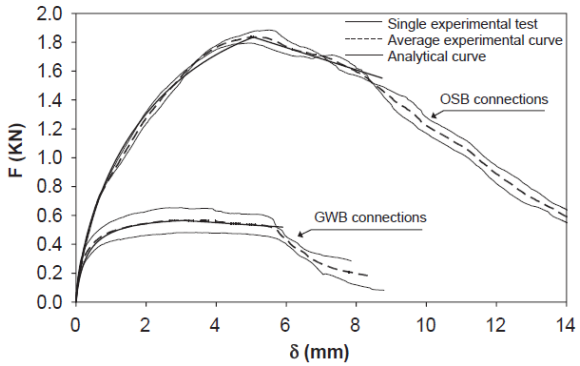

Figure 3.5. Load-Displacement Curves of Sheathing Fasteners (Fiorino *et al.*, 2009 [19]).

The tables including the essential parameters related to the components are given below (Table 3.1 and Table 3.2).

Table 3.1. Wall Parameters (Fiorino *et al.*, 2009 [19]).

h (mm)	2500
b (mm)	1200
l (mm)	2400
t_p (mm)	9.0 (OSB panels), 12.5 (GWB panels)
A (mm^2)	440
E (MPa)	200000
G (MPa)	1400 (OSB panels), 750 (GWB panels)
K_a (kN/mm)	45

Table 3.2. Sheathing Fasteners Parameters (Fiorino *et al.*, 2009 [19]).

Parameters	OSB sheathing fasteners	GWB sheathing fasteners
k_o (kN/mm)	3.31	2.34
k_h (kN/mm)	-0.11	-0.01
F_0 (kN)	8.73	0.7
F_u (kN)	1.55	0.52
F_p (kN)	1.84	0.57
δ_p (mm)	5.09	3.09
δ_u (mm)	8.74	5.9
α	0.43	0.84

where k_0 is the initial stiffness; k_h is the slope of the straight line (hardening line) asymptote of the assumed Richard and Abbott's curve; F_0 is the intersection between the hardening line and the δ=0 axis; F_u is the conventional ultimate load on the analytical response curve; α is a shape parameter regulating the sharpness of transition from the elastic to the plastic behavior (for α large enough a bilinear response is obtained). The values of the parameters k_0, k_h, F_0, F_u, and α are defined by considering the following conditions:

- k_0 is equal to the initial stiffness of experimental curve.
- k_h, F_0, and α are determined by imposing that the analytical curve intersects the experimental curve at the following three points: (1) conventional elastic point (δ_e, F_e); (2) peak point (δ_p, F_p); (3) a point (δ_x, F_x), with $\delta_e < \delta_x < \delta_p$, defined in such a way to minimize the difference between the areas under the analytical and experimental curves (A1 = A2, see Fig. 3.4) for $0 < \delta < \delta_p$.
- Fu is determined in such a way to minimize the difference between the areas under the analytical and experimental curves (A3 = A4, see Figure 3.4) for $\delta_p < \delta < \delta_u$.

(*** It should be noted that all of the information regarding the acquisition of the Richard and Abbott model described above is cited from the paper proposed by Fiorino *et al.*, 2009 [19] ***)

Load-displacement relationship of the screw model which is generated for the analytical study in this thesis is given below (Figure 3.6). Due to the differences described previously, Richard and Abbott model has not been adopted directly to the analytical model; however it played an important role as a reference for the starting point. The comparison between Richard and Abbott model and the model which was created for the analytical study is also presented in Figure 3.6.

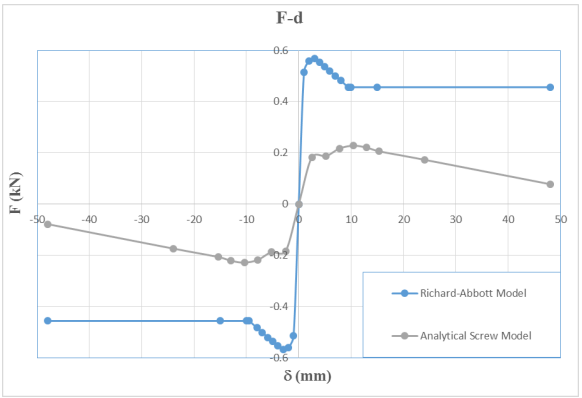

Figure 3.6. Richard-Abbott Model vs. Analytical Screw Model.

As can be observed from the presented figure, analytical screw model for 200/300 mm screw spacing which refers to 200 mm spacing in the edges and 300 mm in between is obtained with a trial and error solution taking Richard and Abbott model as a

reference starting point. Because of the difference between the properties of the CFS shear panels used in the experimental process of acquiring Richard-Abbott model and features of CFS shear panels used in the experiments with respect to the scope of this thesis, the gap between Force-Displacement relationships of these two models is understandable. Besides, the difference between these behaviors does not exceed reasonable mathematical limits. As a result of the development of this analytical screw model, the analyses of the bare frame and cold-formed steel shear panel yielded a perfect match between experimental and analytical results (Figure 3.8 and Figure 3.11).

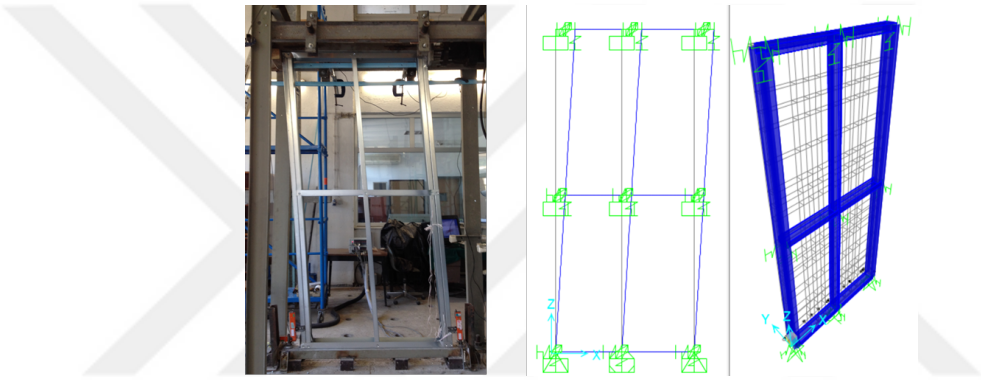

Figure 3.7. Analytical Model of the Bare Frame.

The analytical model of the bare frame is set up mainly characterized by nine nonlinear links at the corner intersections (Figure 3.7). These nonlinear links are defined by SAP2000 in order to represent the pin connections assembling frame sections to each other without contribution to the lateral stiffness of the whole system.

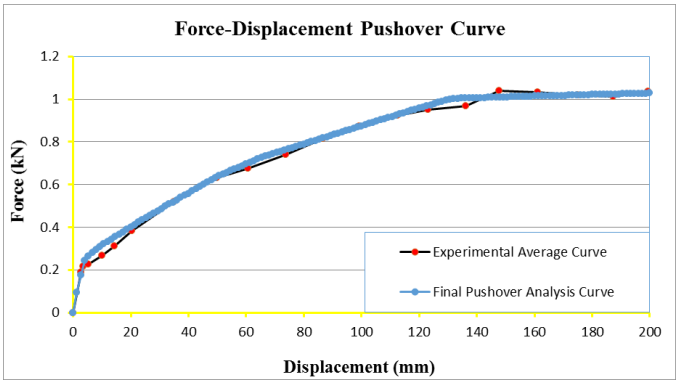

Figure 3.8. Comparison between Analytical and Experimental Curves of Bare Frame.

Posterior to the acquisition of the reasonable match between analytical and experimental curves for bare frame system, the study can be extended to further observation including a CFS shear panel constructed on the bare frame system.

3.5. Analytical Study of the CFS Shear Panel Sheathed with Board Type 1

The analytical model of the cold-formed steel shear panel sheathed with board type 1 was constructed on the bare frame system which was checked analytically in the previous part (Figure 3.9). Since the analytical force-displacement curve of the bare frame system has a reasonable match with that of experimental results, shear panel sheathed with board type 1 was modeled and developed relying on the model generated for bare frame system with additional nonlinear links representing sheathing-to-frame fasteners. Accordingly, the results of experiments were compared to that of analytical study and a very good convergence was also obtained for analytical study of the CFS shear panel sheathed with board type 1. Furthermore, mechanical properties of board type 1 as well as cold-formed steel grade st37 are provided by the manufacturer company (Table 3.3).

Table 3.3. Mechanical Properties of Board Type 1 and CFS.

Properties	Modulus of Elasticity, E (MPa)	Weight per unit Volume (kg/m^3)	Poisson's Ratio
Board Type 1	3053 in short direction 2404 in long direction	640	0.167
CFS	203395	7849	0.3

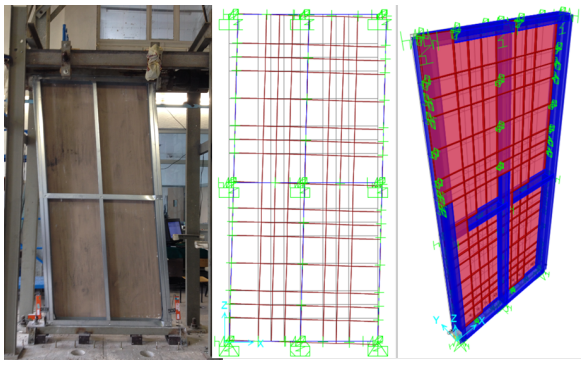

Figure 3.9. Analytical Model of the CFS Shear Panel with Board Type 1.

The nonlinear links representing the screws connecting the frame elements to each other and the fasteners connecting the sheathing to the frame system can be clearly seen in Figure 3.10.

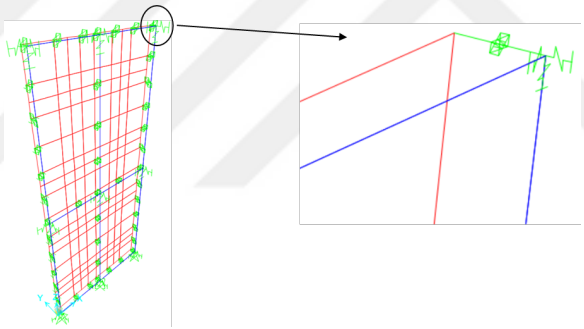

Figure 3.10. Nonlinear Links Representing Sheathing-to-Frame Fasteners and Frame Fasteners.

The behavior of the cold-formed steel framed shear panel is fundamentally characterized by strong nonlinearity resulting from sheathing-to-frame fasteners. Therefore, additional nonlinear links were defined between board type 1 and frame system following the screw model described in section 3.4. These nonlinear links are representing the screws connecting board type 1 to the frame system with a spacing of 200 mm in the edges and 300 mm in between as described in Appendix A.1 (Figure A.1). The convergence between results of experimental study conducted on cold-formed steel framed shear panel sheathed with board type 1 and analytical study performed on the model of CFS shear panel sheathed with board type 1 can be investigated in Figure 3.11.

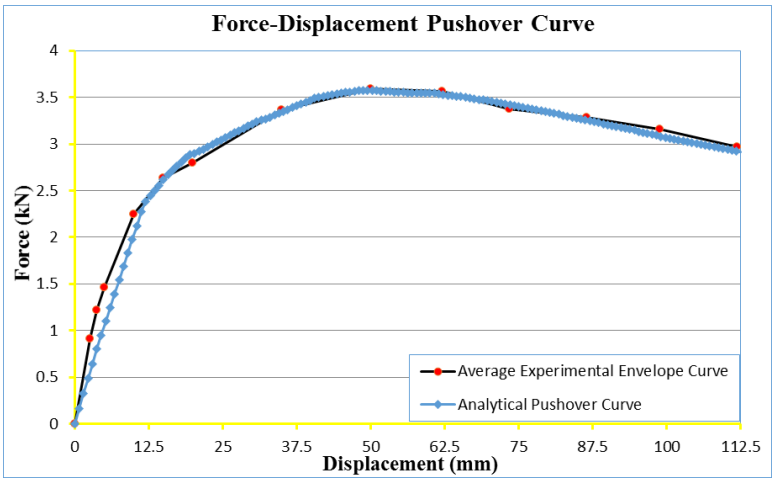

Figure 3.11. Comparison between Analytical and Experimental Curves of CFS Shear Panel Sheathed with Board Type 1.

As can be noticed, a significant convergence between analytical and experimental results is acquired for the full shear panel as well. It should be noted that average experimental envelope curve is obtained by taking the average of the results coming from three successive experiments conducted in the laboratory on cold-formed steel shear panels sheathed with board type 1. With the proposed screw model described in section 3.4, this substantial match is received.

4. ANALYTICAL STUDY OF A TYPICAL ONE-STORY CFS STRUCTURE

4.1. Introduction

Since a reasonably efficient convergence between analytical results and experimental outcomes is supplied, which is acquired as a collaborated two successive phases starting from analysis of bare frame and followed by analysis of cold-formed steel framed shear panel, the analytical study has been extended to be applied on a typical one-story residential structure. The ultimate objective of this application is to assure the capability of cold-formed steel structures to possess a sufficient performance in seismic prone regions such as Turkey.

4.2. Properties of the Structure

The geometric properties of this particular cold-formed steel framed structure is determined arbitrarily based on the essential needs which may be arisen for a one-story residential structure (Figure 4.1). This structure is assumed to be located in seismic zone 1 with the soil-site conditions regarding Z3 (Table 4.1).

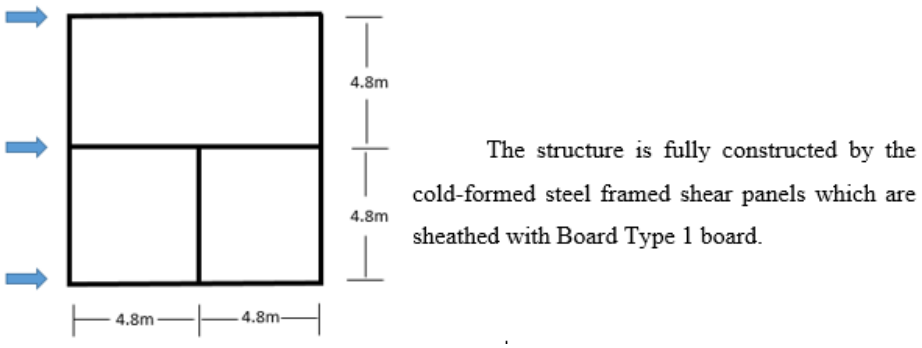

Figure 4.1. Top View of the Structure.

Table 4.1. Parameters of the Structure.

Seismic Zone, A_o	1st Seismic Zone, A_0=0.4
Soil Class, T_A and T_B	Z3 Soil Class, T_A=0.15, T_B=0.6
Importance Factor, I_0	Residential Building, I_0=1

All of these parameters are taken from Turkish Earthquake Code 2007 [3] in order to determine the design earthquake demand which may occur on this structure.

4.3. Model of the Structure

The model of the structure is constructed by making use of the analytical model developed for the cold-formed steel framed shear panel sheathed with board type 1. In other words, load-bearing system of the structure is constructed by shear panels which is purely the fundamental mentality behind cold-formed steel framed structures. It should be noted that the analysis has been conducted in x-global direction. As it is known, one cold-formed shear panel has dimensions of 2.4*1.2 m (height * width). As a result, in x-direction for the length of 9.6 m, three CFS shear panels which have dimensions of 2.4*9.6 m (height * width) were constructed. In y-direction for the length of 9.6 m, two CFS shear panels which have dimensions of 2.4*9.6 m (height * width) and for the length of 4.8m, one CFS shear panel which has dimensions of 2.4*4.8 m (height * width) were constructed. This application has been taken as a simplifying assumption because if all the directions had been defined by the CFS shear panel with the dimensions of 2.4*1.2 m, the analysis would have required the detailed modeling of intersection points which may itself be a subject of a possible future work. Gravity loads resulting from the self-weight of the cold-formed steel shear panel are taken into account by utilizing the SAP2000 software by means of self-weight multiplier. Apart from this, distributed gravity loads arising from the dead and live loads are assigned to the top track of the cold-formed steel shear panels by means of tributary area. Consequently, gravity loads are assigned to the frame system as a uniformly distributed load. The

quantity of these gravity loads and calculation process is shown in Table 4.2

$$W_{wall} = W_{sp} * n_{sp} \tag{4.1}$$

$$W_{floor} = \left(W_{sp} * \frac{A_{str}}{A_{sp}} \right) + W_{alum} \tag{4.2}$$

$$W_{alum} = \gamma_{alum} * V_{alum} \tag{4.3}$$

where W_{sp} is weight of one shear panel considering two-sided sheathing (for dimensions of 2400 mm of height and 1200 mm of width, Figure A.1 and Table 3.3), n_{sp} is number of shear panels (for 2400/1200 mm dimensions), A_{str} is area of the plan view of the structure, A_{sp} is area of one shear panel (for 2400/1200 mm dimensions), γ_{alum} is weight per unit volume of alum, V_{alum} is volume of alum, W_{alum} is weight of alum, W_{floor} is weight of the floor and W_{wall} is weight of the walls.

Table 4.2. Calculation of Gravity Loads Resulting from Walls and Floor.

W_{sp} (kg)	67.2
n_{sp}	44
A_{str} (m^2)	92.2
A_{sp} (m^2)	2.9
γ_{alum}(kg/m^3)	1200
V_{alum} (m^3)	4.6
W_{alum} (kg)	5520
W_{floor} (kg)	2957
W_{wall} (kg)	7656

However, W_{wall} and W_{floor} are taken as 4000 kg and 8000 kg including the effect of insulation and installation.

Weight as a distributed gravity load on the slab (W_{dist}) can be calculated as follows:

$$W_{dist} = \left(\frac{W_i}{A_{str}}\right) \tag{4.4}$$

In Equation 4.4, W_i represents weight of any kind. Accordingly, weight as a distributed load on the slabs resulting from walls, floor, roof, snow and live load can be presented as shown in Table 4.3.

Table 4.3. Calculation of Gravity Loads Distributed along the Slab.

W_{wall} (kN/m^2)	0.4
W_{floor} (kN/m^2)	0.8
W_{roof} (kN/m^2)	1.05
W_{snow} (kN/m^2)	0.5
W_{live} (kN/m^2)	2

Calculations were completed according to 1.4 D + 1.6 Q load combination where D and Q represent dead and live load, respectively. Gravity load acting on the exterior shear panels (W_{ext}) can be calculated using Equation 4.5.

$$W_{ext} = \frac{1}{3} * (1.4\,[W_{floor} + W_{roof}] + 1.6\,[W_{snow} + W_{live}]) * A_{str} \tag{4.5}$$

Weight as a distributed gravity load on the top track of the exterior shear panels and interior shear panels ($W_{d,t,e}$ and $W_{d,t,i}$) can be calculated as follows:

$$W_{d,t,e} = \frac{W_{ext}}{l * n_l} \tag{4.6}$$

$$W_{d,t,i} = W_{dte} * 2 \tag{4.7}$$

where l represents length of shear panels and n_l refers to the number of shear panels

for this length. Accordingly, weight as a distributed gravity load on the top track of the exterior shear panels and interior shear panels can be calculated as 5 kN/m and 10 kN/m, respectively (Figure 4.2).

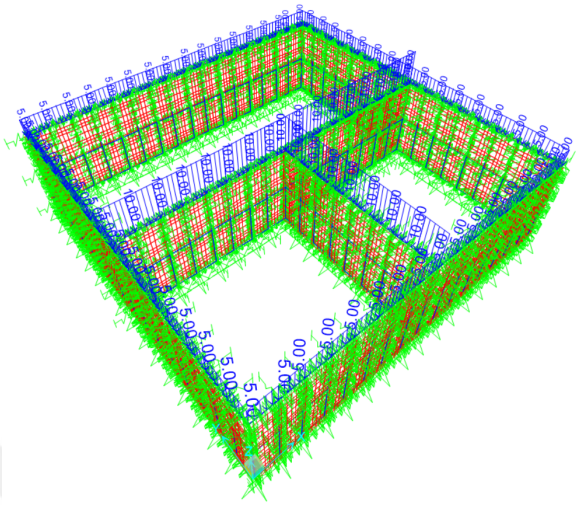

Figure 4.2. Model of the CFS Structure Including Distribution of Gravity Loads.

4.4. Modification of the Nonlinear Links Due to the Effect of Gravity Load

It must be noticed that behavior of the nonlinear links will vary according to the contribution of gravity loads since gravity loads apply on the cold-formed steel frame and there is a direct connection between nonlinear links and the frame system. In reality, behavior of the screws would also change as the gravity load acting on the shear panel varies due to the direct connection between the sheathing, screws and the frame system. In order to calibrate the load-displacement relationship of the nonlinear links, three set of tests were conducted on shear panels sheathed with board type 1 under the effect of 10 kN/m distributed gravity load. The view of the shear panel under the effect of gravity load and the analytical model of this shear panel in SAP2000 are presented in Figure 4.3. The modified last form of nonlinear links which supplies a reasonable match between analytical pushover curve and average experimental load-displacement curves and comparison of load-displacement curves can be seen in Figure 4.4 and Figure 4.5.

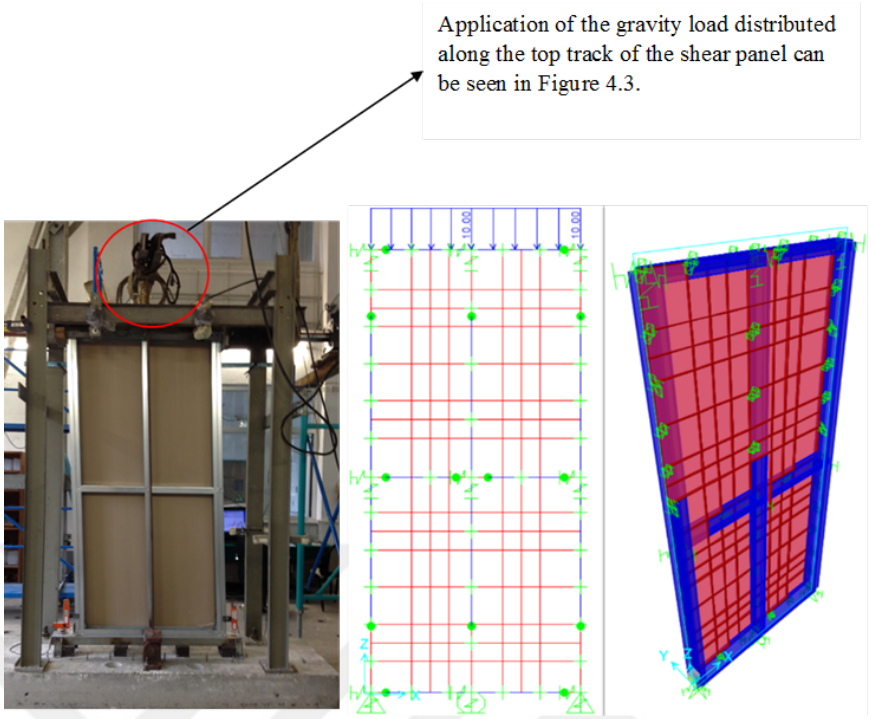

Figure 4.3. Shear Panel with Gravity Load and Analytical Model of the Shear Panel.

It should be noted that gravity load is applied as a point load, but this point load is assumed to be transferred to the top track of the shear panel as a distributed load because of the rigid structure of the loading beam which transfers the lateral load applied by the actuator to the top track of the shear panel.

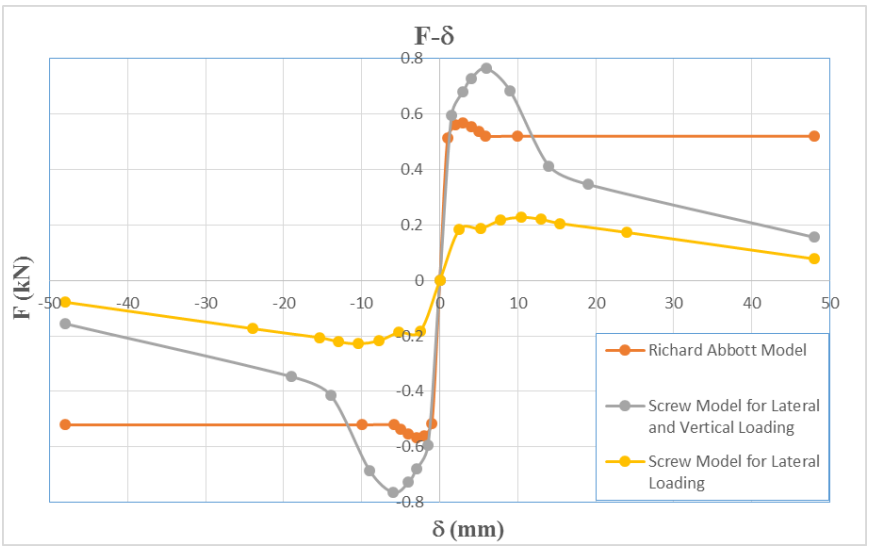

Figure 4.4. Modified Screw Model Including the Effect of Gravity Loading.

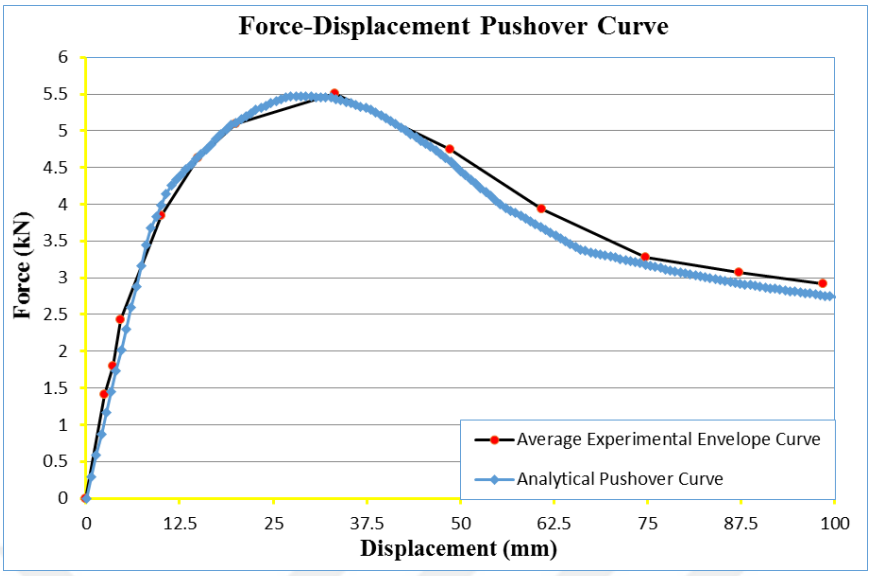

Figure 4.5. Comparison between Analytical and Experimental Pushover Curves under the Effect of Gravity Loading for CFS Shear Panels Sheathed with Board Type 1.

4.5. Pushover Analysis of the Structure

Subsequent to the acquisition of the model of the cold-formed steel framed residential one-story structure including the modified behavior of the nonlinear links under the effect of gravity loading which represent sheathing-to-frame fasteners, pushover analysis has been performed on the top level of the structure in order to be capable of determining the capacity of the structure (Figure 4.6). The check of the structure against the possible design earthquake proposed by Turkish Earthquake Code 2007 [3] is done with respect to the base shear and performance point obtained from modal capacity curve. In other words, the demand occurring on the structure coming from the design earthquake is compared to the capacity of the structure obtained via structural analysis results in terms of base shear and performance point.

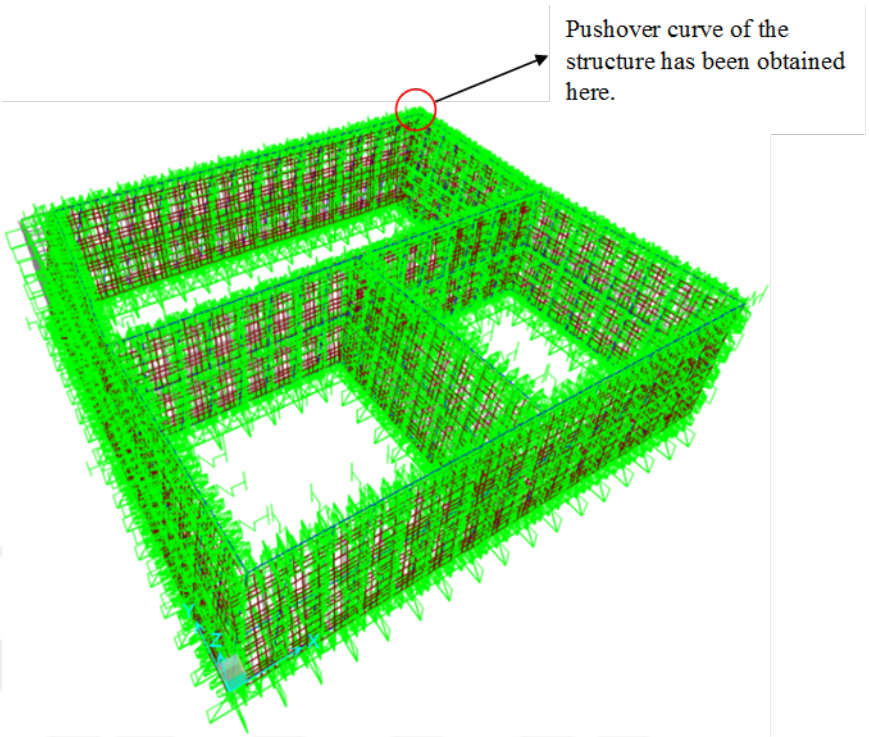

Figure 4.6. Deformed Shape of the Structure after Pushover Analysis.

After pushover analysis of the one-story cold-formed steel framed structure is completed, the capacity of that structure in terms of base shear can be observed from the pushover cure (Figure 4.7).

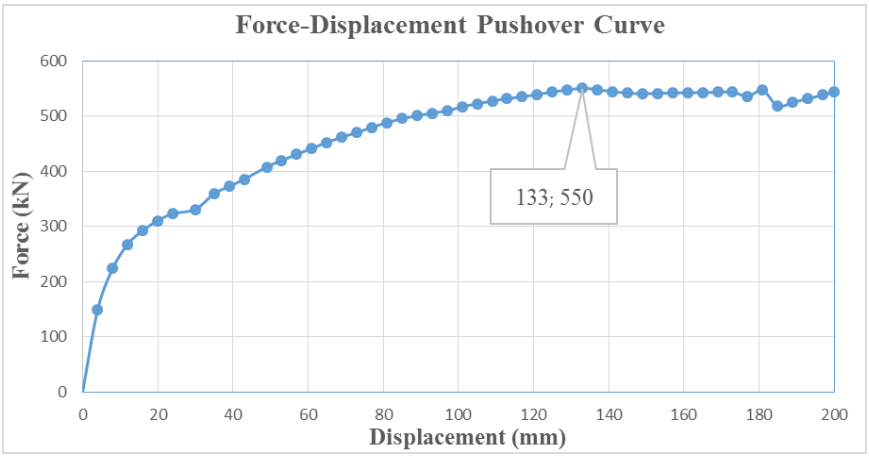

Figure 4.7. Pushover Curve of the Structure.

It can be explicitly seen that capacity of the structure in terms of base shear is 550 kN. In order to obtain the demand which may occur on this structure from the design

earthquake, period of the structure for characterization of that particular structure must be calculated. Characteristic period of the structure has been calculated with the following method:

- Modal analysis conducted on the structure with the characterization of the non-linear links with their initial stiffness as linear elastic links

In order to obtain the demand occurring on the structure in terms of base shear, weight of the structure, thus mass of the structure must be determined. The weight of the structure is taken from the analysis of the structure under gravity loads in the base reaction form (Table 4.4).

Table 4.4. Weight of the Structure.

TABLE: Base Reactions				
OutputCase	CaseType	GlobalFX	GlobalFY	GlobalFZ
Text	Text	KN	KN	KN
DEAD	LinStatic	2.33E-13	-1.72E-13	331.154

Weight is calculated as 331 kN from base reactions obtained by the structural analysis under gravity loads. Mass of the structure can be calculated through Equation 4.8.

$$\mathrm{m} = \frac{\mathrm{W_{str}}}{\mathrm{g}} \tag{4.8}$$

where m is mass of the structure, W_{str} is weight of the structure and g is gravitational acceleration. Mass of the structure is calculated as 33.8 tons.

$$\mathrm{k_0} = \tan\theta \tag{4.9}$$

where k_0 is the initial stiffness of the nonlinear links and tan θ represents the slope of the initial line. Initial stiffness of the nonlinear links is computed as 0.4 kN/mm^2.

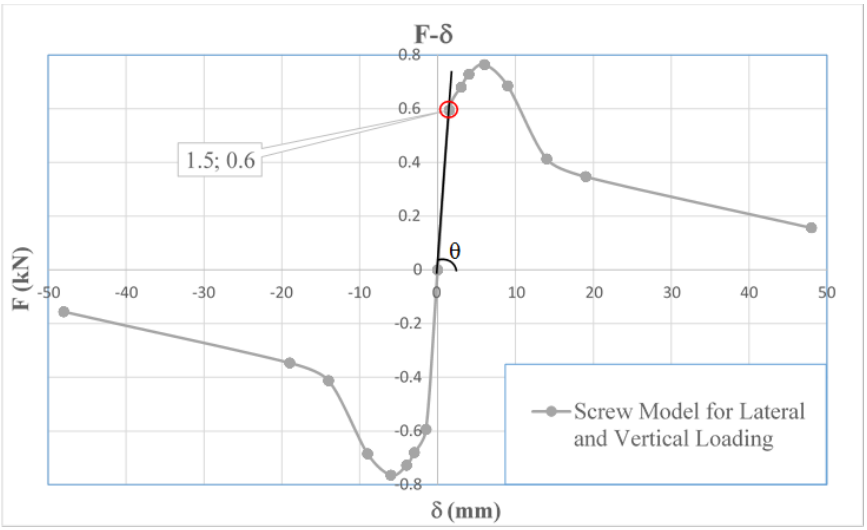

Figure 4.8. Initial Stiffness of the Nonlinear Link Elements.

During modal analysis which was conducted in order to determine the characteristic period of the structure, nonlinear links have been adjusted again with their initial stiffness as linear-elastic links (Figure 4.8). Modal analysis which was conducted on the structure via idealized linear elastic links yielded the characteristic period of the structure as 0.23 sec (Table 4.5 and Figure 4.9).

Table 4.5. Period Calculation via Structural Modal Analysis.

TABLE: Modal Participating Mass Ratios				
OutputCase	StepType	StepNum	Period	UX
Text	Text	Unitless	Sec	Unitless
MODAL	Mode	1	0.226743	0.85
MODAL	Mode	2	0.16958	0.07942
MODAL	Mode	3	0.142078	0.01723
MODAL	Mode	4	0.140102	0.005519
MODAL	Mode	5	0.129808	1.26E-06
MODAL	Mode	6	0.114655	2.44E-05
MODAL	Mode	7	0.095008	0.0003556
MODAL	Mode	8	0.090808	0.02356
MODAL	Mode	9	0.078107	2.18E-05
MODAL	Mode	10	0.077319	0.0000451
MODAL	Mode	11	0.071879	1.334E-06
MODAL	Mode	12	0.07183	4.87E-04

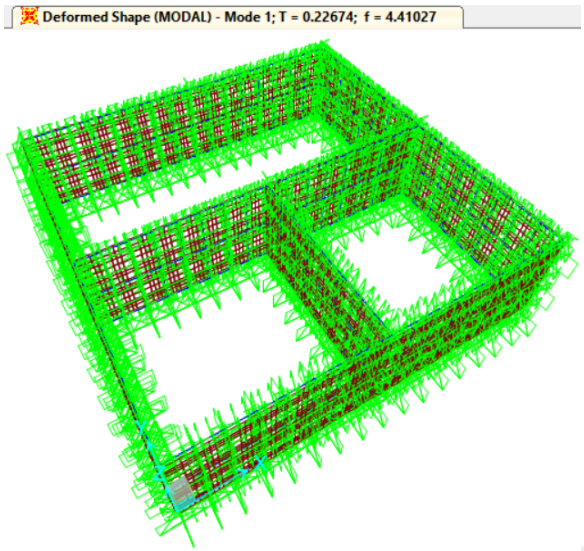

Figure 4.9. Period Calculation via Structural Modal Analysis.

With the simultaneous observations done on the deformed shape of the structure under modal analysis and tabular form of modal participating mass ratios, it can be deduced that characteristic period of the structure is obtained as 0.23 second in the x-direction since the highest mass participation occurs in the first mode of x-direction.

4.6. Force-Based Performance Assessment of the CFS Structure

With the acquisition of characteristic period of the structure, performance check of the structure in terms of base shear can be carried out by utilizing the design spectrum proposed by Turkish Earthquake Code 2007 [3] (Figure 4.10). This design spectrum represents the possible worst case scenario earthquake which has ten percent probability of exceedance in fifty years. Since the characteristic period of the structure is calculated and other spectrum parameters relevant to the properties of the structure and the location of the structure are known, the demand in terms of base shear which may arise from the design earthquake can be computed.

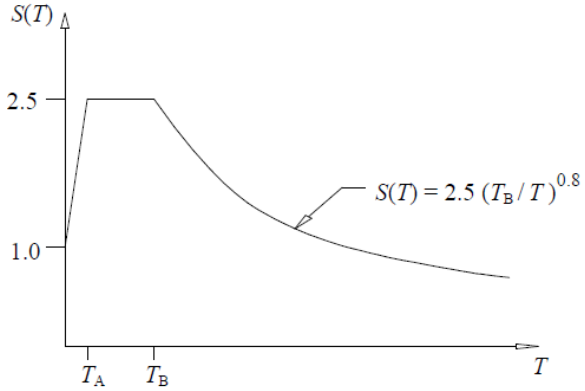

Figure 4.10. Spectrum Coefficient (TEC 2007 [3]).

$$\mathrm{S\,(T)} = 1 + 1.5\frac{\mathrm{T}}{\mathrm{T_A}}, (0 \leq T \leq T_A) \tag{4.10}$$

$$\mathrm{S\,(T)} = 2.5, (\mathrm{T}_A < \mathrm{T} \leq \mathrm{T}_B) \tag{4.11}$$

$$\mathrm{S\,(T)} = 2.5, (\mathrm{T}_B < \mathrm{T}) \tag{4.12}$$

Table 4.6. Spectrum Characteristic Periods (TEC 2007 [3]).

Local Site Class According to Table 6.2	T_A (second)	T_B (second)
Z1	0.1	0.3
Z2	0.15	0.4
Z3	0.15	0.6
Z4	0.2	0.9

Table 4.7. Effective Ground Acceleration Coefficient, A_0 (TEC 2007 [3]).

Seismic Zone	A_0
1	0.4
2	0.3
3	0.2
4	0.1

Table 4.8. Building Importance Factor, I_0 (TEC 2007 [3]).

Purpose of Occupancy or Type of Building	Importance Factor (I_0)
4. Other buildings Buildings other than above defined buildings. (Residential and office buildings, hotels, building-like industrial structures, etc.)	1

Total base shear demand (V_t) can be calculated via weight of the structure (W), spectral acceleration coefficient ($A(T_1)$) and seismic load reduction factor (R_a (T_1)) according to the parameters listed below:

- First seismic zone A_o=0.4
- Z3 soil class T_A=0.15, T_B=0.6
- Building importance factor, I_0=1
- $R_a(T_1)$=1, since performance assessment is of concern

$$V_t = \frac{WA(T_1)}{R_a(T_1)} \tag{4.13}$$

From Equation 4.13, total base shear demand can be calculated as 331 kN. Ac-

cordingly comparison between demand and capacity can be carried out.

$$\begin{aligned} &331\mathbf{kN} < 550\mathbf{kN} \\ &\mathbf{DEMAND} < \mathbf{CAPACITY} \end{aligned} \tag{4.14}$$

From this simple structural analysis, it can be concluded that use of light-weight cold-formed steel structures in earthquake-prone regions like Turkey, yields considerably reliable consequences.

4.7. Displacement-Based Performance Assessment of the CFS Structure

Despite the fact that performance assessment of the particular CFS framed structure was already carried out with respect to the base shear demand resulting from the design spectrum proposed by TEC 2007 [3], it would be efficient to evaluate the performance once more according to the performance point of the structure. Performance point of the structure is obtained through using the conversion of pushover curve to modal capacity curve following the specifications proposed in TEC 2007 (Figure 4.12). After acquiring the performance point of the structure, the performance of the structure can be assessed by checking the damage levels occurring on the structure at a level of top displacement which corresponds to the performance point

$$\mathrm{a}_1^{(\mathrm{i})} = \frac{\mathrm{V}_{\mathrm{x1}}^{(\mathrm{i})}}{\mathrm{M}_{\mathrm{x1}}} \tag{4.15}$$

$$\mathrm{d}_1^{(\mathrm{i})} = \frac{\mathrm{u}_{\mathrm{xN1}}^{(\mathrm{i})}}{\phi_{\mathrm{xN1}}\Gamma_{\mathrm{x1}}} \tag{4.16}$$

$$\mathrm{M}_{\mathrm{x1}} = \frac{\mathrm{L}_{\mathrm{x1}}^2}{\mathrm{M}_1} \tag{4.17}$$

$$L_{x1} = \sum_{i=1}^{N} m_i \phi_{xN1} \tag{4.18}$$

$$M_1 = \sum_{i=1}^{N} m_i \phi_{xN1}^2 \tag{4.19}$$

$$\Gamma_{x1} = \frac{L_{x1}}{M_1} \tag{4.20}$$

where $a_1^{(i)}$ is modal acceleration defined for the first mode of vibration in x-direction for i^{th} step of the pushover analysis, $d_1^{(i)}$ is modal displacement defined for the first mode of vibration in x-direction for i^{th} step of the pushover analysis, $V_{x1}^{(i)}$ is base shear for the first mode of vibration in x-direction for ith step of the pushover analysis, $u_{xN1}^{(i)}$ is top displacement for the first mode of vibration in x-direction for i^{th} step of the pushover analysis, M_{x1} is effective mass defined for the first mode of vibration in x-direction, ϕ_{xN1} is amplitude of the first mode shape at the top of the building (N^{th} story) defined for the first mode of vibration in the x-direction, Γ_{x1} is participation factor defined for the first mode of vibration in x-direction and M_1 is modal mass defined for the first mode of vibration.

ϕ_{x11} is obtained as 4.6 mm from the deformed shape of the structure during modal analysis in x-direction for the first mode (Figure 4.11). Accordingly, essential parameters for modal capacity curve can be calculated (Table 4.9).

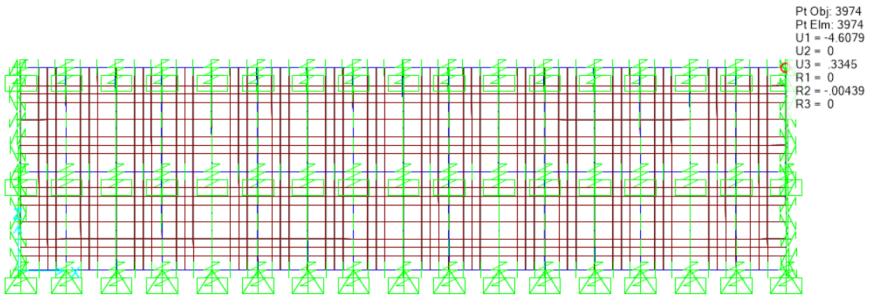

Figure 4.11. Amplitude of the First Mode Shape in x-direction.

Using the Equation 4.15 and Equation 4.16 which were proposed previously, modal capacity curve can be acquired prior to determining the performance point (Figure 4.13).

Table 4.9. Calculation of Essential Parameters for Modal Capacity Curve.

Floor	m_1(ton)	Φ_{xN1}(m)	mi*Φ_{xN1}	mi*Φ^2_{xN1}	L_{x1}	M_1	M_{x1}	Γ_{x1}
1	33.8	0.005	0.169	0.000845	0.169	0.000845	33.8	200

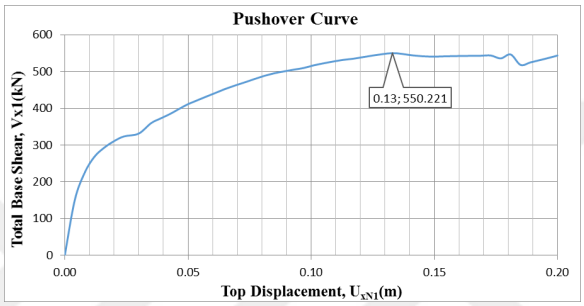

Figure 4.12. Pushover Curve of the Structure.

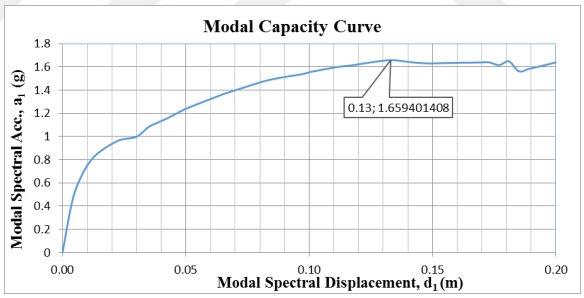

Figure 4.13. Modal Capacity Curve of the Structure.

To be able to find the performance point of the structure, demand spectrum must be obtained. For this purpose, specifications proposed in TEC 2007 were utilized.

Nonlinear inelastic spectral replacement, S_{di1}, in the first step of the pushover analysis, shall be obtained with Equation 4.21 depending on the linear elastic spectral replacement S_{de1}, which corresponds to $T_1^{(i)}$ first period regarding the first (dominant) mode calculated based on linear elastic behavior:

$$S_{di1} = C_{R1} * S_{de1} \tag{4.21}$$

Linear elastic spectral replacement, S_{de1} is calculated from elastic spectral acceleration S_{ae1} regarding first mode in the first step of pushover analysis (Equation 4.22):

$$\mathrm{Sde1} = \frac{\mathrm{S_{ae1}}}{\left(2\pi/\mathrm{T_1^{(1)}}\right)^2} \tag{4.22}$$

Ratio of spectral displacement C_{R1}, is determined depending on the value of first period of vibration, $T_1^{(1)}$. Structures which have first period of vibration, $T_1^{(1)}$, smaller than T_B, that also refers to the structure in the scope of this thesis, C_{R1} is calculated with the Equation 4.23.

$$C_{R1} = \frac{1 + (\mathrm{R_{y1}} - 1) * \mathrm{T_B}/\mathrm{T_1}}{\mathrm{R_{y1}}} \tag{4.23}$$

R_{y1} is the strength reduction factor pertinent to the first mode and calculated with the Equation 4.24.

$$\mathrm{R_{y1}} = \frac{\mathrm{S_{ae1}}}{\mathrm{a_{y1}}} \tag{4.24}$$

S_{ae1} is the elastic spectral acceleration and a_{y1} is the equivalent yield acceleration related to the first mode and it can be obtained from the peak value of modal capacity curve (Equation 4.25).

$$\mathrm{S_{ae1}} = \mathrm{A_0 IS\,(T)}\, g \tag{4.25}$$

Calculation of the essential parameters in order to be able to determine the performance point of the structure is given in Table 4.10.

Table 4.10. Calculation of Essential Parameters for Performance Point.

T_1 (second)	0.23
T_B (second)	0.6
a_{y1} (m/s^2)	16.3
S(T)	2.5
S_{ae1} (m/s^2)	9.81
R_{y1}	0.6
C_{R1}	1
S_{de1} (m)	0.01
$d_1^{(p)}$=S_{di1} (m)	0.01

Performance point of this particular one-story structure turned out to be 0.01 m. Performance point can also be shown in graphical form with the comparison of capacity curve and demand spectrum.

Following the acquisition of the demand spectrum for that particular one-story structure, performance point can be demonstrated in graphical form (Figure 4.14). From the demonstration of graphical acquisition of performance point, it can be seen that performance point turned out to be 0.01 m which is the same as previous calculation.

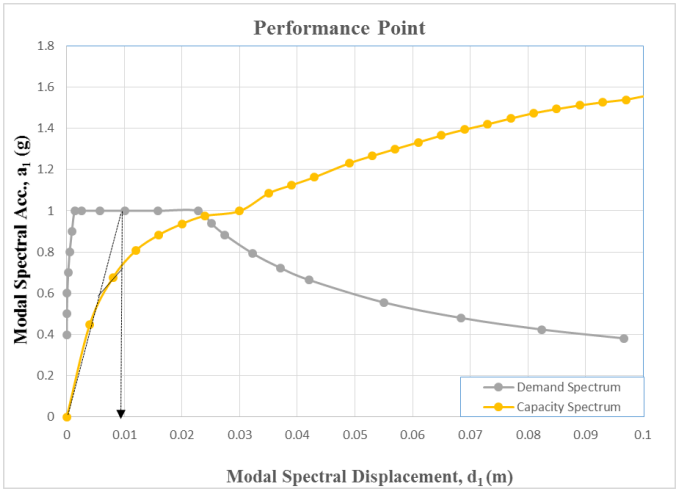

Figure 4.14. Performance Point of the Structure.

As a result of the acquisition of the performance point as 0.01 m of cold-formed steel framed one-story structure, the performance evaluation can be achieved based on the damages that occurred at a top displacement level of 0.01 m = 10 mm. Recalling the experimental study performed on cold-formed steel shear panels sheathed with board type 1, performance of this one-story structure is definitely adequate since no considerable damage was observed at a top displacement level of 10 mm (Figure B.1.).

5. CONCLUSIONS AND FUTURE WORKS

In this chapter, the main conclusions which can be drawn according to the study completed so far in the content of this thesis have been presented. Some of the conclusions regarding the chapters were already drawn in the sections of concern, yet a broader adjustment to the conclusions is carried out herein to illustrate the main picture in an efficient way. Since the potential of cold-formed steel construction is substantially high, there are always prospective future works which may come as a result of recent research. This topic has already reached a sufficiently accomplished development; however, there is still a really large available field for further developments as well as extended research since a simple change in components of cold-formed steel construction may change the behavior significantly such as screw spacing, type of screws, type of board, board thickness, steel thickness, anchorage properties, effect of gravity load and so forth.

5.1. List of Conclusions

- Cold-formed steel structures have started to be used widely in the last decades due to various favorable sides such as lightness, easy practices, dimensions, transportability, high strength and ductility, environmental advantages, cost-management and time-effectiveness.
- Besides advantageous sides, vulnerability to all kinds of buckling due to its small thickness, isolation problems and such drawbacks have always kept the research on this topic available and many further developments have been applied to cold-formed steel structures.
- Due to the high potential of the cold-formed steel structures, the research on cold-formed steel structures and materials have always extended to further studies.
- In order to see the performance of CFS construction against earthquakes, in earthquake-prone regions such as Turkey, a considerable sum of experiments have been conducted in the Structures Laboratory of Bogaziçi University in the scope of this thesis.

- Apart from assuring the performance of CFS structures against earthquakes, it was also desired to develop an analytical model by SAP2000 software [4] which represents the lateral load-displacement behavior of a particular CFS framed shear panel.
- Experimental study has been carried out on a variety of specimens with cold-formed steel frame including different kind of sheathings all based on gypsum wallboard.
- Results of all of the experiments differed from each other in terms of ductility and load bearing capacity; however, it was truly significant to see that no brittle type of failure was observed for none of the specimens sheathed with gypsum wallboard. It is always desired to design the structures to interfere with the brittle type of failure in any case which is only valid with sufficient energy absorption capacity, in other words, ductility. Prevention of brittle failure was the fundamental goal of all of the CFS shear panels and experiments revealed that this ultimate goal was achieved.
- As a matter of fact, as long as a different type of sheathing is applied to the shear panel, the behavior changed and results differed from each other. According to the site conditions where CFS structure will be built, the selection of the appropriate board can be done.
- Subsequent to the completion of experimental study, an analytical model representing the load-displacement relationship of a specific CFS shear panel was developed. After coming up with a reasonable convergence between analytical results coming from the model of the particular CFS shear panel and experimental outcomes, the study has been extended to be applied on a typical one-story structure located in a seismically active region such as Turkey.
- Consequently, after the analytical study of the one-story structure was completed, the performance check of the structure has been carried out with respect to the base shear and performance point obtained from pushover analysis. Demand on the structure was acquired from the design spectrum of Turkish Earthquake Code 2007 to be compared to the capacity. Comparison between capacity and demand has explicitly manifested that constructing CFS structures in seismic-prone regions such as Turkey is safe and sound as long as it is done with an

adequate engineering supervision and application.

5.2. List of Future Works

- As a future work, analytical study can be improved in terms of the screw model supported by a certain number of experiments which may be conducted on screws to characterize the load-displacement behavior of the screws similar to the research carried out by Fiorino *et al.*, 2009 [19].
- An initiative to the effect of screw spacing on the behavior of cold-formed steel shear panels has already been done in the Structures Laboratory of Bogaziçi University but it is not included in this thesis because it may be extended more successfully in the scope of a project in the future.
- Effect of gravity loads on the shear panels may also be a part of extended research about CFS shear panels because with today's technology, the majority of construction with CFS systems is done for low-rise and mid-rise residential applications. However, with a further study regarding the combination of gravity loads as a result of increase in number of stories, it is likely to see a wider range of CFS construction all over the world involving high-rise buildings, as well.

APPENDIX A: PANEL TECHNICAL DRAWINGS (AUTOCAD)

A.1. L1001 Shear Panels

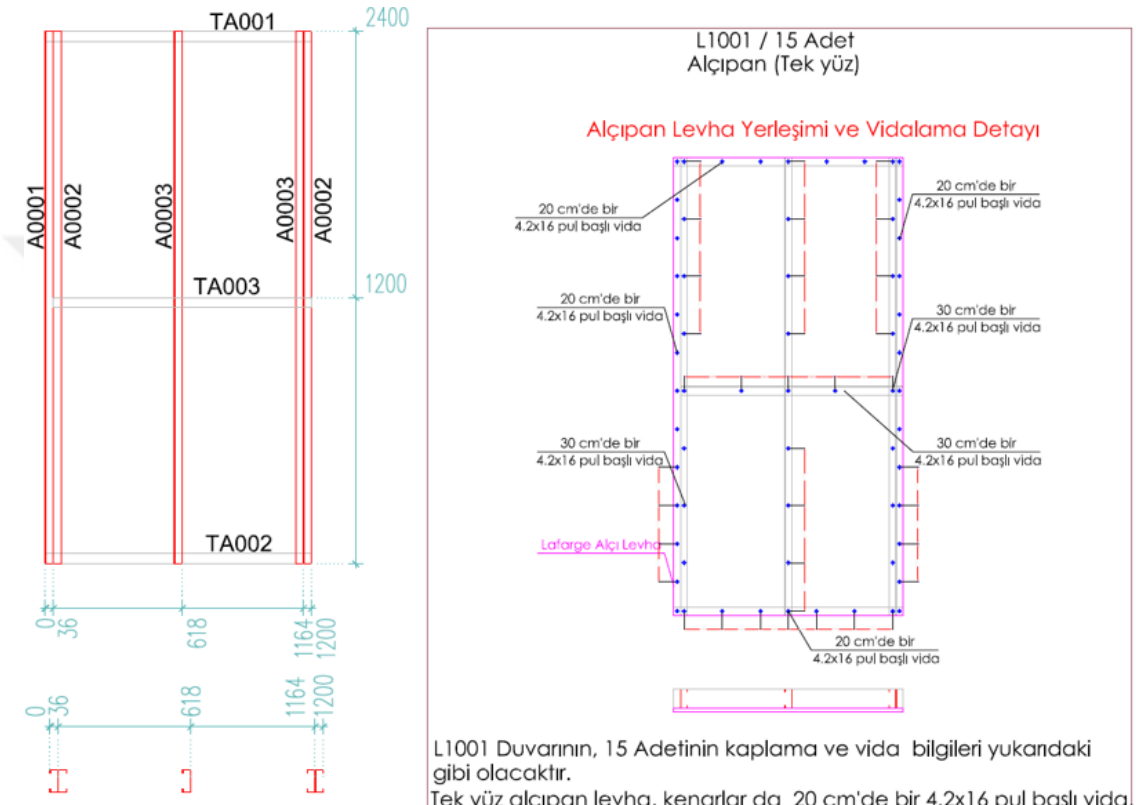

L1001(18)

POZ	ADET	KESİT	UZUNLUK(mm)	AĞIRLIK(kgs)
A0001	1	AK-CM9910	2398	3.2613
A0002	2	AK-CM9910	2398	6.5226
A0003	2	AK-CM9910	2398	6.5226
TA001	1	AK-CS10110	1200	1.632
TA002	1	AK-CS10110	1200	1.632
TA003	1	AK-CS10110	1164	1.583
-	-	Grand Total:		21.1535
-	-	Diagonal Length:	2683	

Figure A.1. L 1001 Panel Technical Drawing (Provided by the Manufacturer Company).

PNL-O1 named panels possessing 0.9 mm steel thickness were manufactured according to the configuration shown above (Figure A.1). Six of shear panels sheathed with board type 1 and board type 2 were produced based on this configuration.

A.2. L1002 Shear Panels

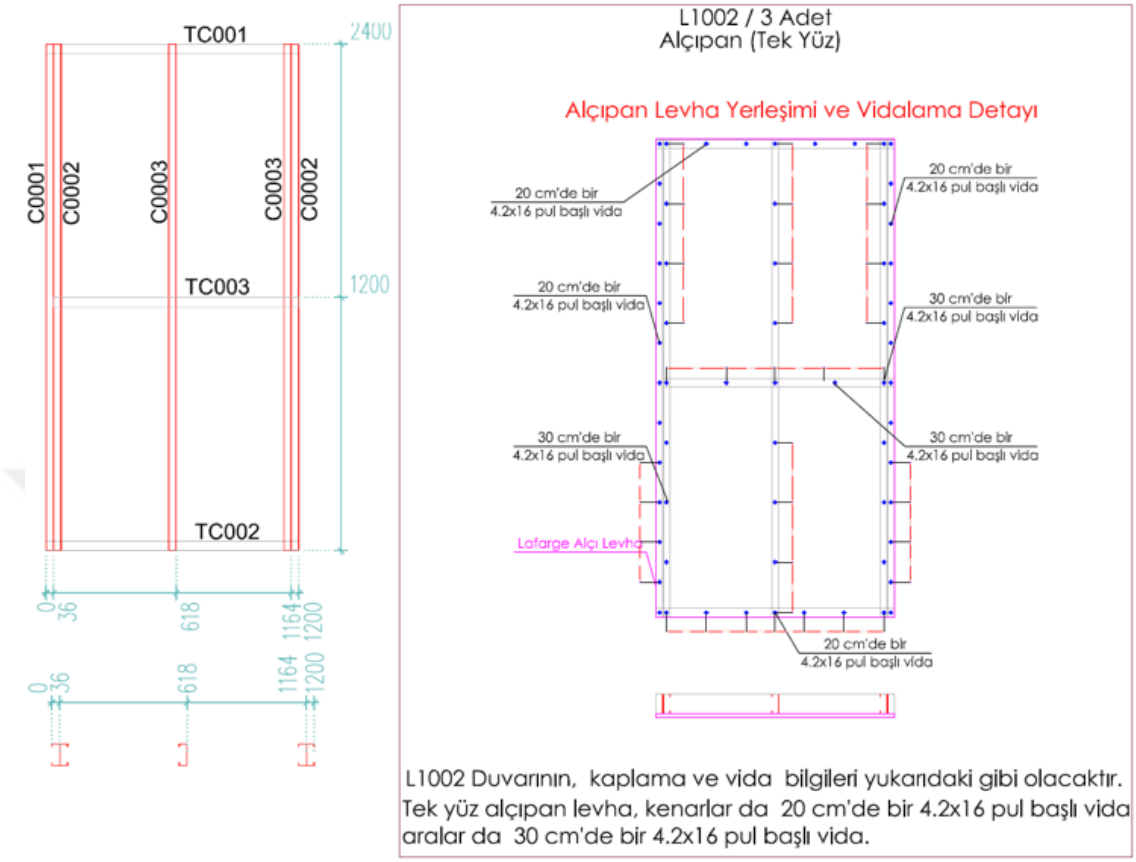

L1002(3)				
POZ	ADET	KESİT	UZUNLUK(mm)	AĞIRLIK(kgs)
C0001	1	AK-CM9915	2397	5.4172
C0002	2	AK-CM9915	2397	10.8344
C0003	2	AK-CM9915	2397	10.8344
TC001	1	AK-CS10215	1200	2.712
TC002	1	AK-CS10215	1200	2.712
TC003	1	AK-CS10215	1164	2.6306
-	-	Grand Total:		35.1406
-	-	Diagonal Length:	2683	

Figure A.2. L 1002 Panel Technical Drawing (Provided by the Manufacturer Company).

PNL-O2 named panels possessing 1.5 mm steel thickness were manufactured according to the configuration shown above (Figure A.2). Three of shear panels sheathed with board type 2 were produced based on this configuration.

APPENDIX B: PHOTOS OF DAMAGES OBSERVED AT CERTAIN TOP DISPLACEMENT LEVELS



Figure B.1. Damages Observed on Shear Panels Sheathed with Board Type 1 at a Top Displacement of 10 mm.



Figure B.2. Damages Observed on Shear Panels Sheathed with Board Type 1 at a Top Displacement of 15 mm.

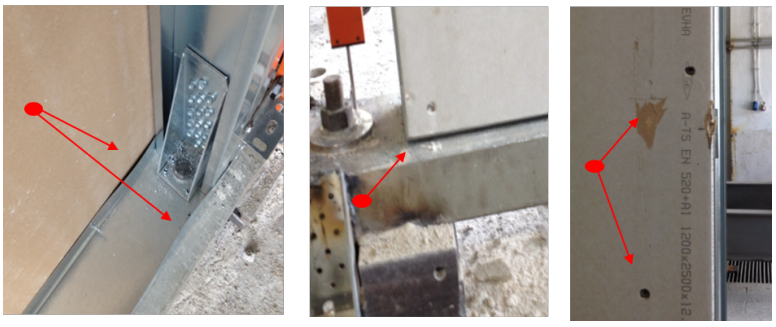

Figure B.3. Damages Observed on Shear Panels Sheathed with Board Type 1 at a Top Displacement of 20 mm.



Figure B.4. Damages Observed on Shear Panels Sheathed with Board Type 1 at a Top Displacement of 35 mm.



Figure B.5. Damages Observed on Shear Panels Sheathed with Board Type 1 at a Top Displacement of 50 mm.

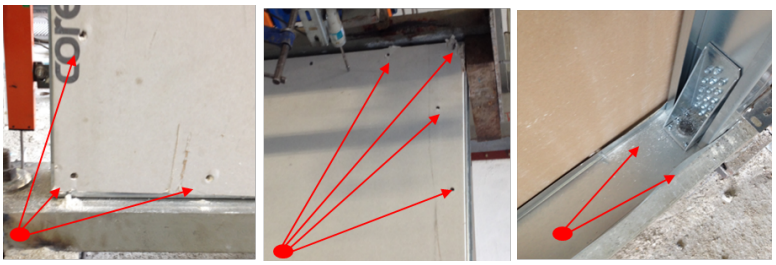

Figure B.6. Damages Observed on Shear Panels Sheathed with Board Type 1 at a Top Displacement of 62.5 mm.

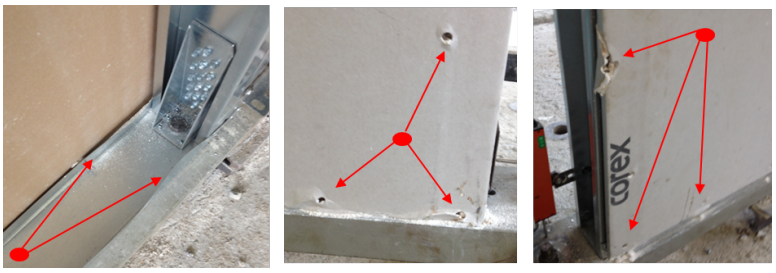

Figure B.7. Damages Observed on Shear Panels Sheathed with Board Type 1 at a Top Displacement of 75 mm.

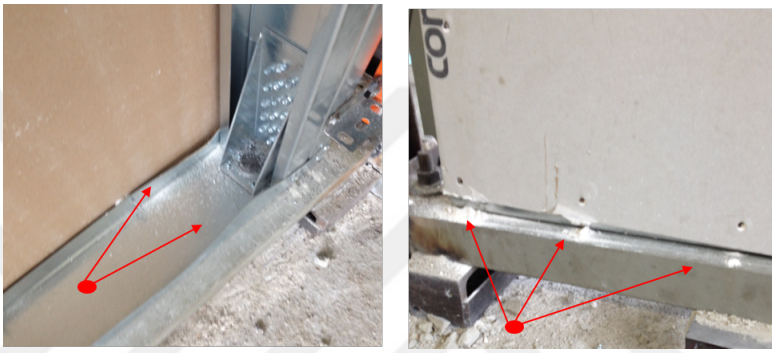

Figure B.8. Damages Observed on Shear Panels Sheathed with Board Type 1 at a Top Displacement of 87.5 mm.

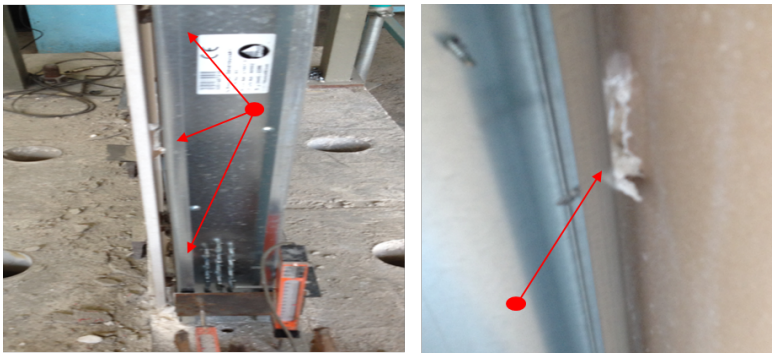

Figure B.9. Damages Observed on Shear Panels Sheathed with Board Type 1 at a Top Displacement of 100 mm.

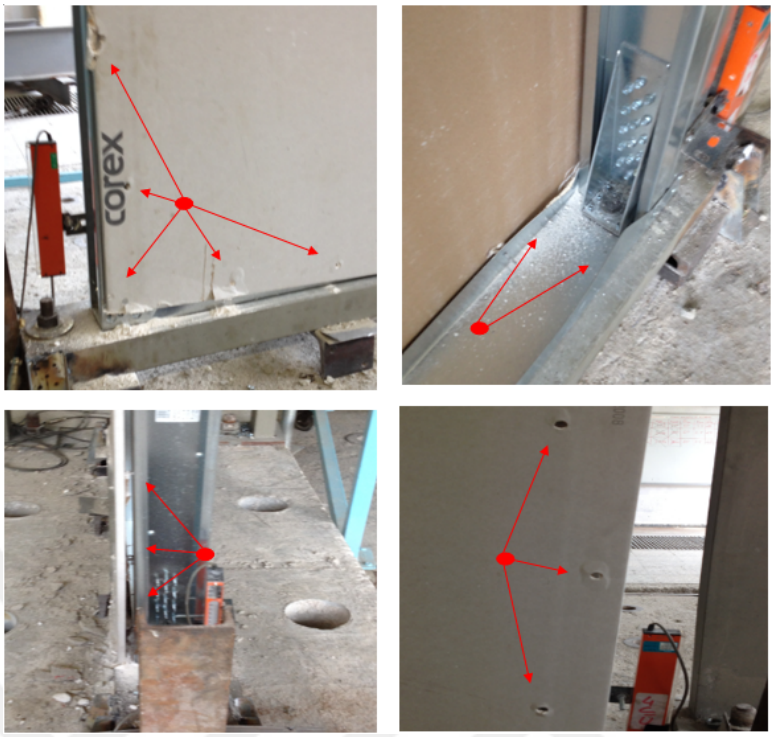

Figure B.10. Damages Observed on Shear Panels Sheathed with Board Type 1 at a Top Displacement of 112.5 mm.

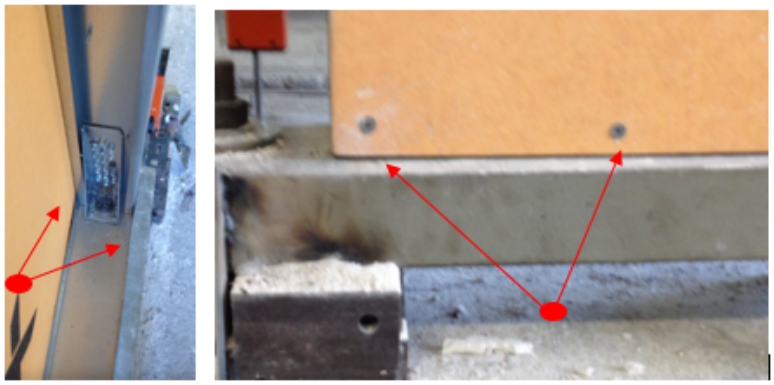

Figure B.11. Damages Observed on Shear Panels Sheathed with Board Type 2 (0.9 mm Steel Thickness) at a Top Displacement of 10 mm.

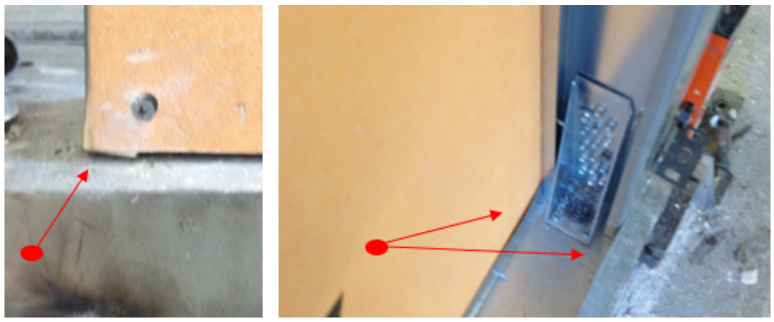

Figure B.12. Damages Observed on Shear Panels Sheathed with Board Type 2 (0.9 mm Steel Thickness) at a Top Displacement of 15 mm.



Figure B.13. Damages Observed on Shear Panels Sheathed with Board Type 2 (0.9 mm Steel Thickness) at a Top Displacement of 20 mm.

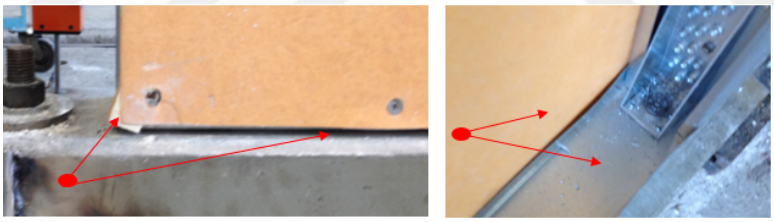

Figure B.14. Damages Observed on Shear Panels Sheathed with Board Type 2 (0.9 mm Steel Thickness) at a Top Displacement of 35 mm.

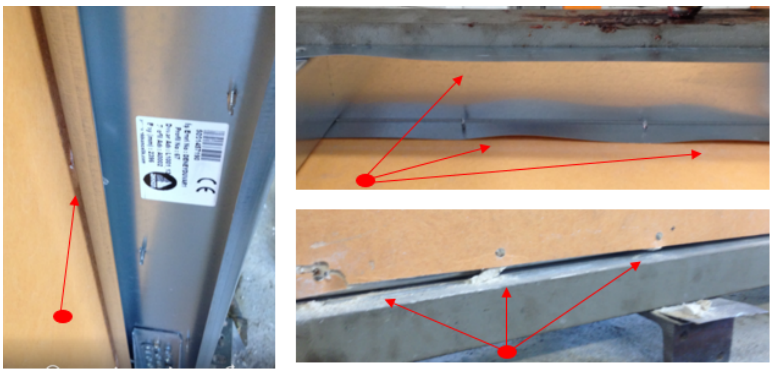

Figure B.15. Damages Observed on Shear Panels Sheathed with Board Type 2 (0.9 mm Steel Thickness) at a Top Displacement of 50 mm.

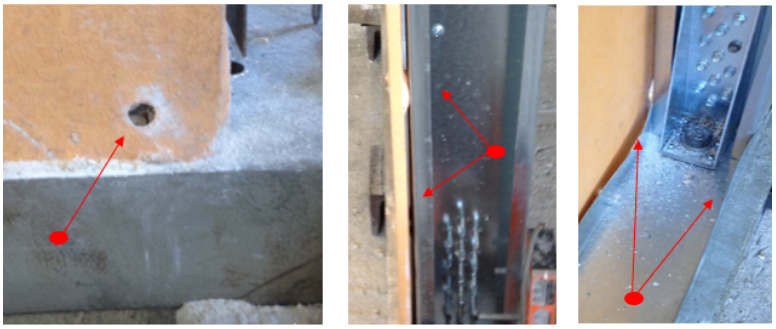

Figure B.16. Damages Observed on Shear Panels Sheathed with Board Type 2 (0.9 mm Steel Thickness) at a Top Displacement of 62.5 mm.

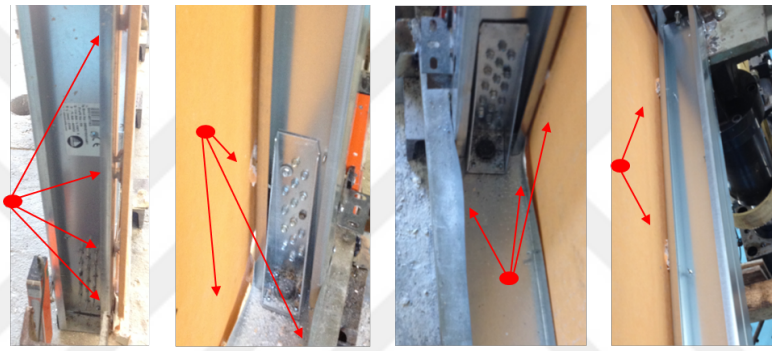

Figure B.17. Damages Observed on Shear Panels Sheathed with Board Type 2 (0.9 mm Steel Thickness) at a Top Displacement of 75 mm.

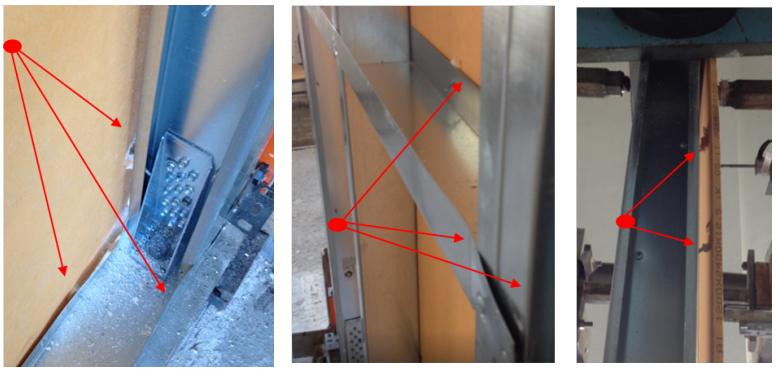

Figure B.18. Damages Observed on Shear Panels Sheathed with Board Type 2 (0.9 mm Steel Thickness) at a Top Displacement of 87.5 mm.

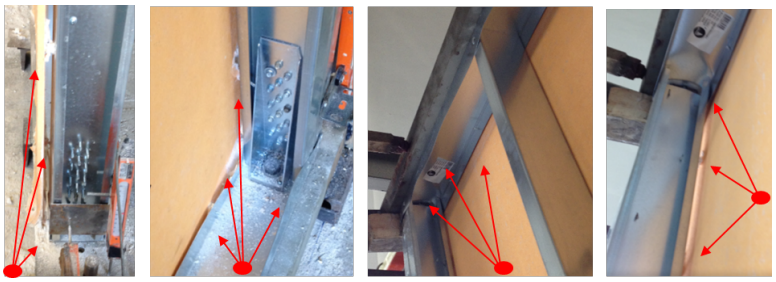

Figure B.19. Damages Observed on Shear Panels Sheathed with Board Type 2 (0.9 mm Steel Thickness) at a Top Displacement of 100 mm.

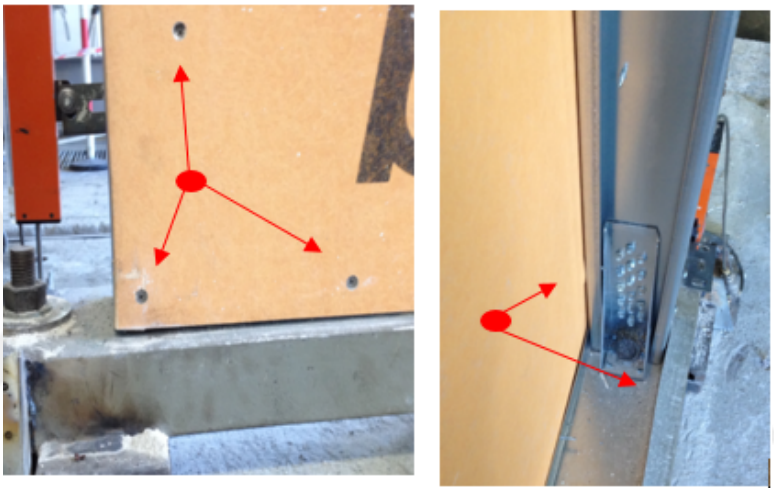

Figure B.20. Damages Observed on Shear Panels Sheathed with Board Type 2 (1.5 mm Steel Thickness) at a Top Displacement of 10 mm.

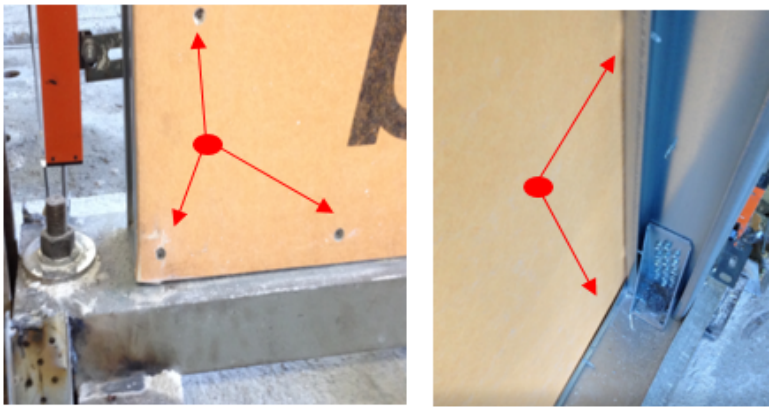

Figure B.21. Damages Observed on Shear Panels Sheathed with Board Type 2 (1.5 mm Steel Thickness) at a Top Displacement of 15 mm.

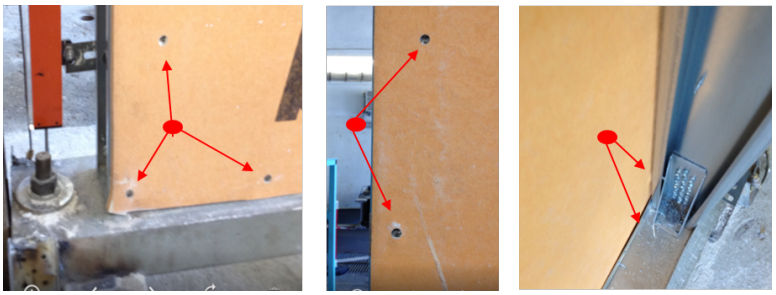

Figure B.22. Damages Observed on Shear Panels Sheathed with Board Type 2 (1.5 mm Steel Thickness) at a Top Displacement of 20 mm.

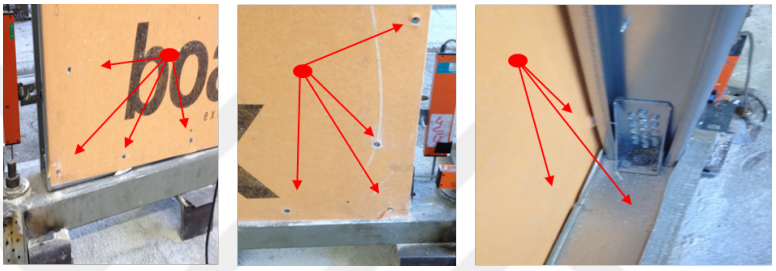

Figure B.23. Damages Observed on Shear Panels Sheathed with Board Type 2 (1.5 mm Steel Thickness) at a Top Displacement of 35 mm.

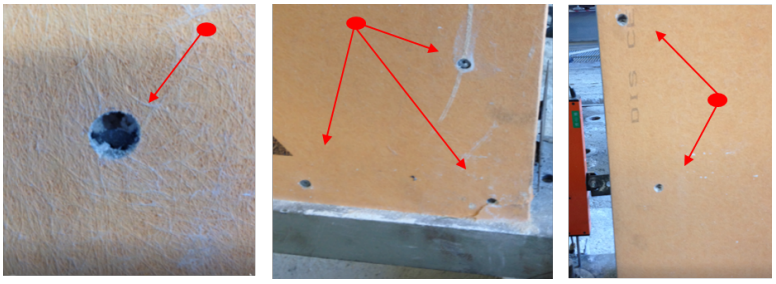

Figure B.24. Damages Observed on Shear Panels Sheathed with Board Type 2 (1.5 mm Steel Thickness) at a Top Displacement of 50 mm.

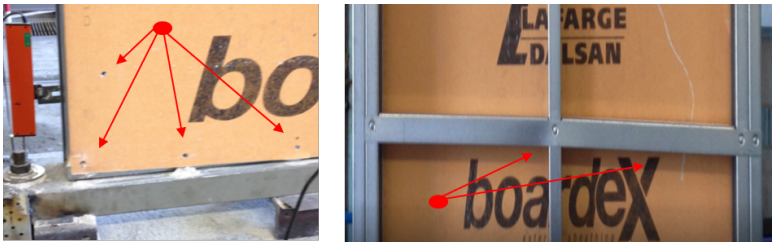

Figure B.25. Damages Observed on Shear Panels Sheathed with Board Type 2 (1.5 mm Steel Thickness) at a Top Displacement of 62.5 mm.

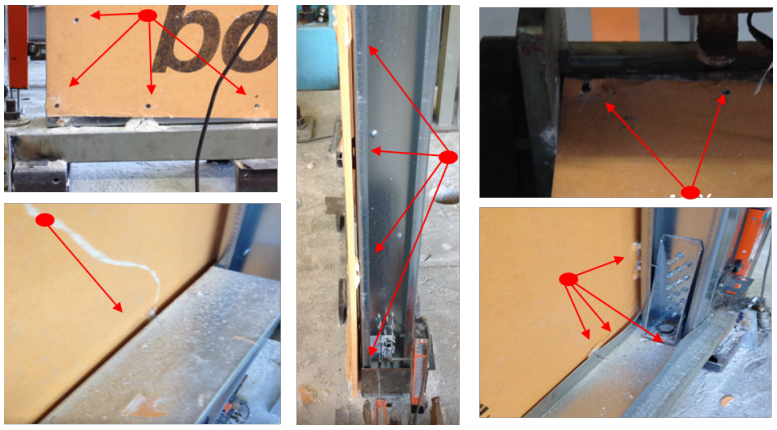

Figure B.26. Damages Observed on Shear Panels Sheathed with Board Type 2 (1.5 mm Steel Thickness) at a Top Displacement of 75 mm.

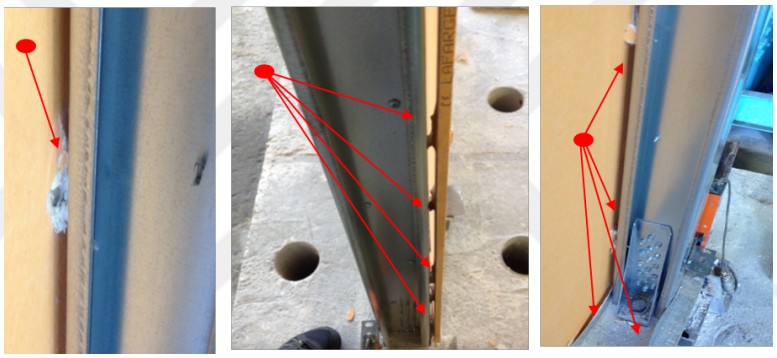

Figure B.27. Damages Observed on Shear Panels Sheathed with Board Type 2 (1.5 mm Steel Thickness) at a Top Displacement of 87.5 mm.

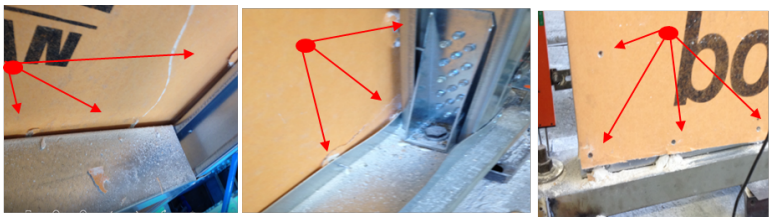

Figure B.28. Damages Observed on Shear Panels Sheathed with Board Type 2 (1.5 mm Steel Thickness) at a Top Displacement of 100 mm.

REFERENCES

1. Turkish Earthquake Code, 2007, "Specification of Buildings to be Built in Disaster Areas", *The Ministry of Public Works and Settlement*, Ankara.

2. American Iron and Steel Institute -S213-07, 2007, "North American Standard for Cold-Formed Steel Framing-Lateral Provisions", Washington, D.C., *American Iron and Steel Institute*-S213-07.

3. American Society for Testing and Materials E2126, 2011, "Standard Test Methods for Cyclic (Reversed) Load Test for Shear Resistance of Vertical Elements of the Lateral Force Resisting Systems for Buildings", *American Society for Testing and Materials International, West Conshohocken*, PA, 2006, DOI: 10.1520/E2126-11, *www.astm.org*.

4. Computers and Structures Increment SAP2000 v17, 2015, "Integrated Finite Element Analysis and Design of Structures1, *Computers and Structures Increment*, Berkeley, California, USA.

5. Miller T.H., Pekoz T., 1993, "Behavior of cold-formed steel wall stud assemblies", *Journal of Structural Engineering*, Vol.119, No.2, pp. 641-651.

6. Miller T.H., Pekoz T., 1994, "Behavior of gypsum-sheathed cold-formed steel wall studs", *Journal of Structural Engineering*, Vol. 120, No. 5, pp. 1644-50.

7. Serrette, S. L, K. Ogunfunmi., 1996, "Shear Resistance of Gypsum-Sheathed Light-Gauge Steel Stud Walls", *Journal of Structural Engineering*, Vol. 122, No. 4, pp. 383-389.

8. Serrette, S.L., J. Encalada, M. Juadines, H. Nguyen, 1997, "Static Racking Behavior of Plywood, OSB, Gypsum and Fiberbond Walls with Metal Framing", *Journal of Structural Engineering*, Vol. 123, No. 8, pp. 1079-1086.

9. Fülöp, L.A. and D. Dubina, 2004, "Performance of wall-stud cold-formed shear panels under monotonic and cyclic loading Part I: Experimental research", *Thin-Walled Structures*, Vol. 42, pp. 321-338

10. Fülöp, L.A. and D. Dubina, 2004, "Performance of wall-stud cold-formed shear panels under monotonic and cyclic loading Part II: Numerical modelling and performance analysis", *Thin-Walled Structures*, Vol. 42, pp. 339-349.

11. Rogers, C.A., A.E. Branston, F.A. Boudreault and C.Y. Chen, 2004, "Steel Frame / Wood Panel Shear Walls: Preliminary Design Information For Use With The 2005 NBCC", *13th World Conference on Earthquake Engineering*, No: 1999, Vancouver, Canada.

12. Corte, G. D., L. Fiorino and R. Landolfo, 2006, "Seismic Behavior of Sheathed Cold-Formed Structures:Numerical Study", *Journal of Structural Engineering*, Vol. 132, No:4, pp. 558-569

13. Landolfo, R., L. Fiorino and G.D. Corte, 2006, "Seismic Behavior of Sheathed Cold-Formed Structures:Physical Tests", *Journal of Structural Engineering*, Vol. 132, No:4, pp. 570-581.

14. Xu, L. and Martinez, J., 2006, "Strength and Stiffness Determination of Shear Wall Panels in Cold-Formed Steel Framing", *Thin-Walled Structures*, Vol.44, pp. 1084-1095.

15. Fiorino, L., G. D. Corte and R. Landolfo, 2006, "Lateral Response of Sheathed Cold-Formed Shear Walls: An Analytical Approach", *18th International Specialty Conference on Cold-Formed Steel Structures*, pp. 603-619.

16. Fiorino, L., G. D. Corte and R. Landolfo, 2007, "Experimental Tests on Typical Screw Connections for Cold-formed Steel Housing", *Engineering Structures*, Vol. 29, pp. 1761-1773.

17. Simsir, C.C and A. Jain, 2008, "Nonlinear Analysis of Woodframe Shear Walls", *The 14th World Conference on Earthquake Engineering*, Bejing, China.

18. Dubina, D., 2008, "Behavior and performance of cold-formed steel-framed houses under seismic action", *Journal of Constructional Steel Research*, Vol. 64, pp. 896-913.

19. Fiorino, L., O. Iuorio and R. Landolfo, 2009, "Sheathed cold-formed steel housing: A seismic design procedure", *Thin-Walled Structures*, Vol. 47, pp. 919-930

20. Landolfo, R., L. Fiorino and O. Iuorio, 2010, "A Specific Procedure for Seismic Design of Cold-Formed Steel Housing", *Thin-Walled Structures*, Vol. 6, No:1, pp. 603-618.

21. Rogers, C.A., Velchev, K., Comeau, G. and Balh, N., 2010, "Evaluation of the AISI S213 seismic design procedures through testing of strap braced cold formed steel walls", *Thin-Walled Structures*, Vol.48, pp. 846-56.

22. Schafer, B.W., Z. Li and C.D. Moen, 2010, "Computational modeling of cold-formed steel", *Thin-Walled Structures*, Vol. 48, pp. 752-762.

23. Fiorino, L., O. Iuorio and R. Landolfo, 2012, "Seismic analysis of sheathing-braced cold-formed steel structures", *Engineering Structures*, Vol. 34, pp. 538-547

24. Peterman, K.D., N. Nakata and B.W. Schafer, 2014, "Hysteretic characterization of cold-formed steel stud-to-sheathing connections", *Journal of Construction Steel Research*, Vol. 101, pp. 254-264.

25. Peterman, K. D and B. W. Schafer, 2014, "Sheathed Cold-Formed Steel Studs under Axial and Lateral Load", *Journal of Structural Engineering*, Vol. 140(10): 04014074.